UNIVERSITÀ
DEGLI STUDI
FIRENZE

DOTTORATO DI RICERCA IN NEUROSCIENZE

CICLO XXXIV

COORDINATORE Prof. Nicoletta Berardi

Myopathologic readouts identification in dystrophinopathies trough comparative analyses of human and animal models muscles

Settore Scientifico Disciplinare MED/26

Dottorando

Dott. Cardone Nastasia

Tutore

Prof. Malandrini Alessandro

Coordinatore

Prof. Berardi Nicoletta

Anni 2018/2021

Alla mia famiglia

UNIVERSITÀ
DEGLI STUDI
FIRENZE

DOTTORATO DI RICERCA IN NEUROSCIENZE

CICLO XXXIV

COORDINATORE Prof. Nicoletta Berardi

Myopathologic readouts identification in dystrophinopathies trough comparative analyses of human and animal models muscles

Settore Scientifico Disciplinare MED/26

Dottorando

Dott. Cardone Nastasia

Tutore

Prof. Malandrini Alessandro

Coordinatore

Prof. Berardi Nicoletta

Anni 2018/2021

Abstract

Duchenne Muscular Dystrophy (DMD) is an X-linked lethal muscle disorder, his incidence is relatively common 1:5000 male births. DMD is caused by mutations in the *DMD* gene encoding Dystrophin. Dystrophin is a crucial component of the dystrophin-associated glycoprotein complex which has a structural function providing stability to skeletal muscle. Loss of dystrophin leads to progressive muscle impairment and later-on DMD patients and ultimate to cardio-respiratory failure, as no cure available.

Dystrophin deficient mdx-mice model show a mild phenotype and do not display the gradual dramatic muscle loss observed in DMD patients (3). For this reason, a new model of DMD has been developed. It is a rat model with a deletion of exon 52 in DMD gene (R-DMDdel52) deletion that led to a complete loss-of-function of dystrophin.

The aim of this project is to obtain a comprehensive comparative pathophysiology analysis of DMD human, mdx mice and R-DMDdel52 rats, and to find new histopathologic readout useful for the follow up, but more important for the develop of new therapies strategies.

We analyzed 21 human quadriceps and deltoids muscle biopsies at the age of 1-7 years old divided in 4 groups, according to age and compare it with *Tibialis anterior* (TA), of rats and mice at different time points.

The markers of interest were fibrosis markers, inflammation markers, and muscle regeneration capacity markers all of it represents the principal hallmarks of DMD those were used to highlight similarity and/or differences between DMD human biopsies and rodent models, and to describe the disease progression.

We mainly focalized our attention on better understand the muscle stem cell behavior in all the samples. Studying Pax7+ Muscles stem cells (SC) and the regeneration process (eMyHC). We described a reduction of regenerative capacities of the muscles over time in DMD humans as well as in animal models, by quantifying the regenerating myofibers. Moreover, we firstly demonstrated the acquisition of a senescence phenotype specifically in DMD SCs, by evaluating the expression of senescence markers (p16, p21 and yH2AX).

Indeed, in DMD patients and rats, a progressive exhaustion of stem cells has been observed with an early acquisition of senescence traits. In contrast, mdx4cv mice, did not show senescence markers, possibly explaining the milder phenotype of this model.

The ultimate goal of this project was to draw up histopathological guidelines necessary for the follow up of the disease and useful for any clinical and therapeutic studies.

Myopathologic readouts identification in dystrophinopathies trough comparative analyses of human and animal models muscles

SUMMARY

Myopathologic readouts identification in dystrophinopathies trough comparative analyses of human and animal models muscles

1.INTRODUCTION

1.1 Skeletal muscle

Skeletal muscle is the most abundant tissue of the human body, comprising approximately the 40% of total body mass. Skeletal muscle tissue is one of most dynamic and plastic tissues of the human body and contains 50-75% of all body proteins, is mainly composed of water (75%), proteins (20%) and other substances such as inorganic salt, fat, carbohydrates (5%) (Frontera et al., 2015).

There are three types of muscles: skeletal and cardiac, also defined striated, and the smooth muscle. Skeletal muscle is responsible for every voluntary and conscious action; the cardiac muscle is involuntary and tridimensionally organized to form the heart. The heart pump the blood throughout the body. The smooth muscles are contained in various organs such as blood vessels, stomach, bladder, airways, uterus, they are involuntary or hormone-regulated and have different macroscopic and microscopic organization compared to the striated ones (Webb C et al., 2003).

The skeletal muscles can be viewed as a biomechanical device that convert chemical energy to physical work. Their primary function is to generate strength and contract in order to support locomotion, respiration, posture, and hearth functionality. Skeletal muscles are essential for multiple functions, and they interact with various components such as nerves for impulse transmission, and vasculature for optimal tissue oxygenation (Shandrin et al., 2017; Dumont et al., 2015). From a metabolic perspective, the skeletal muscle contains a regulatory and metabolic machinery regulating cellular homeostasis. With this respect, it has multiple roles including the storage of amino-acids and carbohydrates, production of heat and the maintenance of core temperature, contribution to basal metabolism, consumption of oxygen and ATP during physical activity and exercise (Frontera et al., 2015).

1.1.1 Macroscopic and microscopic morphology of skeletal muscle

The skeletal muscle is composed by muscle cells also called myofibers, separated by different layers of connective tissue. The epimysium is the outer layer surrounding the entire muscle; the perimysium delimits each bundle of muscle fibers including blood vessels and nerves; and the

endomysium surround each muscular fiber. Bundles of myofibers form the fascicle, bundles of fascicle form the muscle tissue inside the above mentioned three concentric layers of fibrotic tissue. The muscles are encapsulated by the extracellular matrix and supported by the cytoskeletal networks (Mukund et al., 2019; Frontera et al., 2015).

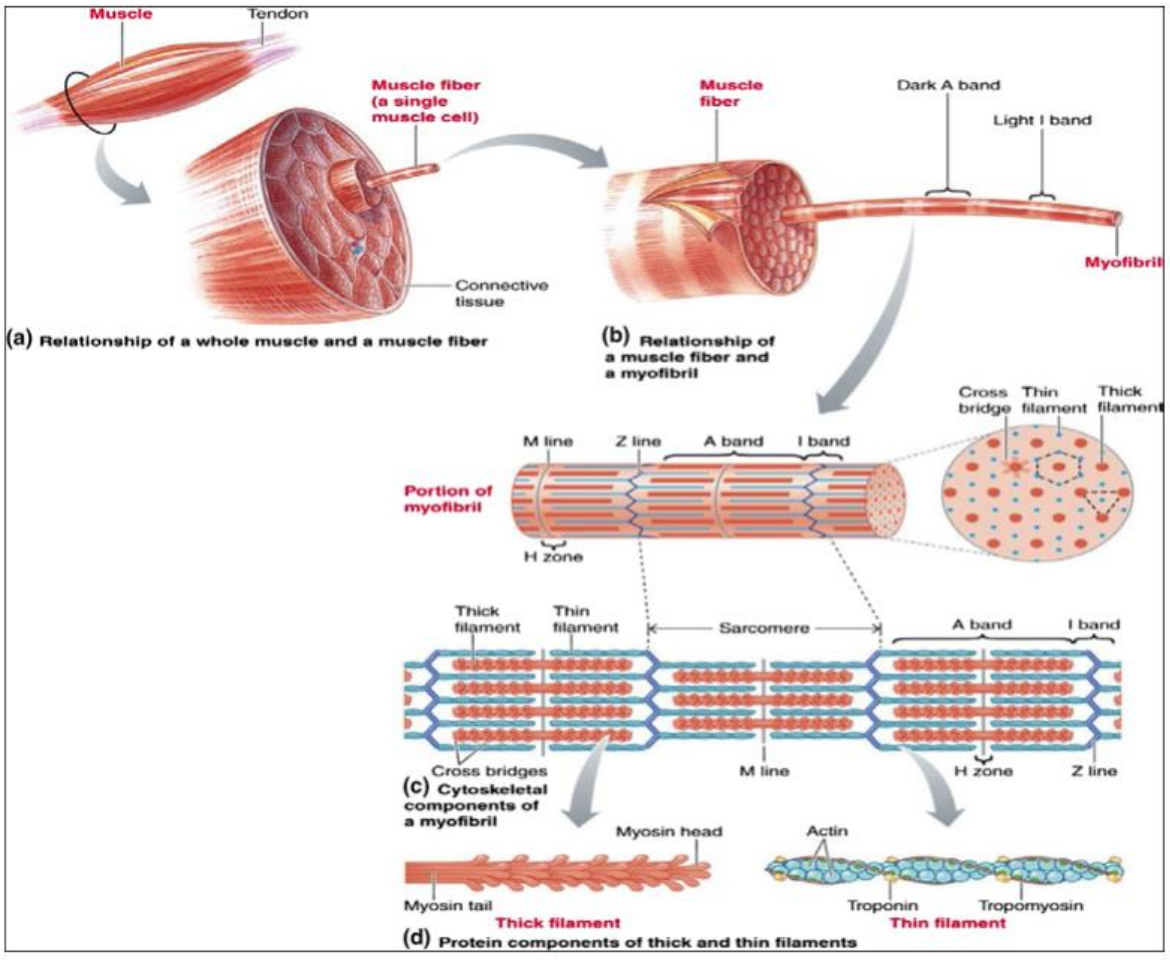

Figure 1 *Skeletal muscle structure: representation of the epimysium, the perimysium, and the endomysium connective tissues, which surround muscle, fascicles and myofibers respectively. Enlargement of one sarcomere and cross-sectional view of a sarcomere cut through in different locations. (Frontera et al., 2015)*

The myofibers are syncytia composed by hundreds of post-mitotic nuclei sharing the same cytoplasm that are generated by the fusion of myoblasts during development. Some myoblasts do not fuse with the developmental myofibers but migrate in the space between the sarcolemma and the basal lamina forming the skeletal muscle stem cells, also known as satellite cells (SCs). Muscle SCs are able to differentiate upon muscle injury, contributing to muscle repair and regeneration (Shandrin et al., 2017).

A single muscle fiber has approximate dimensions of 100µm in diameter and 1cm in length, with anatomic variation; each muscle fiber contains several myofibrils and it's surrounded by a cell membrane called sarcolemma. The cytoplasm is called sarcoplasm. The myofibers sarcoplasm comprises thousands of myofibrils forming different striations. The two most abundant myofilaments are actin and myosin and the represent approximately 70–80 % of the total protein content of a single fiber. The ultrastructural analysis of the skeletal muscle allowed to identify different bands and lines, constituting the sarcomere structure, which is the basic contractile machinery of skeletal muscle.

Each sarcomere is formed by thick and thin filaments whose arrangement gives the sarcomere a striated, band-like pattern. The sarcomere is the area between two Z lines (or Z disks) and consist of overlapping arrays of thick (myosin) filaments and thin (actin) filaments. Running through the center there is the I (isotropic) band (lighter area), comprising the thin filaments connected by the nebulin to the Z band. Thick filaments are located at the center and are connected by titin at the M line, that is placed in the middle of the sarcomere. Thin and thick filaments are comprised in the area that includes the A (anisotropic) and the H bands (Martini et al., 2012).

1.1.2 Muscle contraction

The contraction process is the result of the interaction between the thick and thin filaments of each sarcomere. The thin filaments are composed by monomers of globular actin that polymerize in filamentous actin. A complex of troponin and tropomyosin is associated with the actines. Tropomyosin forms a long chain that covers the active sites, thus preventing the actin-myosin interaction, while troponin is responsible for tropomyosin stabilization. Thick filaments contain a double strand myosin chain twisting together, with an elongated tail and two globular heads that are the binding site for the hydrolysis of ATP. Only one of the heads is always in contact with actin any time (Mukund et al., 2019).

Structures involved in the contractions are the T tubule systems and the Neuromuscular Junction. The T tubule system are invaginations of the sarcolemma that conducts the nerve action potential from outside to the inside of the cell. The sarcoplasmic reticulum (SR), which is responsible for the storage, release and uptake of calcium. The calcium is stored in terminal cisternae, two terminal cisternae in close contact with T tubule (one on each side) giving rise to the triad (Martini et al., 2012).

The neuromuscular junction is a modified chemical synapse where the electrical signals are conducted to the axon terminal (presynaptic region), where are located many vesicles containing acetylcholine (Ach). On the other side there is the muscle motor plate. This specialized multi-folded postsynaptic region contain the acetylcholine receptors (AChRs). Between the presynaptic and postsynaptic areas there is a space called the synaptic cleft filled with a specialized matrix known as synaptic basal lamina (Rodriguez Cruz et al., 2020).

The muscle contraction is activated when a neural signal created in the brain or in the spinal cord starts. It is subordinated to the onset of electrical event that occurs within the sarcolemma. The nervous impulse arrives by the NMJ at the triad structure where the calcium is stored, activating depolarization activity (action potential), managed by sodium and potassium channels (Exter et al., 2010).

Upon stimulation the Ach pool is released and binds the receptors on the postsynaptic membrane of the sarcolemma; this is followed by an open of the ionic channels and a releasing of sodium across the membrane, creating the action potential. Action potential triggers depolarization of T tubule which is immediately followed by a large and fast release of calcium from the sarcoplasmic reticulum, enough to trigger the contractile response of myofibrils. The released calcium binds to the regulatory protein troponin C of the complex troponin-tropomyosin, thus determining the displacement of the tropomyosin from the actin active sites within the thin filaments. The exposure of these active sites allows the binding of the head of the myosin molecule with actin. This event is corroborated by the presence of ATP. The ATPase is located in the myosin head, which promotes the detachment of myosin from actin and the formation of a new actin-myosin cross-bridge. The ATPase, in the myosin head, hydrolyzes the ATP resulting in the release of chemical energy that is transformed into mechanical work during the actin–myosin interaction. The end of the cycle is marked by the subsequent ADP release that leads to the formation of a new acto-myosin rigor complex, which will be in turn dissociated by ATP binding, thus starting a new cycle (Radàk et al., 2018; Exter et al., 2010).

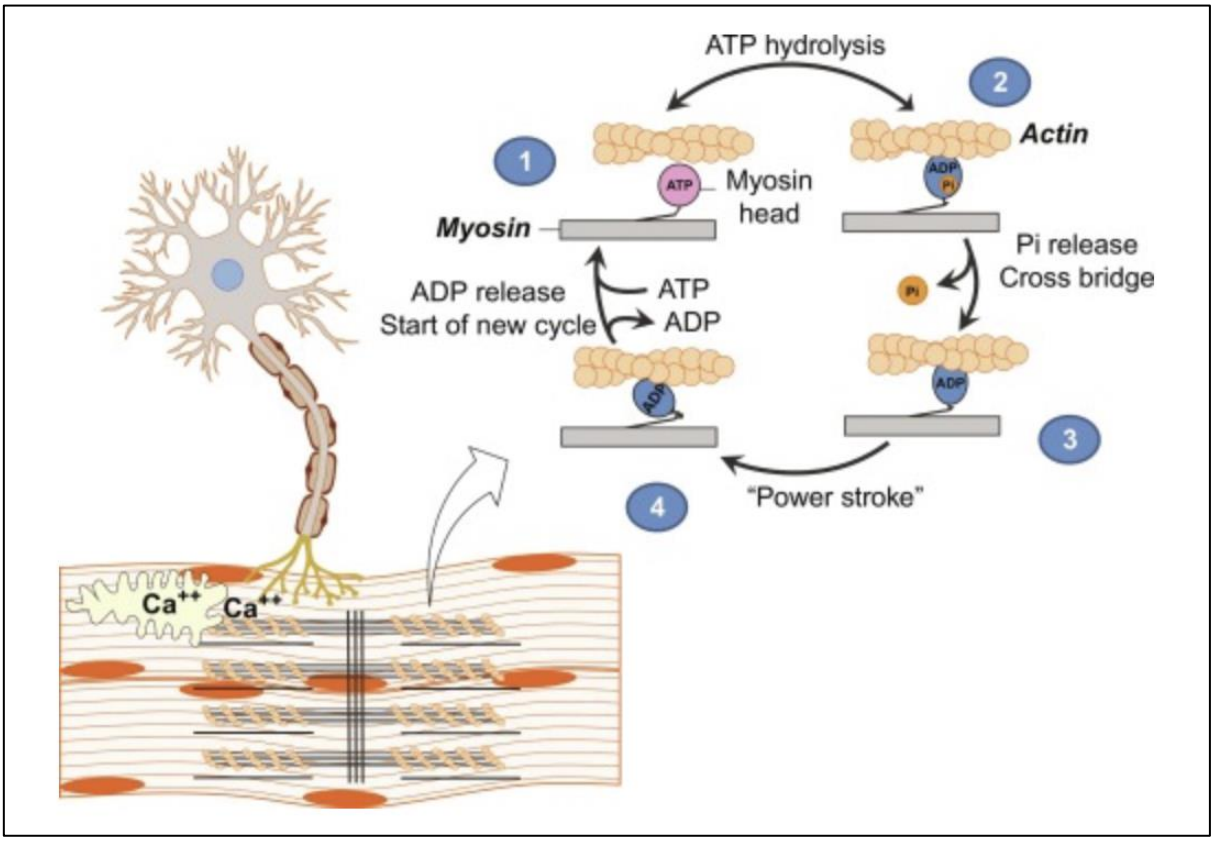

Figure 2 *Muscle contraction cycle. Action potential across T-tubule system realizing Ca++ ions. Ca++ ions bind troponin which allow myosin-actin binds. Sliding of myosin-actin binds produce the muscle contraction and require ATP (modified from Radàk 2018).*

1.1.3 Muscle fiber types

One important characteristic of skeletal muscle is its heterogeneity. In fact, it is composed of fibers that owe variable biochemical, mechanical, and metabolic properties. These properties were used to classify the fiber types. Nowadays the common identifier of muscle fiber types is the contractile protein Myosin Heavy Chain (MyHC). MyHC is a molecular motor that converts chemical energy into mechanical force and is indispensable for body movement and heart contractility. MyHC presents a wide number of isoforms, is encoded by a multigene family and differentially distributed in human muscles, and among different species in a tissue- and stage-specific manner (Schiaffino et al., 2010; Galpin et al., 2012).

It exists two kinds of fibers, type 1 and type 2 fibers.

The type 1 or slow-twitch muscles rich in oxidative enzymes, mitochondria and myoglobin, specialized in continuous activity. Muscles with a predominance of type 1 fibers are called red muscles (Glancy et al., 2011).

Type I or Slow Oxidative fibers express MyHC-β/slow isoform, encoded by *MYH7* gene. These fibers are rich in myoglobin and mitochondria, and they are characterized by slow contractile properties and aerobic metabolism, high resistance to fatigue and low myosin ATPase activity (Talbot et al., 2016).

Type 2 or fast-twitch muscles, identified as white muscles, specialized for phasic activity and characterized by glycolytic metabolism.

Type IIa or Fast Oxidative-Glycolitic fibers express MyHC-IIA isoform, encoded by *MYH2* gene. These fibers presents both oxidative and glycolytic enzymes and they are characterized by a fast-twitching phenotype, and an aerobic metabolism.

Type IIb or Fast Glycolytic or Fast Fatigable fibers express MyHC-IIB isoform encoded by *MYH4* gene. These fibers are rich of glycolytic enzymes, low in myoglobin and mitochondria. The metabolism of this fiber type is an anaerobic metabolism, typical of white muscles such as diaphragm or EDL. They are characterized by short but intense contraction and high myosin ATPase activity.

Type IIx or Fast Intermediate fibers: expressing the MyHC-IIX isoform encoded by *MYH1* gene. They share fast-twitching properties with other fast MyHC isoforms (2A and 2B) but present an intermediate resistance to fatigue and higher contraction capacity (Talbot et al., 2016).

This classification is representative for mammalian limbs fiber types. However, there are several other muscle groups expressing different isoforms of MyHC. For example, there are atypical muscles in head and neck such as Extraocular muscles, jaw and other neck muscles that presents atypical muscle fibers (Schiaffino et al., 2011).

Embryonic MyHC encoded by *MYH3* and fetal MyHC encoded by *MYH8* are expressed during development and in regenerating muscle fibres (Tajsharghi et al., 2013).

Different muscles can have different predominance of fibers, reflecting the adaptation of the muscle to different patterns, enabling the muscle to participate to different activities, depending on the metabolic request. This property is called muscle plasticity or malleability (Schiaffino et al., 2011).

Further, the muscle responds to different stimuli: nervous, steroids, hormones, aging, inactivity and the response to stimuli is fiber type specific. Recently it has been demonstrated that myofibers of adult mice can also adapt their contractile and metabolic properties depending on external stimuli, by activating or repressing a set of specific genes, such as the *MYH* genes (Dos Santos et al., 2020).

1.1.4 Myogenesis

In vertebrate, during embryonic development, skeletal muscles of all body, except craniofacial muscles, derived from the somite (Bismuth et al., 2010). Somites are metameric organizations originating from the segmentation of the parassial mesoderm. The somites are subdivided in three regions: the dermomyotome expressing Pax3, which subsequentially divides into dermatome from which originate the cutaneous dermis; and myotome from which originate the skeletal muscles of the body and the limbs; the third region is the sclerotome which contribute to give rise to the cartilage of the spinal cord and ribs and the occipital region of the skull.

The muscles of the head are derived from paraxial mesoderm and prechordal mesoderm (Buckingam et al., 2003).

Skeletal muscle development is a multistep process. Founder stem cells are specified and progressively turned into muscle progenitor cells with a myogenic-specific commitment.

The first step is the migration and the delamination of progenitor cells, which co-express transcriptional factors – paired box 3 and 7 (Pax3 and Pax7), the upstream regulators of the myogenesis (Buckingam et al., 2015).

The delamination of dermomyotome is followed by a downregulation of Pax3 while progenitor cells start expressing the myogenic regulatory factors (MRFs): Myf5, Mrf4 and/or MyoD giving rise to the primary myotome formation. These factors are essential for skeletal muscle, determining the skeletal muscle cell identity and are considered the gatekeepers for the myogenesis (Tajbakhsh et al., 2009).

The last factor needed for the determination of skeletal muscle cell identity is Myogenin, driving the terminal differentiation of muscle progenitor cells into mononucleated elongated fibers expressing desmin and myosin (Relaix et al., 2006).

Several regulatory genes are necessary for myogenesis (Tajbakhsh., 1997) that willl not be discussed here.

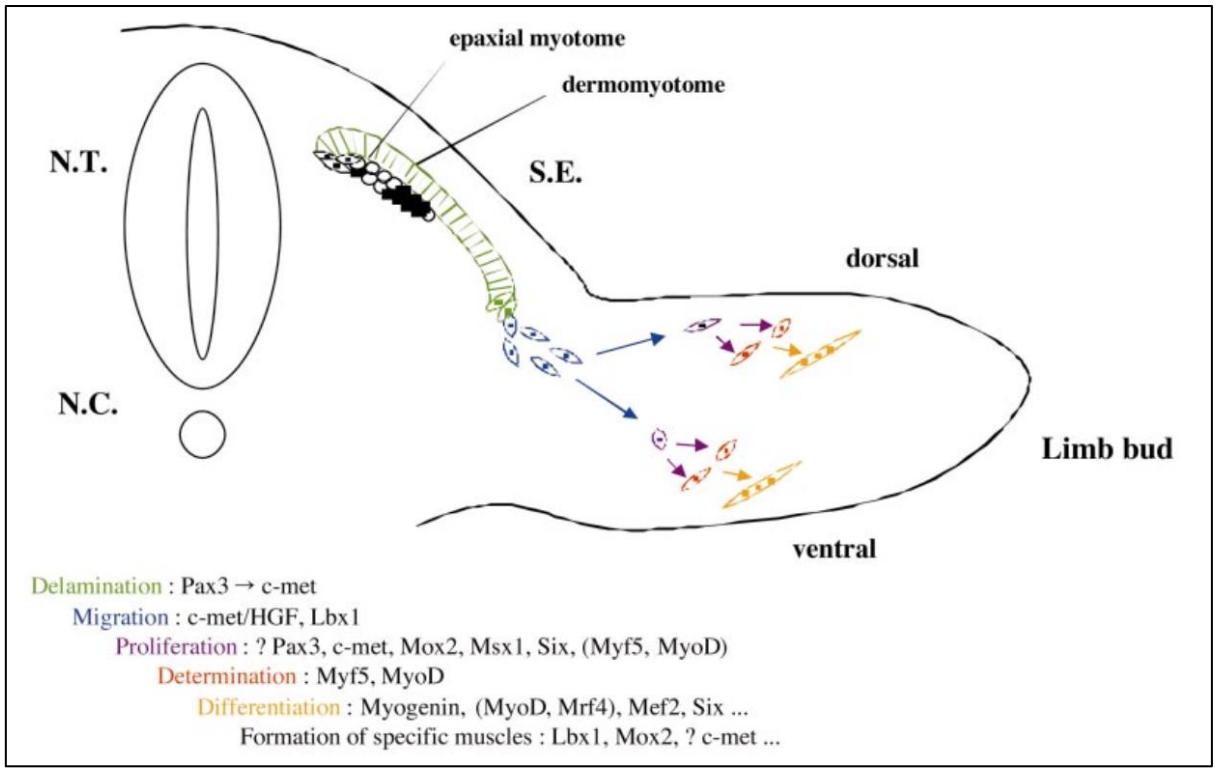

Figure 3 *Muscles formation in the limbs, schematic representation with different stages and genes potentially involved. NC, notochord; NT, neural tube; SE, surface ectoderm (modified from Buckingam et al 2003).*

Only a fraction of myogenic progenitors terminally differentiates during primary myotome formation. These myogenic progenitors are used as a scaffold for the successive waves of myogenic cells formation, to sustain muscle growth during development (Relaix et al., 2006).

The primary myotome formation is followed by a cascade of specific myogenic waves in successive distinct steps involving different types of myoblasts: embryonic and foetal myoblasts and satellite cells (Biressi et al., 2007).

The myogenic mononucleated progenitors, expressing slow MyHC starts to fuse into myotubes forming the secondary fibers. Secondary, the fibers are surrounded by primary fibers, but they differentiate from the expression of MyHC, the secondary fibers express the fast MyHC isoform (Hutcheson et al., 2009).

Subsequently, the muscle masses undergo very extensive growth in the foetal period and postnatally. This expansion has been recently attributed to a population of muscle progenitor

cells already present at the embryonic stage located in the central part of the dermomyotome. These skeletal muscle progenitor cells coexpress Pax3 and Pax7, can differentiate into skeletal muscle fibers during embryogenesis, and are present as a reserve cell population within the growing muscle mass during prenatal and postnatal life (Tajbakhsh., 2009; Relaix., 2006; Messina et al., 2009).

The third population of cells are known as satellite cells (SCs), are recognized only after the formation of secondary fibers as mononucleated cells lying between basal lamina and sarcolemma (Cossu et al., 2005). This population of cells contribute to the muscle mass growing, after being activated by myogenic factors they undergo several cells division producing mature fibers that fuse and forms new fibers. In the meanwhile, few of these cells does not differentiate and return to quiescence in order to maintain the progenitor pool (Collins et al., 2005).

1.1.5 Satellite cells and muscle regeneration

Skeletal muscle has the great ability to regenerate upon acute injury and chronic degeneration in muscular dystrophies. This process is mainly managed by muscle satellite cells (SCs) which are activated and then proliferate and differentiate (Frontera et al., 2015).

Satellite cells were described for the first time in 1961 by Alexander Mauro as “dormant myoblast”. Discovered by electron microscopy for their atypical localization between the sarcolemma and the basal lamina (Mauro et al., 1961). Lately described as population of small, mononucleated cells with a heterochromatic nucleus surrounded by a small amount of cytoplasm that constitutes around 2-10% of total muscle nuclei in adult skeletal muscle (Hawke et al., 1985).

SCs, are characterized by an increased nuclei/cytoplasm ratio, a reduced organelle content, and a small nucleus with an abundance of inactive chromatin and they are quiescent (G0) in mature skeletal muscle (Chargé et al., 2004; Schultz et al., 1978). In physiological conditions, SCs are required for the postnatal muscle growth, and a decreasing in the numbers of SCs during aging has been reported (Dumont et al., 2015; Chargé et al., 2004).

SCs are activated in response to injury, therefore these enter the cell cycle and proliferate. They have the capability to migrate to damaged places where they differentiate into myoblast and fuse to destroyed fibers or to each other to form *de novo* multinucleated myofibers. Importantly,

as SCs are a type of adult stem cells they can both differentiate to generate muscle progenitors indispensable for muscle repair, and self- renew and replicate themselves to maintain the SCs pool. SCs can undergo symmetric division when two identical cells are generated or asymmetric division giving rise to both myogenic progenitor cell and stem cell (Yin et al., 2013).

The main regulators of satellite cells physiology, and myogenic potential are transcriptional factors – paired box 3 and 7 (Pax3, Pax7) and myogenic regulatory factors (MRFs). Their sequential activation and repression are crucial for proper myogenesis (Le Grand et al., 2007). Pax7 is a canonical marker expressed in both quiescent and activated (proliferating) SCs in many species including human (Seale et al., 2000). Pax-3 (Pax-7 paralogue) plays important role during embryonic myogenesis, however, in adult skeletal muscle is restricted to certain type of muscles, for example, diaphragm. In contrast Pax7 is uniformly present in SCs from the majority of muscle types (Relaix et al., 2006; Seale et al., 2000). Pax7 plays a pivotal role in regulating SCs function, it induces satellite cells specification by regulating expression of some MRFs (von Maltzahn., et al 2013).

Quiescent SCs do not express MRFs, which are sequentially expressed during myogenesis in activated SCs, proliferating myoblasts, and mature myofibers (Le Grand et al., 2007). The MRFs are: Myf5 (myogenic-factor 5), MyoD (myogenic determination factor), myogenin, MRF4 (muscle regulatory factor) that are member of class II basic helix-loop-helix family of transcription factors (Hernández-Hernández et al., 2017). Myf5 is the only MRF expressed by quiescent MuSCs, which, when activated, start to express MyoD, while adult myoblasts exspress MyoD and Myf5. Differentiation of myoblasts into mature fibers starts after the downregulation of Pax genes and the upregulation of myogenin and MRF4 (Bentzinger et al., 2012). Following several rounds of proliferation, myogenic cells exit the cell cycle, start to differentiate, and begin to fuse to damaged myofibers or fuse to each other to form new myofibers. Myogenic differentiation is an irreversible procedure driven by hierarchical gene expression. Since the induction of MyoD or myogenin expression can induce MEF2 expression, while overexpression of MEF2, in turn, increases MyoD expression and myoblast differentiation (Yin et al., 201; Dumont et al., 2015).

Finally, newly formed myofibers are characterized by the expression of unique developmental myosin isoforms such as embryonic myosin heavy chains (eMyHC), coded by the myosin

heavy chain 3 (*MYH3*) and has centrally localized nuclei which is the main feature of regenerating myofiber (Schiaffino et al., 2015).

The Skeletal muscle displays an extraordinary regenerative capacity. Whether the muscle injury is inflicted by trauma of genetic defects, muscle regeneration follows three distinct and overlapping phases: inflammation, tissue reconstruction, and tissue remodeling (Relaix et al., 2015; Dumont et al., 2015; Baghdadi et al., 2018). The typical appearance of a muscle in regeneration shows newly formed myofibers of small caliber and with centrally located myonuclei within the regenerated muscle.

1.1.6 Skeletal muscles disorders: the muscular dystrophies

Disorders that affect the muscle tissue are termed myopathies, since they are determined by a primitive structural or functional muscle defect that establishes a pathological condition. The vast group of myopathies can be further classified as inherited and acquired (Gao et al., 2015).

The muscular dystrophies (MDs) are a clinically, biochemically and genetically heterogeneous group of inherited degenerative disorders characterized by progressive muscle wasting and weakness of variable distribution and severity (Malfatti et al., 2017).

Given the widespread of muscle tissue throughout the body, it is well sustained the presence of several types of dystrophies which differ among them for the severity of muscle weakness, degree of progression, inheritance type, age of onset, and selective muscle involvement (Gao et al., 2015; Yiu et al., 2015).

Here we will focus on an early onset muscular dystrophy, the Duchenne Muscular Dystrophy (DMD), which is caused by loss of function mutations in the gene encoding dystrophin (Duan et al., 2021).

1.2 Duchenne muscular dystrophy

Duchenne muscular dystrophy (DMD, OMIM#310200) is a rare devasting chromosome X-linked disease that affect approximately 1:5000 boys and 1:50000000 girls (Starosta A et al., 2021). DMD is due to mutations in the *DMD gene* encoding Dystrophin, that prevent the production of the muscle isoforms of dystrophin (Duan et al., 2021).

DMD boys are diagnosed in childhood since they present a stereotyped presentation with walking or climbing stairs difficulties, frequent falls, and the presence of Gower's sign (patients need to use the harms to stand up) (Birnkrant et al., 2018). Natural history studies showed that DMD patients lose the ambulation at around 12 years of age becoming wheelchair bounded (Blake et al., 2002). DMD is also associated with cognitive impairment, low IQ score and speech delay (Mirski et al., 2014). Successively the patients develop a severe muscular atrophy, cardiomyopathy and around 20 years of age shows decreased respiratory functions needing assisted ventilation. Finally, all these comorbidities lead to an inexorable decline with death in their 20-40 years old (Duan et al., 2021). This scenario has changed than to the therapy with steroids and codification of standard of care measures for respiratory and cardiac involvement.

1.2.1 DMD gene and its product: Dystrophin

DMD gene is one of the biggest gene in the human body, consisting of 2,4 million bases and localized in the short arm of chromosome X (Xp21) (Keegan., 2020; Muntoni et al., 2003). The coding sequence is made up of 79 exons spanning 14 kilobase pairs (Aartsma-Rus et al., 2006). The TREAT_NMD DMD Global database has reported more than 7000 mutations within the *DMD* gene. Most of them are large mutations (80%) including large (≥1 exon) deletions (68% of total mutations) and large (≥1 exon) duplications (11% of total mutations) (Juan-Mateu et al., 2015; Bladen et al., 2015). Small mutations including small deletions and duplication, and splice site mutations accounted for 20% of total mutation. The database reported also nonsense and missense point mutations <10% of all mutations. Importantly, the majority of described mutations are found within two "hot spots" of the dystrophin gene, one located in the distal region – exons 45-55 and in the proximal region – exons 2-20 (Nakamura et al., 2017).

The 93% of mutations are frameshift in the DMD gene and lead to a premature stop codon, with a truncated and non-functional isoform of dystrophin, characterizing DMD phenotype (Ahn et al., 1993).

In contrast in-frame mutations lead to the synthesis of a partially functional and internally truncated protein for this reason are associated to a milder type of dystrophy such as the Intermediate dystrophinopathies (IMD) or the Becker Muscular Dystrophy (BMD) (Aartsma-Rus et al., 2006).

However, it must be taken in consideration that there are some exceptions: patients carrying frame-shift deletion present a BMD phenotype, and patients with in-frame mutations are

associated with DMD phenotype (Muntoni et al., 2003, Aartsma-Rus et al., 2017). This inconsistence can be partially explained by the presence of alternative splicing of the *DMD* gene or activation of additional translation start sites although it might be caused by others phenomenon (Ferlini et al., 2013). Of note, patients carrying out-of-frame mutation (exon 45 deletion) may present a milder phenotype, due to spontaneous exon 44 skipping that restores the reading frame and allow the production of some functional dystrophin protein (Prior et al., 1997). Subsequent studies on the 44-45 exon skipping, in fact, has been performed and confirmed the milder phenotype of the patients with an increasing in the number of dystrophin positive fibers, suggesting that studies of the clinical trials for exon 44-45 skipping might be useful (Anthony et al., 2014; Dwianingsih et al., 2014).

The dystrophin, product of *DMD* gene, is an enormous protein of 427kDa. It is localized at the cytoplasmatic face of the sarcolemma and represent the most important member of the dystrophin-associated protein complex (DAGC) (Gao et al., 2015).

Dystrophin has four main functional domains: 1. actin-binding amino-terminal domain, 2. Rod domain, 3. cysteine-rich domain, 4. C-terminal domain (Koenig et al., 1998).

The N-terminal actin-binding domain (ABD_1) contains 2 calponin homology domains (ch1.; ch2) and binds directly to F Actin linking dystrophin to the sarcolemmal actin network. ABD_1 also binds dystrophin to the contractile apparatus in skeletal muscle cells (Stone et al., 2005).

The rod domain contains 24 spectrin repeats and collaborate to form a strong lateral connection with actin filaments (ABD_2). It mediates dystrophin interaction with microtubules, and it is required for the organization of microtubule lattice in skeletal muscle cells (Prins et al., 2009).

The cysteine-rich domain (CRD) of dystrophin is formed by several domains: WW protein-binding module found in several signaling and regulatory molecules, calcium-binding EF-hand motifs (EF1 and EF2), and Zinc-finger domain (ZZ), which is responsible for binding with transmembrane protein like calmodulin in a calcium-dependent manner (Rentschler et al., 1999).

The Carboxy-terminal domain contain two polypeptides that fold into an a-helical coiled coils. Coiled coils are common protein motifs involved in protein-protein interaction. Ct domain provides binding sites for dystrobrevin and syntrophins, mediating their sarcolemma localization (Sadoulet-Puccio et al., 1997).

The dystrophin gene has at least eight promoters that give rise to different isoforms of different molecular mass (Wein et al., 2014). Three full-length isoforms (427kDa) of dystrophin exist: Dp427M muscles localized isoform, Dp427B localized in brain and Dp427P which is expressed in the Purkinje cells. The transcription of these three isoforms is controlled by three different promoters in the upstream localization of the first exon (Muntoni et al., 2003). The synthesis of the shorter isoforms of dystrophin depends by internally localized promoters. Dp260 is the retinal isoform (D'Souza et al., 1995); Dp140 is expressed in brain (Lidov et al., 1995); Dp116 is the Schwann cells isoform (Byers et al., 1993); Dp71 is characteristic of non-skeletal muscle tissues (Hugnot et al., 1992); the shortest isoform is Dp40, a brain localized isoform derived from alternative splicing of Dp71 isoform (Tozawa et al., 2012). However, a greater number of isoforms may be expressed as a consequence of alternative splicing (Fletcher et al., 2013; Feener et al., 1989).

1.2.2 Dystrophin-Associated Glycoprotein Complex (DAGC)

Dystrophin is a major structural element of the dystrophin-associated glycoprotein complex (DAGC). The structure of the dystrophin protein preserves the integrity and stability of the sarcolemma exerting a protective role against mechanical stress due to repeated contractions, by creating a link between the subsarcolemmal cytoskeletal actin and the extracellular matrix through the DAGC (Ervasti et al., 1993; Matsumura et al., 1994).

Together with dystrophin, dystroglycan is a central component of the DAGC. Dystroglycan is encoded by DAG1 gene and is initially expressed as a single protein, then is cleaved into α-dystroglycan and β-dystroglycan (Ibraghimov-Beskrovnaya et al., 1992). β-dystroglycan is a transmembrane protein binding the cysteine-rich domain of dystrophin, moreover, is a regulator of the cytoskeleton organization providing transduction through the extracellular matrix (Sotgia et al 2000). The N-terminal end of β-dystroglycan interacts with the α-dystroglycan which is a highly glycosylated peripheral membrane protein binding the basal lamina. These two subunits are necessary for the stability and the linkage between cytoskeleton and ECM (Ervasti et al., 1993).

Other components of DAGC are the sarcoglycans (SG). The main function of sarcoglycans is to facilitate interactions between cytoskeleton and ECM. Those are a single-pass transmembrane family and are divided in 4 subunits α-, β-, γ-, and δ (Talts et al., 1999). The sarcoglycans are tightly associated with sarcospan which is composed by four transmembrane

domains. SG complex and sarcospan maintain mechanical stability of sarcolemma and contribute to signal transduction (Gao et al., 2015). Mutations in genes encoding sarcoglycans were identified in patients suffering from limb-girdle muscular dystrophies (LGMD) and showed to be associated with cardiomyopathy. Mutation in one gene lead to deficiency of all components of the SG complex (Nigro et al., 1996, Barresi et al., 2000).

The intracellular part of DAGC is composed by α-dystrobrevin, syntrophins, and nitric oxide synthase (nNOS). Dystrobrevin links the other members of the complex with the cytoskeleton interacting with dystrophin, syntrophinn. The crucial role of these interactions is the transductions of stress signals, thus are expressed proteins such as the presence of nNOS, kinase-3 (Noguchi et al., 1995; Brenman et al., 1996).

Syntrophins are scaffold proteins interacting with the other proteins of DAGC. The main role is to connect the DAGC to the nitric oxide signaling (Brenman et al., 1996).

Mutations in any of these components cause inherited autosomal muscular dystrophies (Dalkilic et al., 2003).

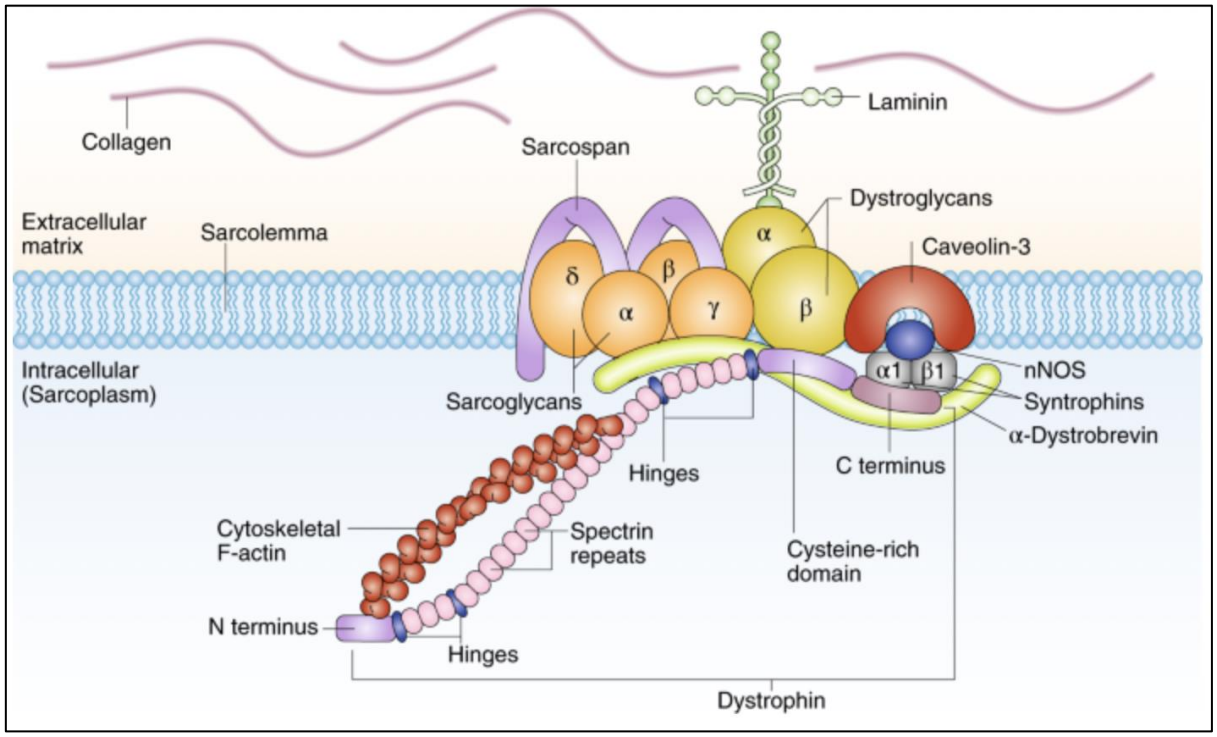

Figure 4 *Representation of Dystrophin -associated glycoprotein complex.*

1.2.3 Pathophysiology of Duchenne muscular dystrophy

Dystrophin has a structural role in the DAGC linking the internal cytoskeleton to the ECM. The DAGC is destabilized when dystrophin is absent, resulting in the loss of the linkage and an instability of the sarcolemma leading to cycles of degeneration/regeneration of myofibers occurring within the muscle (Shahnoor et al., 2015). This membrane instability caused by the lack of dystrophin also lead to contraction-induced damages with release of cytoplasmatic contents. Consequently, there is an activation of the innate immune response recruiting MHC I and II, T and B cells, muscle necrosis, increased oxidative stress, fibrosis tissue replacement and finally, loss of muscle functionality (Rosemberg et al., 2015). However, the pathophysiology of the DMD is still somehow unclear and further studies are needed in order to develop novel treatments.

1.2.3.1 Disruption of sarcolemma

DAGC disruption makes cells more susceptible to mechanical damage and may cause structural defects in the plasma membrane such as subsarcolemmal lesions that lead to membrane and permeability alterations (Mokri et al., 1975). Therefore, the intracellular content can easily leak from destroyed myofibers and muscle enzymes such as Creatine Kinase (CK) (Rosalki et al., 1989) or lactate dehydrogenase (LHD) (Ibrahim et al., 1981), and growth factors (D'Amore et al., 1994; Kaye et al., 1996). Serum CK level are used as a diagnostic tool as their level are greatly elevated in DMD affected boys and is often increased in DMD female carriers (Hoffman et al., 1992). Although CK is a great marker to screen newborns (Mendell et al., 2013), it is not appropriate to monitor disease progression or response to therapies because its level declines considerably with age and might be also affected by exercises and other muscle injuries (Hathout et al., 2016).

Serum proteins such as albumin and immunoglobulins, which are typically found in the blood, are accumulated in damaged, necrotic myofibers (Amthor et al., 2004; Bradley et al., 1998). Degenerating or necrotic myofibers are observed in muscle biopsies even before the onset of clinical symptoms. Necrotic fibers are usually observed in clusters in both human samples and animal models. Necrotic fibers are exposed to neutrophils and macrophages invasion and undergo phagocytosis (Blake et al., 2002).

1.2.3.2 Inflammation

Damage and necrosis of myofibers lead to activation of the innate immune system and excessive inflammatory response. Dystrophic muscles are invaded by inflammatory cells such as macrophages, lymphocytes, eosinophils. The chronic inflammation contributes to the progression of the disease (Villalta et al., 2015).

Changes in sarcolemma permeability leads to the leak of cytoplasmatic contents which migrate in the ECM triggering the immune response. These contents are for example nucleic acids or heat shock proteins, known as damage/danger-associated molecular pattern (DAMP). DAMPs bind the toll-like receptors (TLR) activating their pathway and activating NFkB signaling. After the activation of these inflammatory pathways the complement is activated accordingly, so therefore an increasing of MHC class I and II and the expression of cytokines, chemiokines, growth and adhesion factors is observed in the muscle (Rosemberg et al., 2015; Henriques-Pons et al., 2014; Chen et al., 2005).

In addition to macrophages and white cells, other inflammatory cells can contribute to the progression of the disease inducing apoptosis through sarcolemmal interactions. Particularly the T-helper (CD4+), cytotoxic (CD8+) and regulatory lymphocytes are found in skeletal muscle of DMD (Spencer et al., 2001; Spencer et al., 1997).

1.2.3.3 Muscle regeneration

DMD is characterized by repeated cycles of degeneration and regeneration of myofibers (Guiraud et al., 2019), but regenerative capacity of DMD muscles is impaired despite the high number of SCs (Reimann et al., 2000).

The lack of dystrophin and the subsequent alterations in the DAGC impact also on the satellite cells. SCs lose their polarity in the absence of dystrophin, this loss of polarity impact on kinetics and cells proliferation. These lead to a number of abnormal asymmetric divisions. Lack of asymmetric division leads to a loss of myogenic progenitor cells, impairing muscle regeneration (Dumont et al., 2016, Keefe et al., 2015). Recent studies demonstrate that in the dystrophic niche of SCs should be some signal that impact on the proliferation. Has been demonstrated that once removed the SCs from the dystrophic niche, they start to proliferate like SCs derived from healthy muscles (Boldrin et al., 2015; Meng et al., 2015). However it cannot be excluded

the hypothesis of cell-autonomous defect present in DMD-mutant satellite cells, defect which contributes to the pathogenesis of DMD (Dumont et al., 2016).

SCs could be also affected by inflammatory cells and factors, for example IL10 secreted from macrophages which stimulate cells proliferation (Villalta et al., 2009), TNFα activate SCs and induces transition from G1 to S and has been demonstrated that IL6 induce SCs proliferation. Macrophages play different roles in muscle repair according to their state of activation, once activated produce reactive oxygen species, exhibit proinflammatory functions, and may enhance both damage of dystrophin-deficient myofibers and myogenic cell proliferation (Villalta et al., 2009, Desguerre et al., 2009).

Another hypothesis is the satellite cells exhaustion model. After subsequent cycles of regeneration and degeneration the SCs results in progressive loss of their regenerative capacity, a shortening of telomers and induced premature senescence (Decary et al., 2000).

1.2.3.4 Fibrosis

In physiological conditions, deposition of ECM is needed for supplying a scaffold for new myofibers, however, the excessive secretion of collagen, elastin, fibronectin and glycosaminoglycans induces the formation of non-functional, fibrotic tissue in skeletal muscle as well as in the heart (Kharraz et al., 2014; Birnkrant et al., 2018). The main profibrotic factor has been identified. It is the transforming growth factor-beta (TGFβ) (Biernacka et al., 2011). TGFβ increases expression of profibrotic genes such as collagen type I or connective tissue growth factor (CTGF), the synthesis of matrix proteins, promoting ECM deposition (Leask et al., 2004). Important levels of TGFβ has been shown in plasma and skeletal muscle of DMD patients, these levels were positively correlated with collagen deposition (Ishitobi et al., 2000; Bernasconi et al., 1995).

In DMD the regenerative capacity will be loss during time and the muscle tissue is replaced with fibrotic and adipose tissue (Deconinck N et al., 2007). One of the main sources of TGFβ are the inflammatory cells infiltrated in DMD muscles, like lymphocytes and macrophages (De Paepe et al., 2013).

Another important contribution in muscle regeneration and muscle replacement with adipose tissue and fibrotic tissue is given by the fibro-adipogenic progenitors (FAPs) (Joe et al., 2010). FAPs are multipotential cells capable to give rise to both fibroblast and adipocytes. They express factors such as interleukin-6 (IL6) and insulin-like growth factor-1 (IGF1) which could

affect muscle regeneration, moreover FAPs can give rise to ectopic adipocytes which accumulate in degenerating muscles (Uezumi et al., 2010; Heredia et al., 2013).

Fibrosis is one of the main hallmarks of DMD and has many negative consequences, impacts on the muscle functionality, including heart, and reduces the number of myofibers potentially target for therapies (Kharraz et al., 2014).

1.2.3.5 Angiogenesis and circulation

Dystrophin is not only expressed in muscle cells, but also in satellite cells and endothelial cells, suggesting that a lack of dystrophin can impact on angiogenesis (Podkalicka et al., 2019). Angiogenesis is the new formation of capillaries and vessels in the tissues, an efficient blood circulation is needed for the correct functionality of muscle tissues since the vessels deliver oxygen and various metabolites (Podkalicka et al., 2019). Firstly, Leinonen in 1979 and then Miike et al in 1987 demonstrated abnormalities in blood vessels structure on DMD muscles biopsies. The basement membrane was more than double in DMD compared to control, and they showed an increase in the numbers and in the area of capillaries. Moreover, degenerating capillaries were founded (Miike et al., 1987; Leinonen et al., 1979). In fact, later, elevated levels of VEGF were found in DMD patients compared to controls, confirming anomalies in DMD muscle angiogenesis (Saito et al., 2009).

Nitric oxide (NO) is a potent vasodilator and is found to be relevant in DMD pathophysiology (Podkalicka et al., 2019). NO is produced by NO-syntase (n-NOS) which is a component of the DAGC (Grozdanovic et al., 1999). In dystrophin deficient cells n-NOS lose his subsarcolemmal anchorage leading to a reduction of his activity and expression followed by lower levels of NO. This reduction may contribute to the progression of the dystrophic phenotype (Kasai et al., 2004; Brenman et al., 1995). In absence of NO, during exercise, ischemia may occur in DMD muscles due to the lack of oxygen (Sander et al., 1995; Crosbie et al., 2001).

A reduction in the expression of nNOS in muscles of DMD dystrophic patients has been found compared to children with other myopathies (Sander et al., 2000).

NO is also founded to be implicated in myofiber differentiation (Lee et al., 1994), moreover may act as an epigenetic regulator of the expression of n-NOS in DMD myofibers, impairing the muscle development and regeneration (Colussi et al., 2009).

Other processes and molecular pathways are identified to play an important role in the progression of DMD phenotype such as oxidative stress, mitochondrial disfunction and autophagy anomalies (De palma et al., 2012, Podkalicka et al., 2019).

1.2.4 Hystopathology of Duchenne muscular dystrophy

In 1868 Duchenne was following up a group of children with muscle weakness and hypertrophy of some muscles. By performing a needle biopsy and analyzing the muscle tissue, he discovered the proliferation of fibrotic tissue and the abnormal presence of adipose tissue (Duchenne et al., 1868).

Muscle biopsy analysis enormously contributed to describe the morphologic phenotype of the disease in the muscle, and to understand biological and molecular mechanism of the disease. Analyzing in details muscle biopsies led the researchers to performing deeper analysis, thanks to that, a lot of molecular mechanisms has been understood throughout years. Moreover, the hallmarks of DMD have been founded by analyzing muscle biopsies and are nowadays the target of multiple therapies, such as givinostat which target fibrosis and others (Dubowitz et al., 2021).

Nowadays muscle biopsies for DMD are performed less than before, since the diagnosis of DMD is molecular. The muscle biopsy is still mainly performed to discriminate Becker from Duchenne, as in Becker muscles a percentage of dystrophin is still expressed (Dubowitz et al., 2021). Nevertheless, a detailed analysis of a muscle biopsy is very important, because it gives a lot of information about the disease, on the possible etiological steps of muscle alteration; the finding of all the characteristic markers of the muscle disease (explained below) in the biopsy, allows the clinicians to simplify the differential diagnosis of Duchenne muscular dystrophy, therefore helps to direct in the right diagnostic screening step.

Importantly, clinical severity cannot be judge only by the grade of the pathology, but in the meantime, a Becker cannot be discriminate from a Duchenne only referring to the muscle biopsy, must be a combination of the two. However, the biopsy gives us information before the manifestation of clinical signs, because pathological changes can be observed in DMD muscles since early stages and even in utero (Merrick et al., 2009).

The classical histological features in DMD muscles can be appreciated with the Hematoxylin & Eosine (H&E) staining. The blown Myopathologic phenotype consists of fibers size variability with atrophic and hypertrophic fibers, so an heterogeneity in the size of the fibers

can be appreciated. The smallest fibers can be the fibers in regeneration (described below). Immature centrally nucleated fibers are observed representing the muscle regeneration, but also fibers with sarcolemma internal nuclei are observed. Multiple internal nusclei fibers are not so common in DMD and BMD rather than other myopathies, however their fibers can be also found representing the splitting fibers and sometimes the necrotic fibers (Dubowitz et al., 2021). Basophilic small mononucleated fibers are the regenerative ones which shows a prominent central nucleus and are pale in the H&E staining. The newly formed fibers can be better detected with Embryonic-Myosin Heavy chain (*Myh3* gene) Immuno Fluorescence (IF), or Foethal-Myosin Heavy chain IF. Usually, these fibers are expressed in the muscle in cluster and are the fibers derived from the degenerative and regenerative cycles occurring in DMD muscles. Unfortunately, the regenerative capacity will be loss during time (Deconinck et al., 2007; Taylor et al., 1997; Ribeiro et al., 2018).

Another common myopathic feature is that the Myosin-Heavy chain expression in the muscles has a predominance of Type I myosin slow fibers, because it has been reported that glycolytic fast-twitch fibers (Type IIb) are preferentially affected by the disease, whereas oxidative Type I fibers are almost spared (Webster et al., 1988; Yuasa et al., 2008).

There is a contingent of necrotic fibers, isolated or in clusters. In these necrotic spots phagocytes and other inflammatory infiltrates are always presents. The necrotic fibers are pale in H&E and Gomori staining, the necrosis is usually segmented, affecting firstly one part of the fiber that will be later phagocyted entirely (Dubowitz et al., 2021).

Where there is necrosis, presence of infiltrated inflammatory infiltrates is always present. Macrophages in myo-phagocytosis are those in greater number, but also T cells, basophils and mast cells can be appreciated. In contrast Eosinophils and B cells are rare (Dubowitz et al., 2021; Deconinck N et al., 2007; Bradley et al., 1972). Large round hypercontracted fiber can be also observed, as a characteristic of other muscular dystrophies, they are intensively stained and correspond to damaged fibers (Dubowitz et al., 2000).

It is well known that the fibrosis is one the main characteristics of DMD muscles, and the deposition of fibrotic tissue increases with the progression of the disease (Peverelli et al., 2015). The localization of fibrotic tissue is mainly endomysial, but it accumulates also in perimysium (Nix et al., 2020). An old interesting study on muscle biopsies, where they tried to correlate muscles parameters with clinical signs, shows that endomysial fibrosis is the only

myopathologic parameter in human DMD significantly correlated with poor motor outcome and age at ambulation loss (Desguerre et al., 2009).

Fat tissue substitution occur in DMD muscles after multiple cycles of degeneration, when the muscle is not able to regenerate properly anymore, and is another histological finding that can be seen with H&E staining in muscle biopsies. Other stainings such as Black Sudan, Bodipy and Oil Red O can be used for a qualitative and semiquantitative analysis of fat-tissue infiltration. Adipose tissue is usually observed in the perimysium but can be found in the endomysium too, and the presence of fat tissue in the muscle increases with the progression of the disease (Bayliss et al., 1972; Qiu et al., 2017; Mehlem et al., 2013; Dubowitz et al., 2021).

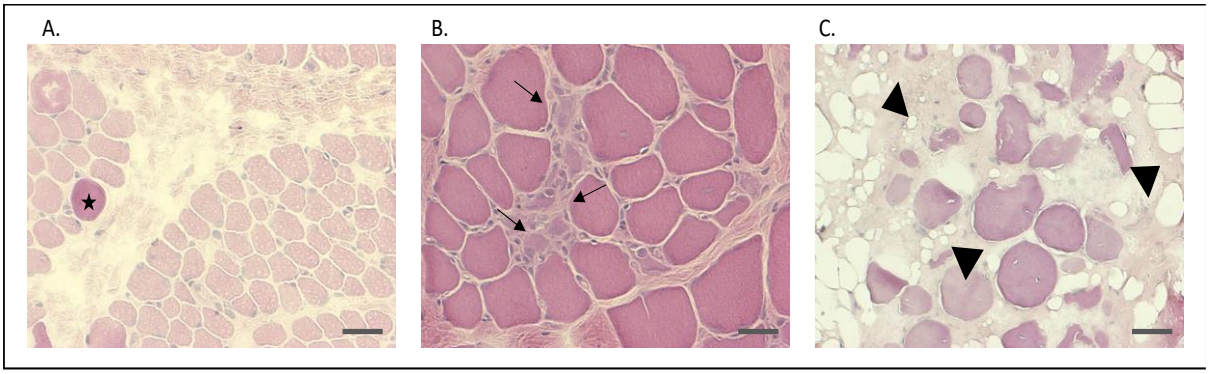

Figure 5 *H&E of DMD muscle biopsies: a) hypercontracted rounded damaged fibers (star), differences in the morphology of fibers, endomysial fibrosis and perymisial fibrosis; Scale bar 200 μm b) fibrosis, basophilic contents (inflammatory infiltrated cells, arrows); Scale bar 100 μm c) muscle from an old patient, the muscle structure is completely lost, the fibers are all damaged and heterogeneous in size and shape, wide areas of fibrotic tissue, fat tissue substitution (black triangles). Scale bar 100 μm*

Although nowadays the diagnosis of Duchenne is made by looking for the mutation in the gene, the muscle biopsy is very important to see the expression of dystrophin and thus discriminate Becker from Duchenne (Dubowitz et al., 2021). Dystrophin, as described above, is a very huge protein and has four domains. As the position and the size of the mutation in the *DMD* gene may vary, is essential to use the antibody which correspond to the right domain to avoid false negatives. The monoclonal antibodies commonly used to recognize these different epitopes are: DYS1 which is directed for the Rod-domain; DYS2 targeting the C-terminal and DYS3 directed to the N-term domain. All the three antibodies are required for the diagnosis because, according to the mutation, they can recognize the fibers which express dystrophin. For example, if the mutation is localized in the Rod-domain only using DYS2 and DYS3 will be possible to see the fibers expressing dystrophin.

In addition is so important to perform a biopsy and to use these three antibodies when the diagnosis is difficult. Since the *DMD* gene is very big, the mutation cannot be detected easily with standard molecular techniques meanwhile the absence of dystrophin is easily detected with IF, western blots or Immuno-Histo Chemistry (IHC). Sometimes the expression of dystrophin, according to the domain, helps the clinician to direct for in-depth research of the mutation in that portion of the gene (Dubowitz et al., 2021).

Characteristic of DMD muscle biopsies is the diffuse absence of dystrophin in the subsarcolemmal localization, except of few fibers that express dystrophin in affected muscles better defined as the so called 'revertant fibers' (Nix et al., 2020).

These fibers expressing dystrophin can be detected in some DMD cases and may result by the restoring of the reading frame occurring with alternative splicing and the antibodies may detect minor transcripts (Lu et al., 2000). The revertant fibers are usually lower in intensity compared to healthy muscles, and not the entire length of the revertant fiber always express dystrophin because only a focal part of the sarcolemma is revertant (Dubowitz et al., 2021). The accumulation and the persistence of revertant fibers increase with age in DMD patients (Fanin et al., 1995; Fanin et al., 1992).

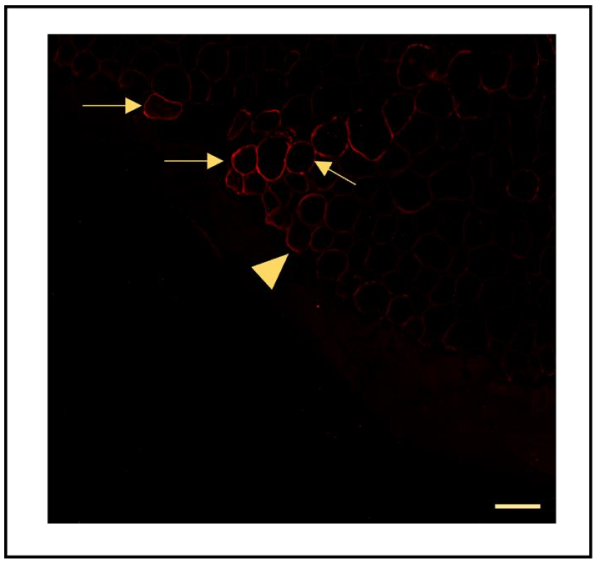

Figure 6 *Cluster of dystrophins revertant fibers in a DMD muscle. Revertant fibers (arrows) trace of dystrophin (yellow triangle) Ab: Dys1. Scale bar 50μm.*

Another marker used for the differential diagnosis of Duchenne muscular dystrophy on muscle biopsies is the Utrophin which is the homologue of dystrophin also know, in fact, as Dystrophin-related protein 1 (DRP-1). In physiological condition this protein is not expressed in the muscle, the expression remain confined in the vessels. However, when there is a lack of dystrophin, the utrophin is expressed in the subsarcolemmal face of the fiber. It is thought that this occurs because could be a mechanism of the fiber to mediate the absence of dystrophin (van der Bergen et al., 2015, Burton et al., 1999). So utrophin can be also used as a marker. No correlation was found between the utrophin levels expressed in the muscles and the clinical and histopathological phenotype (Taylor et al., 1997).

Moreover, recently has been observed that in DMD muscles compared to the healthy muscles there is a higher presence of laminin and spectrin (Aarstma-Rus et al., 2019).

The density of capillaries in DMD muscle biopsies was observed and seems to be increased. An increased number of capillaries has been found surrounding a myofiber, compared to control muscles. Moreover, the basement membrane of capillaries in DMD muscles biopsies is thicker compared to control muscles (Leinonen et al., 1979; Podkalicka et al., 2019). In other studies, the numbers of capillaries remain unvariated in DMD muscles comparing with controls (Desguerre et al., 2009).

1.2.5 Clinical features and diagnosis

Since DMD gene is located on chromosome Xp21, this disease typically affects only boys which present only one X chromosome, whereas female carriers are often asymptomatic. DMD affects 1 in 5000 boys worldwide (Starosta et al., 2021). First symptoms appear between 2-5 tears old such as progressive symmetrical weakness, proximal muscle and calf hypertrophy (Reitter et al., 1996). Proximal lower limb and truncal weakness is seen and is followed by upper limb and distal muscle weakness. DMD boys are not able to run and jump. The progression is very fast, untreated DMD boys become wheelchair around 12 years old (Bushby et al., 2012).

Some degrees of mental impairment are usual, about 20% of affected boys have an IQ less than 70; verbal IQ is more impaired than performance IQ. Neuropsychiatric disorders are also associated to DMD such as autism and obsessive-compulsive disorder (Hendriksen et al., 2008).

Orthopedic complications are frequent: scoliosis is present in all non-treated boys and progresses quickly after the loss of ambulation (Smith et al., 1999).

Lately cardiac and respiratory impairment are observed in DMD affected boys. Pneumonia compounded by cardiac involvement is the most frequent cause of death, which happens in non-treated patients during late teens or early 20s (Yiu et al., 2015).

Serum creatine kinase (CK) values are raised 50 to 200-fold above normal from birth in Duchenne muscular dystrophy. CK level is, in fact, a sensitive biomarker for early detection of DMD. Elevated CK level localizes the problem to the muscle and usually results in a referral to a neurologist or neuromuscular specialist for definitive diagnosis, treatment and genetic counselling (Ciafaloni et al., 2009).

For the diagnosis of DMD the most used tools are multiplex ligation-dependent probe amplification (MLPA) assay or comparative genome hybridization array, both are able to identify deletion and duplications. Other types of mutations can be detected using Next-generation-Sequencing (NGS). (Tian et al., 2019 ; Aartsma-Rus et al., 2015 ; Wang et al., 2014; Falzarano et al., 2015). Recently, whole exome sequencing (WES) is used to detect small mutations in DMD patients. Moreover it turned out to be an excellent method to identify female carriers of DMD (Zamani et al., 2022). Detecting *DMD* mutation with WES it allow also to discriminate patients candidates for specific kind of treatments such as Ataluren (Luce et al 2018). However, when the mutation is difficult to find with the canonical molecular methods and if the clinical diagnosis cannot be confirmed by genetic tests, the other only diagnostic method is to perform a biopsy. The muscle biopsy firstly said to the clinician if the dystrophin is expressed or not and the histological findings obtained by biopsies such as variations in fibre size, necrosis, invasion by macrophages replacement by fat and connective tissue help the clinician in concluding the diagnosis, giving precious information (Ciafaloni et al., 2009).

1.2.6 Therapeutic approaches

Unfortunately, there is still no treatment that slows the relentless progression of the disease and that rescues the chronic defect, so the affected males generally die of respiratory or cardiac problems by about age 20. The treatment commonly used to improve patients' life span (but only modestly its quality) regards the use of corticosteroids, mechanical ventilation, and surgery

(Falzarano et al., 2015). However, in the last decades, some interesting and promising therapeutic approaches were proposed.

1.2.6.1 Pharmacological therapy

The onset of muscle degeneration matches with the onset of muscle inflammation. Thus, inhibiting the immune response in dystrophic muscle can delay the progression of muscular dystrophy and prolong ambulation. For this reason, steroidal therapies such as prednisolone, prednisone or deflazacort, are commonly prescribed for DMD patients and so far, are the only pharmacological intervention to show efficacy in slowing the progression of the disease. However, they are associated with side effects such as gastrointestinal symptoms, metabolic and nutritional disorders, central and peripheral nervous system disturbances, and psychiatric disorders (Manning et al., 2015; Matthews et al., 2016).

Recently a new anti-inflammatory steroidal drug with a favorable safety profile was described, the vamolorone (Hoffman et al., 2019). Vamolorone efficacy is higher in DMD because it targets dual nuclear receptors in a manner that simultaneously treats cardiac disease, by acting as antagonist of Mineralcorticoids Receptor (MR) and chronic inflammation pathways by acting as an anti-inflammatory inhibiting NF-kb pathway (Heier et al., 2019). This drug appears to be better tolerated; boys treated with vamolorone showed less side-effects than a corticosteroids standard of care in DMD (Smith et al., 2020).

Fibrosis is one of the most deleterious pathological features of DMD. Therefore, approaches to counter extensive collagen deposition and enhanced expression of TGF-β are being studied. It was shown that an inhibitor of collagen synthesis – halofuginone improves skeletal and cardiac muscle function in *mdx* mice (Turgeman et al., 2008). The anticancer drug, tamoxifen, has been shown to ameliorate dystrophy progression in *mdx* mice, among others through inhibition of TGF-β (241) and is currently investigated in clinical trial (Nagy et al., 2019). A histon deacetylase inhibitor (HDAC) drug known as givinostat significantly reduce fibrosis in mdx mice (Consalvi et al., 2013). In biopsies collected from boys treated with givinostat was observed an amelioration of the phenotype such as a decreasing of fibrosis and necrosis, reduced tissue fatty replacement, increasing in fiber size. Overall, the drug was well tolerated (Bettica et al., 2016). Recently was seen that givinostat act on a mitochondrial level, promoting the biogenesis of mitochondrial as a metabolic remodeling agent (Giovarelli et al., 2021).

1.2.6.2 Gene therapy

Currently several gene therapy strategies are under investigation. This kind of treatment is based on the restoration of dystrophin expression including nonsense mutation read-through, exon skipping, and CRISPR (clustered regularly interspaced short palindromic repeats)/Cas9 (CRISPR-associated protein) method of gene editing (Łoboda et al., 2020).

One approach to restore dystrophin is the nonsense mutation read through. Usable in approximately 13% of affected boys carrying nonsense mutation. The used molecule for this approach is Ataluren (PTC124) which modulate the translational machinery and allow selective ribosomal readthrough of premature stop codon (PTC) during mRNA translation leading to the expression of a functional protein (Welch et al., 2007).

Another interesting approach aiming restoration of dystrophin protein is the exon skipping strategy. Exon skipping is considered one of the most promising gene editing approaches. It's based on the observation the in-frame mutation in BMD patients lead to production of a truncated but functional protein, so it focuses on restoring the reading frame of dystrophin mRNA using AONs (antisense oligonucleotide) (Aartsma-Rus et al., 2009). AONs are 15-30 nucleotides long fragments of RNA or DNA that specifically bind to and hide target exons from the splicing machinery. To protect short molecules of RNA/DNA from degradation by endo and exonucleases, AONs need to be chemically modified (Aartsma-Rus et al., 2010).

The first drug to treat DMD based on exon skipping technology is eteplirsen (PMO) which was conditionally approved by FDA in 2016. Eteplirsen is for patients carrying the mutation between exon 50 and 52, because induce exon 51 skipping, which are approximately 14% (Aartsma-Rus et al., 2017). Other molecules of the same family (PMO) are golodirsen and vitolarsen inducing the exon 53 skipping, both approved by FDA in 2020 (Heo et al., 2020; Roshmi et al., 2019). Exon skipping approach may be used to treat around 80% of patients. However, it would require usage of precisely designed sequence to treat each subgroup of patients, moreover the treatment shows to have limited efficacy and is long-life required administration (Charleston et al., 2018; Cirak et al., 2011).

A strategy that seems to be more efficacious and safer is the gene editing concerning CRISPR-Cas9 (clustered regularly interspaced short palindromic repeat/CRISPR- associated nuclease/helicase) system (Amoasii et al., 2018). This system couples a single guide RNAs (sgRNAs) and Cas9 protein – endonuclease which is able to cleave and correct DNA (Chemello

et al., 2020). Interestingly, it was shown that restoration of only 4-15% of dystrophin present in healthy counterparts can ameliorate dystrophic phenotype in mice (van Putten et al., 2014).

There are also trials aiming at the restoration of dystrophin expression by transfer of its full-length cDNA. Gene replacement is exerted by using recombinant Adenovirus-associated virus (AAV-9) vectors as a system of delivery, which displays preferential tropism for muscle tissue. However, the capacity of AAV vectors, a vehicle for gene therapy, is limited to ~5 kb (Harper et al., 2002).

Therefore, strategies leading to miniaturization of dystrophin expression cassettes have been established. This led to the development of mini- and micro-dystrophins constructs (Li et al., 2006; Ramos et al., 2019). Numerous studies performed so far showed different efficacy of such treatments, however, some of them revealed significant clinical improvement in treated patients (Mendell et al., 2020). Despite seems to be promising there are some limitations overcoming, because AAV is an immunogenic vector and patients may develop the cytotoxic T cell-mediated immune response against AAV and against mini and micro dystrophin (Mendell et al., 2010).

1.3 Duchenne animal models

To date there are more than 60 different models generated to better understand the mechanism of DMD pathogenesis, some of them highlight the main features and hallmark of the disease while others are more useful to test new therapeutic strategies. Non-mammalian and mammalian models have been developed, despite each of it has limitations these where helpful in providing precious information about the disease (McGreevy et al., 2015).

1.3.1 Non-mammalian models

The advantage of non-mammalian model is their physiologic simplicity which allow to better understand some mechanism, and the ease of genetic manipulation that gives us the potential to quickly create models and follow their development in a short period of time. Dystrophin has been seen to be a highly conserved gene, and its homologs has been found in vertebrates and invertebrates such as *Drosophila melanogaster, Caenorhabditis elegans* and *Zebrafish* (Collins et al., 2013).

The Drosophila melanogaster it is relevant because its DAGC contains the major components presents in the mammalian. Moreover, is cheap, very fast to generate with large number of progeny and is simple in the morphology. Drosophila is very useful to study degenerative muscle diseases because their muscles lack of stem cells allowing to differentiate phenotypes that result directly from degeneration from those that result from failure of regeneration (Kreipke et al., 2017). Drosophila was very useful to understand the molecular mechanisms behind Duchenne muscular dystrophy like the connection of DAGC and dystrophin (Plantiè et al., 2015). Several isoforms of drosophila's dystrophin are homologous to the human's dystrophin. Full-length dystrophin deletion mutants of drosophila showed an age-dependent muscle degeneration and a loss of muscle integrity (Potikanond et al., 2018). In later stages has been seen a developing of cardiac impairment in Dys mutants flyes (Plantiè et al., 2015).

Caenorhabditis elegans. Are high-throughput models due to their speed in reproduction and easy to genetically manipulate. The affected nematodes have a widespread degeneration of the muscle, but their muscles are completely different from the mammalian ones, because their fibers do not fuse and do not regenerate. Despite this, mutations in their homologue *dys-1* lead to progressive muscle degeneration. Indeed, these models are used to test molecules that act against degeneration (Gaud et al., 2004). Has also been used to study calcium channel signaling, demonstrating that dystrophin plays an important role in the transmission of muscle tension and membrane stiffness (Zhan et al., 2014).

Danio rerio better known as *Zebrafish* have abundant skeletal muscle and express orthologues of most DAGC proteins with a similar localization as in mammals, and more important in human. (Berger et al., 2010). Dystrophin-deficient zebrafish develop the main hallmarks of the disease such as degeneration/regeneration, necrosis, inflammation; fibrosis, variation in fiber size and activation of SCs. They have been used to study exon skipping therapies. With these studies has been demonstrated that 20-30% of normal dystrophin could be enough to rescue a severe phenotype (Berger et al., 2012).

1.3.2 Rodent models

1.3.2.1 The *Mdx* mouse

The *mdx* mouse is the classical biochemical and genetic mouse model of DMD. It was discovered in 1984 in a colony of C57BL/10ScSn mice based on the increased levels of CK in

serum and histological evidence of myopathy. The mutation occurs spontaneously, it is a point mutation (C toT) in exon 23 of dystrophin gene resulting in a premature stop codon, thus mdx mouse has no detectable dystrophin (Bulfield et al., 1984). This model is well characterized, and similarly to DMD patients exhibit fibrosis, massive inflammation and necrosis, variability in fiber size, and cycle of degeneration and regeneration. However, the phenotype is much milder compared to DMD patient's phenotype (Stedman et al., 1991). In mdx models the progression of the disease is not like the one of the DMD patients despite the lack of dystrophin. More importantly mdx mice do not develop cardiac failure, show the first signs of fibrosis in heart appear at 17 months old, and the most affected muscle is the diaphragm (Quinlan et al., 2004). Moreover, the lifespan of these mice is decreased only of a 25% vs 75% decrease in human (McGreevy et al., 2015). From another line of mice C57BL/10 which has a common origin with C57BL/6 line, were generated alternative genetic variants of mdx models (Im et al., 1996). The mdx^{2cv} has a point mutation in the intron 42, on a splice site acceptor, while mdx^{3cv} carry a point mutation in the splice site acceptor of intron 65, in this model also other isoform of dystrophin are impaired in fact shows cognitive impairment and ocular problems (Li et al., 2008; Vaillend et al., 1999). Mdx^{4cv} has a point mutation in exon 53 which lead to a premature stop codon, and mdx^{5cv} has a point mutation as well, resulting in a new splice site in exon 10, both of these models show a mild phenotype, and compared to mdx they exhibit more revertant dystrophin fibers, (see above) (Danko et al., 1992). Other genetic models has been developed. One is the mouse with mutations affecting other isoforms of dystrophin such as mdx52 (deletion of exon 52) Dmd-null and $mdx^{\beta geo}$ their use was important to better understand the other dystrophin isoforms (Araki et al., 1997; Echigoya et al., 2013; Wertz et al., 1998).

1.3.2.2 Double knockout mice (dko)

Several double knockout mice have been generated trying to humanize the phenotype (McGreevy et al., 2015). Has been shown that the expression of utrophin (Dystrophin homologue) in mdx skeletal muscles is significantly elevated, which could explain the mild phenotype, indeed mice lacking both dystrophin and utrophin were created by crossing *mdx* and *utrophin*-knockout mice (Deconinck et al., 1997). The protective role of *utrophin* in *mdx* mice is revealed in these mice and phenotypically they are the most comparable to the human DMD condition, the symptoms start very early and progress over time. These animals also develop cardiopathy and cardiac fibrosis at the age of 8-10 weeks and die prematurely because of respiratory failure at around 20 weeks of age (Grady et al., 1997; Chun et al., 2012). Another

model developed for study the compensatory effects to the absence of dystrophin is the dko for dystrophin and integrin. Confirming that integrin may partially compensate the muscle degeneration since this model die very early (24-27 days after birth) of cardiorespiratory failure (Guo et al., 2006). To study regeneration and differentiation of the skeletal muscle in DMD a model lacking dystrophin and MyoD was developed (Megeney et al., 1999). The interaction between cytoskeleton and ECM were studied in dko mice for laminin and desmin (McGreevy et al., 2015). Although these models were useful to better understand many different aspects of the disease, the carried mutation that does not occur in nature, making the data difficult to compare and to interpretate.

A very interesting model has been generated based on the observation that in DMD patients the cardiomyocytes have shorter telomeres, approximately 50% shorter than healthy subjects, suggesting that in DMD there is a premature aging of some muscles. Since mice have longer telomeres than humans this can be the reason why they present a milder phenotype (Yucel et al., 2018). Therefore, mdx mice with shorter telomeres has been generated (mdx^{4cv}/mTG^{G2}), and indeed these animals present a more severe phenotype (Sacco et al., 2010).

Mice models are the most widely used animals because of their many advantages, such as cost, small size, easy to handle and maintain, easy to breed. However, they have limitations, the most important is the partial disease modelization/recapitulation.

1.3.2.3 Rat models

Two different rat model have been created in two different laboratories in 2014. One was generated with CRISPR/Cas to induce deletion either in exon 3 e/o 16 (Nakamura et al., 2014), the other was generated utilizing transcription activator-like effector nucleases (TALEN) to induce a point mutation which result in stop codon in exon 23, as was previously found in mouse (Larcher et al., 2014). These animals show a phenotype consistent with DMD disease displaying myonecrosis, cicle of degeneration and regeneration, fatty infiltration, progressive muscle weakness (Nakamura et al., 2014; Leiden et al., 2014). Moreover, these models develop cardiac impairment with fibrosis and dilated cardiomyopathy, for this reason they are considered to be a better model than mdx. (Larcher et al., 2014; Camacho et al., 2016). Despite the DMD-like phenotype, the models developed by Nakamura et al exhibited too much variability among individuals, with large variation in severity, to limit its usefulness in translational research (Nakamura et al., 2014).

A new rat model of DMD with a deletion of exon 52, has been recently developed in our lab (Taglietti et al., submitted). The rat was developed by injecting the Cas9/sgRNA constructs in Sprague dawley zygotes. These rats show a complete absence of dystrophin with rare revertant fibers and an absence of β-dystroglycan. Muscle atrophy and decreased muscle strength was observed. High level of CK has been measured in an early time point and then decreased. The respiratory function was impaired, and the diaphragm is severely affected from 3-weeks old, showing wide areas of fibrotic deposition, necrosis, inflammatory infiltrates, fiber size heterogeneity exacerbating with age. The diaphragm is the most affected organ; however, the severity of the phenotype was showed also in the limb muscles where has been observed atrophy of the fibers and deposition of fibrotic tissue increasing over time. Fat tissue infiltration, high presence of inflammatory cells and significant heterogeneity of fiber size in limb muscles has been also observed, confirming the severity of the phenotype and the widely compromised skeletal muscle.

The heart start to be compromised at 3-months old, showing fibrosis and ECG changes worsening over time. The lifespan of these animals was dramatic reduced, the survival was within 10 to 14 months of life (Taglietti et al., submitted).

1.3.3 Mammalian large models

Characterization and studies on larger DMD model could contribute to the advancement in better understand the pathology. Large model may bridge the gap between human and mice and might greatly contribute to the developing of new therapies strategy.

1.3.3.1 Golden Retriever Muscular Dystrophy (GRMD)

To date around 20 canine muscular dystrophy dogs have been described; Point mutations in dystrophin gene have been found in Cavalier King, Charles spaniel, Golden retriever , Rottweiler and others, which most of them are case reports (McGreevy et al., 2015). The GRMDs currently are the most widely used colonies, described by Cooper and Kornegay, they harbor a splice site mutation in intron 6 of *DMD* gene which occurs in the skipping of exon 7 and a stop codon in exon 8 (Cooper et al., 1988; Kornegay et al., 1988; Sharp et al., 1978). These dogs recapitulate a similar disease progression to that of DMD patients, with intolerance to exercise at 2-3 months, muscle weakness and atrophy, abnormal weight, dysphagia, fibrosis, cardiomyopathy and reduced lifespan (Nakamura et al., 2011). Although the mutation for all the dogs is the same, a variation in the phenotype has been described; this variability can be due

to genetic modifiers such as Osteopontin (SPP1) and Latent Transforming Growth Factor β Binding Protein 4 (LTBP4) (Bello et al., 2019; Kornegay et al., 2017). Moreover, the phenotype of the dogs remains consistent with the phenotype of the patients for a period of around 6-10 months, and then diverge due to the stabilization of diseases in dogs (Kornegay et al 2017). Canine models are useful in pre-clinical research in the developing on new treatment strategies, in particular gene therapies and also to optimize approaches for viral delivery (Amoasii et al., 2018; Kornegay et al., 2010; Le Guiner et al., 2014; Le Guiner et al., 2017).

1.3.3.2 Other models

Interestingly, other large animal models have been founded. Dystrophic cats with large deletions on the promoter of the full-length dystrophin has been identified (Carpenter et al., 1989). These cats show lack of dystrophin, progressive muscle degeneration and regeneration, hypertrophy of the tongue, neck and shoulders, megaesophagus and kidney failure (Nakamura et al., 2001). These cats are not used in research due to their short lifespan and to the different phenotype (Selsby et al., 2015).

Pig genome has been shown to be three more time similar to human than is the mouse one (Wernersson et al., 2013), moreover the anatomical size of pigs is more comparable with humans, in particular the anatomy and the physiology of the heart (Crick et al., 1998); for these reasons porcine models have been also generated. Leading a deletion of exon 52 they show progressive muscle weakness, cardiac arrythmia and consequently shorter lifespan (Klymiuk et al., 2013; Moretti et al., 2020). These models are used to study exon-skipping drugs, and other therapy approaches (Klymiuk et al., 2016). Recently has been discovered that gene editing mitigates the phenotype of porcine models (Moretti et al., 2020). However, these models are difficult to breed and maintain (Klymiuk et al., 2016).

Recently a DMD monkey model was also generated with CRISPR/Cas9 in rhesus monkey. The Cas9 vectors have been designed to target exon 4 and/or exon 46 producing monkey models lacking dystrophin, however these models are still not well characterized (Chen et al., 2015).

2. AIM OF THE STUDY

To perform a comprehensive comparative and molecular phenotyping of DMD Human biopsies, mdx mice biopsies and R-DMDdel52 samples and to provide a unique longitudinal pathophysiological analysis of DMD disease progression. Indeed, comparative analysis will be performed between human, mdx and R-DMDdel52 samples to investigate the progression of DMD in patients and in our model.

We will characterize the principal hallmarks of Duchenne muscular dystrophy in human biopsies, as inflammation, fibrosis, muscle regeneration capacity and fatty infiltration. We will also characterize muscle stem cell behaviour in human biopsies and models samples.

The expected results may help to obtain histopathological outcome measures to be taken in consideration for the development of future clinical trial with different therapeutic approaches and may also be useful to draw up histopathological guidelines necessary for the follow up.

The ultimate goal of this project is to better understand the stem-cell-driven muscle regeneration, that is lost in context of DMD, and from the application of this knowledge on innovative stem-cell-targeted therapies.

3. MATERIALS AND METHODS

3.1 Patients

All human samples were obtained from patients who had signed informed consent form in accordance with the guidelines of the Ethics Committee of the Istituto Giannina Gaslini (Genova, Italy), and of the Henry Mondor Hospital (Creteil, France) including experimental protocols for muscle biopsies.

Muscular biopsies were collected from 17 boys with genetically confirmed diagnosis of DMD, at age range from 0 to 8 years (Table1). Additionally, muscular biopsies were collected from 3 boys with genetically confirmed BMD, at the age of 3 to 16 years (Table 2). Twenty-four 24 histologically normal muscle tissues were considered as control (Table 3).

The muscles were collected and frozen in isopentane, cooled by liquid nitrogen and stored at -80° until processed. Then, tissues were sectioned at 7 μm of thickness on Super Frost Plus slides (Thermo scientific, 10149870) using cryostat (Leica CM3050S; Leica Biosystems), air-dried, and kept at -80°C for further staining.

Table 1 Clinical data of DMD patients

N°id Biopsy	Age at biopsy	Sex	Diagnosis	Muscle	Mutation	Serum CK at biopsy	First clinical sign (years)	Loss of ambulation (years)	Cognitive impairment	Steroids Treatment
P2405	2,6 years	M	DMD	Quadriceps	del 20-44	28206	30 months	11	yes	yes
P2419	10 months	M	DMD	Quadriceps	na	10117	X	X	X	na
P2454	6 years	M	DMD	Quadriceps	del 12-16	26430	4 years	13	no	yes
P2456	11 months	M	DMD	Quadriceps	del 51-54	49450	3 years	walking	no	yes
P2475	5,10 years	M	DMD	Quadriceps	del 49-50	10386	18 months	walking	yes	yes
P2492	3 months	M	DMD	Quadriceps	del 48-54	11681	3 years	X	no	yes
P2493	18 months	M	DMD	Quadriceps	del 48-52	20538	2 years	walking	yes	yes
P2496	5 years	M	DMD	Quadriceps	del 46-47	21458	4 years	walking	no	yes
P2500	9 years	M	DMD	Quadriceps	p.Ile585Phefs*22	15196	7 years	walking	no	no
P2512	6 years	M	DMD	Quadriceps	del 44	29660	5 years	10	no	yes
P2545	7 years	M	DMD	Quadriceps	del 10-43	14286	4 years	walking	no	yes
P2583	3,6 years	M	DMD	Quadriceps	c.9953_9954delAG, p.Glu3318Valfs*15	18767	3 years	walking	no	yes
P2589	3 years	M	DMD	Quadriceps	dup 50	14768	3 years	walking	no	yes
P2619	8 years	M	DMD	Quadriceps	del 49-52	7392	7 years	walking	yes	no
P2639	4 years	M	DMD	Quadriceps	del 44	28830	2 years	X	X	X
P744193	8	M	DMD	Deltoid	c.3427C>T, p.Gln1143*	9400	retard moteur 3	no	no	X
P713567	8	M	DMD	Deltoid	dup2	7395	retard moteur 3	no	no	X

Table 2 *Clinical data of Beckers patients*

N°id Biopsy	Age at biopsy	Sex	Diagnosis	Muscle	Mutation	Serum CK at biopsy	First clinical sign (years)	Loss of ambulation (years)	Cognitive impairment	Steroids Treatment
P2468	3,1 years	M	BMD	Quadriceps	del 52-53	4103	5 years	n	yes	no
P758702	12	M	BMD	Deltoid	c.5154+1G>A	1000	elevation fortuite des CK /intolérence effort	n	no	X
P760934	16	M	BMD	Deltoid	del45-47	5354	Becker, intolérance effort élévation CPK 15y	n	no	X

Table 3 *Clinical data of control patients*

N°id Biopsy	Age at biopsy	Sex	Diagnosis
P2549	2 years	F	encefalopathy
P2585	6 years	M	congenital myasthenia
P2613	14 years	M	ataxia
P2631	1 years	M	encefalopathy
P2652	5 years	F	krabbe
P2657	9 years	F	arthrogryposis
P2721	5 years	F	laxity
P2771	1 years	M	encefalopathy
P2772	1 years	F	Ondine syndrome
P763295	1 years	M	myop cong NEB
P769250	3 years	M	-
P771543	2 years	M	-
P564811	9 years	F	-
P639789	8 years	M	myop cong ryr1
P640321	7 years	M	-
P754733	5 years	M	RPM délétion de 11 Mb sur le chromosome 12 (12q21.1q.21.3)
P773335	7 years	M	-
P769973	7 years	M	-
P567000	1 years	M	RPM mutation de novo du gène KAT6A
P574835	1 years	F	sd HHE décédée
P550400	4 years	F	retard acquisitions atrophie cérébelleuse
P601121	5 years	M	-
P633654	5 years	M	deficit des ceintures
P639789	8 years	M	-

3.2 Animal models

All animal procedures and experiments were performed in accordance with national and European legislation regarding the *in vivo* research and with the *Directive of the European Parliament and of the Council 2010/63/EU of 22 September 2010 on protection of animals used for scientific purposes*. Animals were handled and protocols were approved by ethics committee at the French Ministry (APAFIS #25606-202005311746599).

As a rat model, Sprague Dawley rats with the deletion of exon 52 within the dystrophin gene (*RatDMDdel52*), developed in our lab (Taglietti et al submitted) and control rats (WT) at different time points: 3 – 6 – 12 months old were used. *Mdx*^{4cv} mice and control mice (WT) at C57BL background, at different time points 2 – 6 – 12 – 17 – 20 months old, were analyzed. Animals were kept in specific-pathogen-free (SPF) facility with water and food available *ad libitum* under controlled temperature (around 23°C), humidity (around 55±10%) and 12h light 12h dark cycles.

As the dystrophin gene is located on chromosome X, only males were used for the experiments. Genotyping of animals was performed by polymerase chain reaction (PCR) on DNA isolated from tails or ears.

The euthanasia procedure was performed in accordance with the national and European community guidelines. Rats were anaesthetized by injection with Euthasol which is a pentobarbital based lethal solution at concentration of 100 µl per 100g and sacrificed by cardiac puncture, while mice were sacrificed by cervical dislocation.

3.3 Histopathological analyses

For the histopathological characterization of muscles frozen sections of 7 µm was used. Tibialis anterior (TA) for rats and mice and Quadriceps or Deltoids for human muscles biopsies were analyzed.

3.3.1 Hematoxilin & eosin

Slides were defrosted for around 20 min at room temperature (RT). The slides were dipped in Mayer's hematoxylin (Sigma-Aldrich) for 3 min, rinse in deionized water, and dipped in lithium carbonate solution for 3 seconds (sec), followed by the incubation in eosin for 30 sec. Then slides were washed in distilled water and dehydrated through increasing concentration of ethanol (EtOH): 50%, 70%, 95%, 100%. In the last step, slides were mounted with Eurokitt after being dipped in xylene. Images were taken with an Axio microscope with brightfield light.

3.3.2 Sirius Red

Sirius red staining was used to calculate the percentage of fibrotic area in muscle tissue. Slides were defrosted for 20 min at RT and dipped in 90% EtOH for 2 min prior to beginning the staining. The samples were incubated for 25 min in picro-sirius red solution (Sigma-Aldrich) and then extensively washed in water and dehydrated in 100% EtOH. After the clear in xylene, slides were mounted with Eurokitt. For calculate the percentage of fibrotic area, a Macro was used (Macro-Chazaud_Collagen). Images were taken with Axio microscope. with brightfield light and with a fluorescent light to calculate the fibrotic area with the macro.

3.3.3 Bodipy

The fat tissue infiltration has been calculated with the bodipy staining which stains the adipocytes present between the fibers. Slides were defrosted at RT for 20 min and hydrates in PBS1X for 5 min. Permeabilization was done in 0,5% Triton for 5 min and then blocked in 10% bovine serum albumin (BSA) for 30 min. After washes in PBS 1X, slides were incubated with rabbit anti-laminin (1:800; L9393Sigma-Aldrich) primary antibody for 1 hour (h) at 37°C. After 3x5' washes in 1X PBS the slides were incubated with goat anti-rabbit Alexa Fluor 555 secondary antibody (1:500) and with bodipy (1:500; Invitrogen D3922) for 45 min at 37°C degrees. Nuclei were stained with Hoechst (Sigma-Aldrich B2261), followed by mounting the slides with fluorescence mounting medium (Dako). The percentage of fat infiltration area was calculated with the Macro (Macro-Chazaud_Collagen) and normalized on the total area of the section. The bodipy is calculated as the percentage of area stained in green (Adipose tissue) on the total area of the muscle section.

3.3.4 Immunofluorescence stainings

For the evaluation of the regenerating fibers (positive for embryonic myosin heavy chain, eMHC) and dystrophin, sections were defrosted, hydrated, permeabilized with 0,5% Triton, and blocked in 10% BSA for 30 min at RT. Subsequently, primary antibodies: mouse anti-eMHC (1:400; clone: F1.652; sc-53091, Santa Cruz), mouse anti-dystrophin (1:20, DYS2-CE; DYS1-CE; DYS3-CE; Leica), rabbit anti-laminin (1:400; Sigma-Aldrich, L9393) were added to 1%BSA and applied for overnight (O/N) incubation at 4°C. Next, after repetitive washes, slides were incubated with Alexa Fluor secondary antibodies 1:500. Nuclei were stained with Hoechst (Sigma-Aldrich B2261), followed by mounting the slides with fluorescence mounting medium

(Dako). Images were acquired using a fluorescent microscope and analysed in *ImageJ* software. The number of the eMHC and dystrophin positive fibers was counted on the whole muscle section and normalized to the total number of fibers and then expressed in percentage.

For the analysis on muscle satellite cells (MuSCs), slides were defrosted 20 mins at RT, rehydrated for 5 min in PBS 1X and then fixed with 4% PFA in PBS 1X for 10 min at 4°C. After washes in PBS 1X, slides were placed in cold acetone: methanol (1:1) solution for 6 min at -20°C and then incubated with blocking solution - 10% BSA for 1h RT. Primary antibodies were added to 1% BSA and incubated O/N) at 4°C. The following primary antibodies were used: mouse anti-Pax7 (1:100 Santa Cruz Biotechnology, sc-81648), rabbit anti-ki67 (Abcam, sp6 ab16667), mouse anti-p16 (Abcam Anti-CDKN2A/p16INK4a, Ab108349), p21 (Thermofisher, bs-10129R) and γH2AX (Abcam, ab11174). After repetitive washes, slides were incubated with Alexa fluor secondary antibodies for 45min at 37°C. Laminin staining was performed after the secondary antibody incubation, for 1h at 37°C using a conjugated antibody (NB300-144AF647). Nuclei were counterstained with Hoechst (Sigma-Aldrich, B2261) followed by mounting the slides with fluorescence mounting medium (Dako). Images were acquired using a LSM800 confocal and analysed in *ImageJ* software. The number of Pax7 positive cells and the double positive ($Pax7^+$-$P16^+$ for example) was counted in at least ten acquisition per sample and normalized to total amount of fibers and was estimated by counting the colocalization of $Pax7^+$ with other markers and nuclei.

The inflammatory cells were stained with CD45 (CD45 positive) marker which stains all the inflammatory cells, calculated manually and normalized on the total area of the section expressed in mm^2. To check the number of capillaries (CD31 and isolectine positive), and the number of fibro-adipogenic progenitors (FAPs, PDGFRα positive cells), slides were defrosted for 20 min at RT and rehydrated for 5 min in PBS then were fixed in 4% PFA 1X for 10 min at 4°C. After washes sections were permeabilized with 0,5% Triton and blocked with 10% BSA for 30 min at RT. Mouse anti-PDFRA (1:100 Invitrogen PA5-16571), rat anti-CD31 (1:100 Dako JC70A) for mice and humans and mouse anti-Isolectine (Alexa647 I32450) for rats. CD31 and isolectin are used to highlight endothelial cells allowing the counting the number of capillaries. Only the vessels with a caliber less than 5μm large were considered capillaries and normalized on the area of the section. CD45 (BD biosciences 555843) for rats and Humans and (Novus NB110-93609) for mice, were incubated O/N at 4°C. After repetitive washes, slides were incubated with Alexa fluor secondary antibodies for 45min at 37°C. Nuclei were

counterstained with Hoechst (Sigma-Aldrich, B2261) followed by mounting the slides with fluorescence mounting medium (Dako). Images were acquired using a LSM800 confocal and analyzed in *ImageJ* software. CD45 and PDGFRA positive cells were counted in at least 10 acquisition and normalized to the area of tissue; CD31 and Isolectine were used to count the capillaries. Results were normalized to total number of fibers.

Cross-sectional area (CSA) and centrally nucleated fibers were counted based on immunofluorescent staining of laminin and Hoechst described above. Centrally nucleated fibers were manually counted and CSA of fibers as well as the mean fiber area was evaluated with a Macro developed in Relaix Lab Université Paris-est (UPEC).

3.4 Functional studies

3.4.1 Treadmill test

To assess muscle functionality and performance the treadmill test was performed by 8 degrees downhill run following acclimatization period of 5 days from 0 speed in day 1 and increasing the speed during the following days. Before the test mice were warmed up for 3 minutes at 5 m/min. For the exhaustion treadmill test, mice ran on the treadmill starting from a speed of 8 m/min for 2 minutes, 11 m/min for 2 minutes, 14 m/min for 2 minutes and the speed was increased every two minutes of 3m/min to a final speed of 35 m/min. The test was ended when animals meet the criterion for exhaustion defined by the incapability of the mice to remain on the treadmill belt despite stimulation by electrical padding of gentle touching. Treadmill was performed on 20-months-old mice and 6-months-old rats.

For rats a similar protocol was used, with acclimatation of 5 days and the exhaustion protocol was followed as previously described. Rats used for performing these experiments were 6 months old rats 4DMD and 2WT.

Treadmill experiments were performed using the Exter-3/6 treadmill (Columbus Instruments).

3.4.2 Forelimb grip strength test

Forelimb grip strength was assessed using a grip strength meter (GSM) with a straight pull bar according to the published protocols with modifications (Aartsma-Rus A et al 2014). Briefly,

the animals were gently held by the tail allowing them to grasp the grid using forelimbs. Afterward, mice and rats were moved horizontally toward the bar and pulled back until the grip was released. The measurements were repeated 5 times with a one-minute break in between. The results were calculated as an average from 5 measurements, normalized to body weight, and expressed as N/kg BW. Mice and rats used for these experiments were the same used for the treadmill.

3.4.3 Whole body plethysmography

Whole body plethysmography was used to assess respiratory flow in unrestrained unanesthetized mice and rats, thus allowing us to assess the activity of the diaphragm and how much it is affected, as previously described with modifications (Gosselin et al 2003). Animals (8mdx, 4 C57WT 20 months old mice and 4RDMDdel52 and 5WT 6 months old rats) were introduced into a "free moving" plethysmograph chamber with constant temperature (22± 2 C) and humidity (50 ± 10%), but different volume for mice (around 450 mL) and rats (around 650 mL). The device was calibrated according to manufacturer instructions prior to all data collection installments. Following acclimatation and settling period (around 10 min), a 20 min were recorded; baseline recording was performed in normoxia. Results were analyzed using emka iOX.2 software (Emka Techonologies, Paris)

Respiratory rate (RR), tidal volume (TV), peak inspiratory flow (PIF), minute volume (MV), and peak expiratory flow (PEF), expiratory time (Te), relaxation time (RT), were recorded and analyzed. Then average values were calculated around one per minute for each serial 10 min. Bronchoconstriction was estimated by the Enhanced Respiratory Pause (Penh) index calculated by the formula Penh = (Te/RT) PEF/PIF. RR, TV Te were normalized to body mass (g).

All the functional experiments were performed in a semi-dark room around 6 PM.

3.5 Statistical analysis

Data are presented as mean ± SD and analyzed with the unpaired two-tailed Student's *t*-test to determine differences between two groups. Correlation tests were done using Pearson coefficient of correlation. When comparing two groups with non-normal distribution, Mann-

Whitney test was used. Results were considered statistically significant at p value ≤ 0,05*. GraphPad Prism 9.0 was used for graphs and statistical analysis

4. RESULTS

4.1Histopathological markers

4.1.1 Fibrosis, internalized nuclei, fiber size and morphology

The DMD patients has been divided in four groups according to age, the percentage of centrally nucleated fibers was 9,43 ±5,72 in DMD and 3,16 ±0,90 in controls (CTR) at 1-2 years old with no statistically significant difference between CTR and DMD p=0,3; 8,74 ±4,15 in DMD patients and 0,00 ±0,00 in CTR at 3-4 years old and no statistically significant differences p=0,53; 12,70 ±4,03 in DMD patients and 0,18 ±0,13 in CTR at 5-6 years old and this two group were different p=0,02 * ; 9,86 ±3,23 in DMD and 0,00 ±0,00 in controls patients with more than 7 years old with differences between the two groups p=0,02* (Fig 10 D). The number of fibers with internalized nuclei does not follow a trend over time, with a constant amount.

In BMD patients, the average of the percentage of fibers with internalized nuclei was 7,43 ±4,44 compared to the controls in which was 0,00 ±0,00 but no statistically significance difference was found p=0,16 (Fig 7 D).

In order to evaluate fibrotic changes over time Sirius red staining has been performed on *quadriceps* of patients and controls. The red stained area represents the proportion of collagen which indicates fibrosis (Fig 7 A)

At 1-2 years old the average of the percentage of fibrotic area was 22,65 ±4,05 in CTR and 32,74 ±2,28 in DMDs with no statistically significant difference p=0,055; at 3-4 years old the percentage of fibrotic area was 11,31 ±3,61 in CTR and 30,27 ±2,91 in DMDs patients with a significative difference p=0,015*; in 5-6 years old patients was 25,28 ±1,06 compared with the controls 14,20 ±2,07 and the difference was significant p=0;0032 **; finally, in patients and controls with more than 7 years old was 32,69 ±2,44 and 10,00 ±1,42 respectively and p<0,0001**** (Fig 7 D). In Becker patients the percentage of fibrosis was less than DMDs patients but was also different compared to controls, BMDs 19,94 ±5 and CTR 7,10 ±0,37 p=0,03* (Fig 7 E).

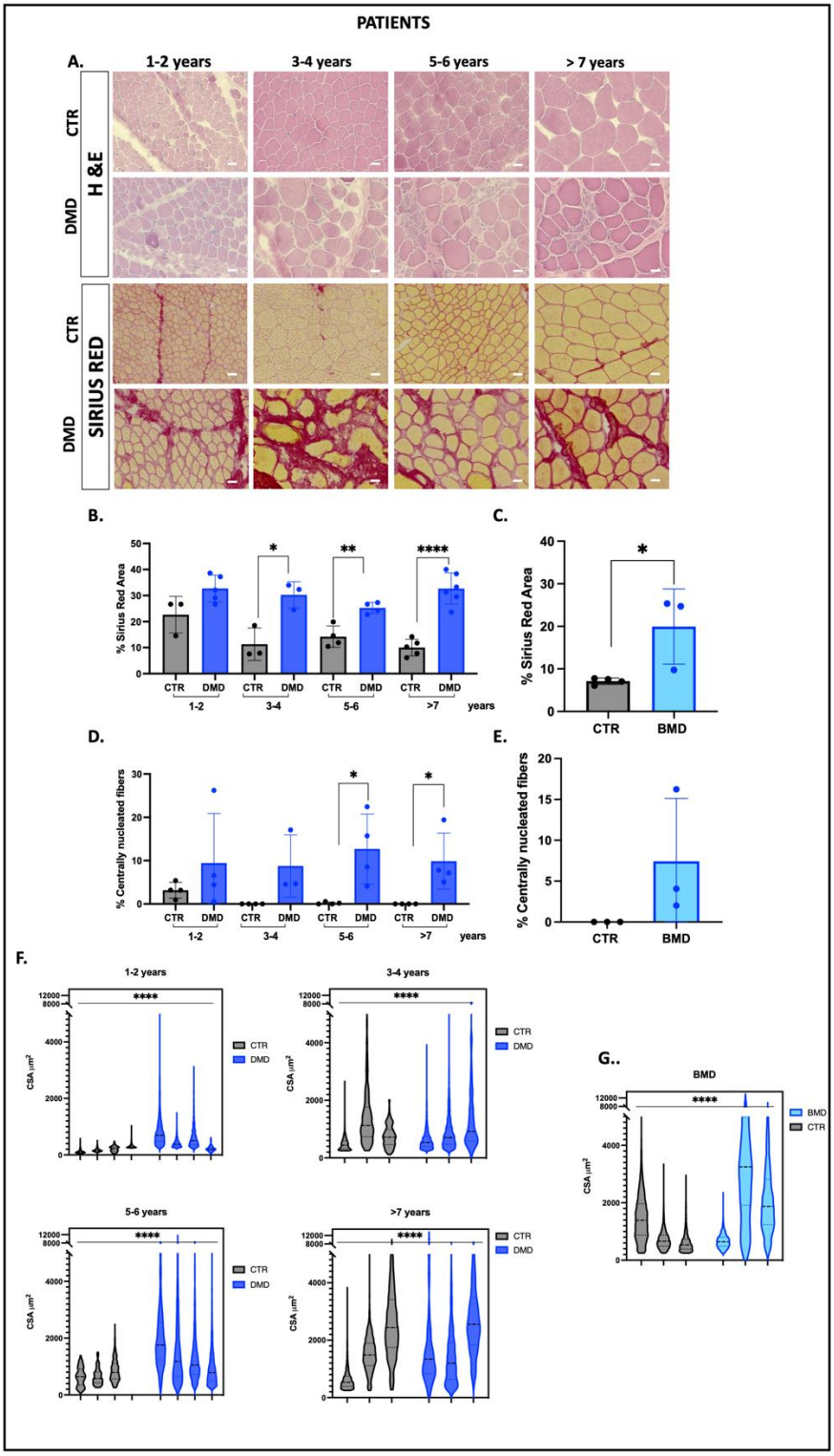

Figure 7 *Dystrophic phenotype of Human DMD and BMD Patients quadriceps compared to age matched histologically normal controls. (A) H&E and Sirius red-stained transverse section of quadriceps biopsies. The scale bar is 20µm. (B) Quantification of Sirius Red staining in DMD patients and controls quadriceps divided in four groups according to age. (C) Quantification of Sirius red area in Becker patients (BMD) and age matched controls. (D) Percentage of centrally nucleated fibers on the total amount of fibers in DMD patients and controls*

*quadriceps divided in four groups according to age. (E) Percentage of centrally nucleated fibers on the total amount of fibers in BMD patients and age matched controls. The data are presented as mean ± SEM; * p≤0,05 Student's t-test (B-C-D-E). (G) CSA Cross Sectional Area of fibers expressed in micrometers square. Violin plots showing the fibers caliber of the quadriceps of each patient. The data are presented as median and quartiles of the total amount of the fibers.*

It was not observed a proper increase in the percentage of fibrotic area in DMDs patients over time (Fig 7 D).

In Fig 7 F. is showed the cross-sectional area of the fibers, indicating their size in the *quadriceps* of patients at different time points. In an early stage the fibers of the controls are much more smaller than DMDs fibers which are more heterogeneous p<0,0001****. In older time points is observed that an important part of the fibers is smaller compared to controls, but there is also a small number of very big fibers, the fiber size heterogeneity is higher in DMDs patients compared to controls, and for all the time points the differences were statistically significant with a p value p<0,0001**** (Fig 7 F). Regarding BMDs fiber size there was more variable among individuals, in one patient the fiber were heterogenous, in another one normal fibers were presents, in any case the difference between BMDs and controls was significant p<0,0001****(Fig 7 G).

The internalized nuclei, the fibrotic tissue, the morphology of fiber size and inflammation are showed in the H&E staining at different time points in Fig 7 A.

The percentage of centrally nucleated fibers, indicating the number of regenerative fibers was 27,36 ±1,86 at 3 months, 30,43 ±1,36 at 6 months 21,97 ±1,42 at 12 months old, for the DMD rats and 1,013 ±0,79 for 3 months old WT, 0,00 ± 0,00 for 6 months old WT and 0,00 ± 0,00 for 12 months WT. The differences between WT and DMD rats were statistically significant in all the time points with a p value of p=0,0001 *** at 2 and 12 months old and p<0,0001**** at 6 months old (Fig 8 B.). The number of fibers with internalized nuclei counting did not follow a trend, it remains high with aging in DMD rats.

In order to evaluate fibrotic changes over time Sirius red staining has been performed on *Tibialis Anterior* muscles, the red stained area represents the proportion of collagen which indicates fibrosis (Fig 8 A). At 3 months old the average of the percentage of fibrotic area was 4,16 ±0,22 in WT rats and 8,28 ±0,69 in DMD rats and the significance was p=0,0073**; at 6 months old 4,41 ±0,64 in WT rats and 10,17 ±0,65 in DMD rats p=0,0033**; at 12 months old 9,166 ±0,35 in WT rats and 23,80 ±0,046 in DMD rats with a significance of p<0,0001****(Fig 8 C). The percentage of fibrotic area increases over time in dystrophic rats (Fig 8 C).

In Fig 8 D. is showed the cross-sectional area of the fibers, indicating the size of them in the *Tibialis Anterior* at different time points. Since 3 months old there are significative differences between DMD and WT rats fibers size in which the size of the DMD are much more smaller and less heterogeneous than WT and is seen the same in older animals the p value for all of them 3,6,12 months old is p<0,0001****(Fig 8 D).

The internalized nuclei, the fibrotic tissue, the morphology of fiber size, inflammation and necrosis are showed in the H&E staining at different time points in Fig 8 A.

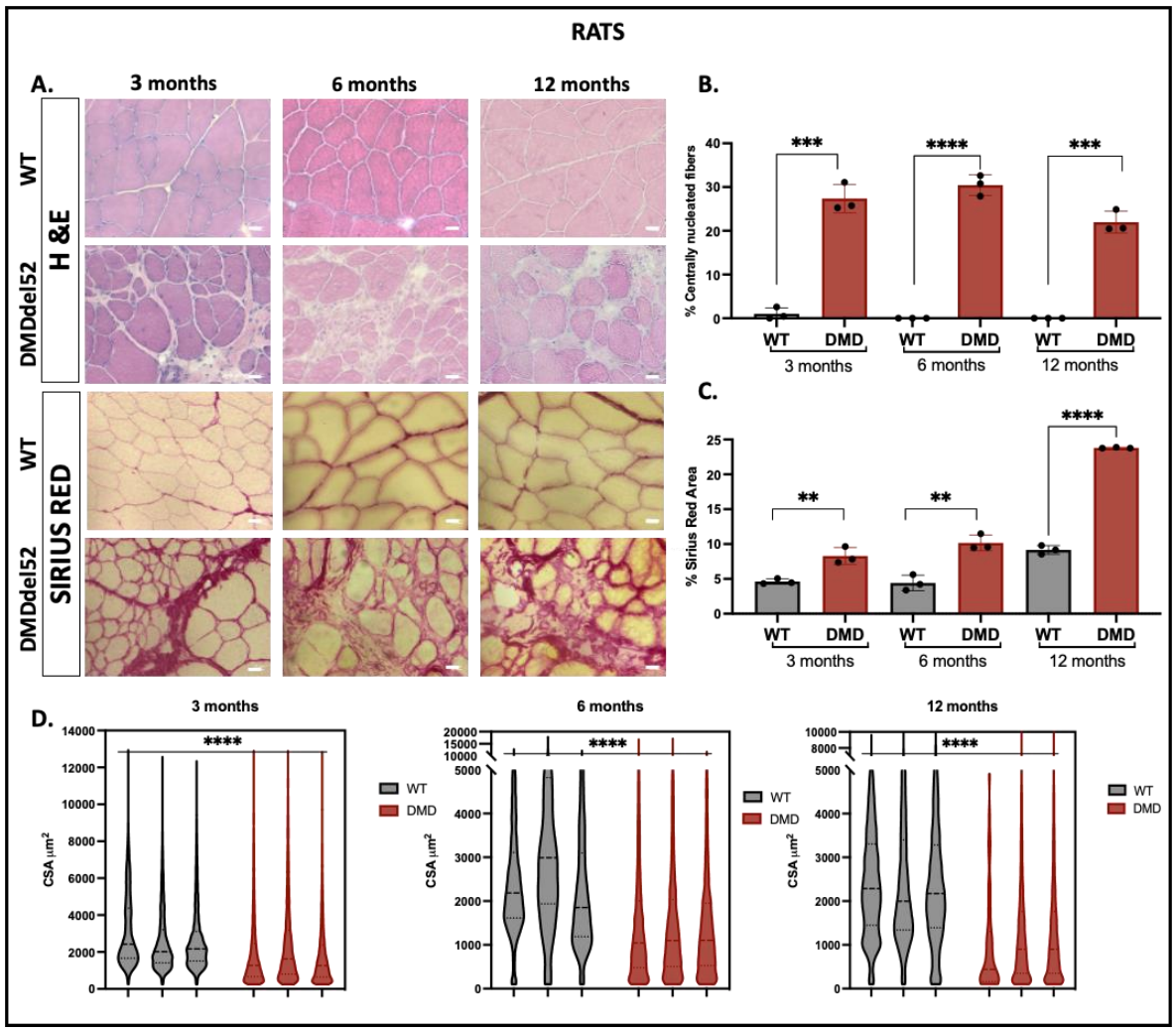

Figure 8 *Dystrophic phenotype of DMD rats Tibialis Anterior compared to age matched WT, the dystrophic pathology increases with age. (A) H&E and Sirius red stained transverse section of Tibialis Anterior of rats. Scale bar is 20µm. (B) Percentage of centrally nucleated fibers on the total amount of fibers at different time points. (C) The fibrotic area increases with age. Percentage of Sirius red area on the total area of the section in WT and DMD rats at different time point. The data are presented as mean ± SEM; * p≤0,05 Student's t-test (B-C). (D) CSA Cross Sectional Area of fibers expressed in micrometers square. Violin plots showing the fibers caliber of the tibialis anterior of each animal. The data are presented as median and quartiles of the total amount of the fibers.*

In mdx^{4cv} mice the percentage of centrally nucleated fibers was 48,70 ±4,60 at 2 months, 75,88 ±3,74 at 6 months 58,41 ±7,81 at 12 months old, 55,16 ±7,11 for the mdx^{4cv} mice and 2,53 ±1,30 for 2 months old WT, 0,43 ± 0,006 for 6 months old WT and 1,84 ± 1,090 for 12 months WT and 6,98 ±2,87 for 17 months old WT. The differences between WT and mdx^{4cv} mice were statistically significant in all the time points with a p value of p=0,0007 *** at 2 months, p<0,0001**** at 6 months, p=0,0020 ** at 12 months old and p=0,0033** at 17 months old (Fig 9 B.). The quantification of fibers with internalized nuclei does not follow a trend over time.

In order to evaluate fibrotic changes over time Sirius red staining has been performed on *Tibialis Anterior* muscles, the red stained area represents the proportion of collagen which indicates fibrosis (Fig 9 A). At 2 months old the average of the percentage of fibrotic area was 3,96 ±0,66 in WT mice and 10,71 ±2,25 in mdx^{4cv} mice and the significance was p=0,04*; at 6 months old 6,05 ±0,63 in WT mice and 8,73 ±0,55 in mdx^{4cv} mice p=0,02*; at 12 months old 7,03 ±0,34 in WT mice and 12,55 ±1,63 in mdx^{4cv} mice with a significance of p=0,03*; at 17 months old 5,13 ±1,47 in WT mice and 12,62 ±1,87 in mdx^{4cv} mice (Fig 9 C). Is not observed an increase in the percentage of fibrotic area in DMD mouse models over time it remains quite stable (Fig 9 C).

In Fig 9 D. is showed the cross-sectional area of the fibers, indicating their size in the *Tibialis Anterior* at different time points. At 2 months old there were differences between mdx^{4cv} and WT mice fibers size but were not significant, the *mdx* fibers are slightly more heterogeneous than WT. Meanwhile at 6, 12 and 17 months old the fiber size of the *mdx* is smaller and less heterogeneous than WT with a significance of p<0,0001****(Fig 9 D).

The internalized nuclei, the fibrotic tissue, the morphology of fiber size, inflammation and necrosis are showed in the H&E staining at different time points in Fig 9 A.

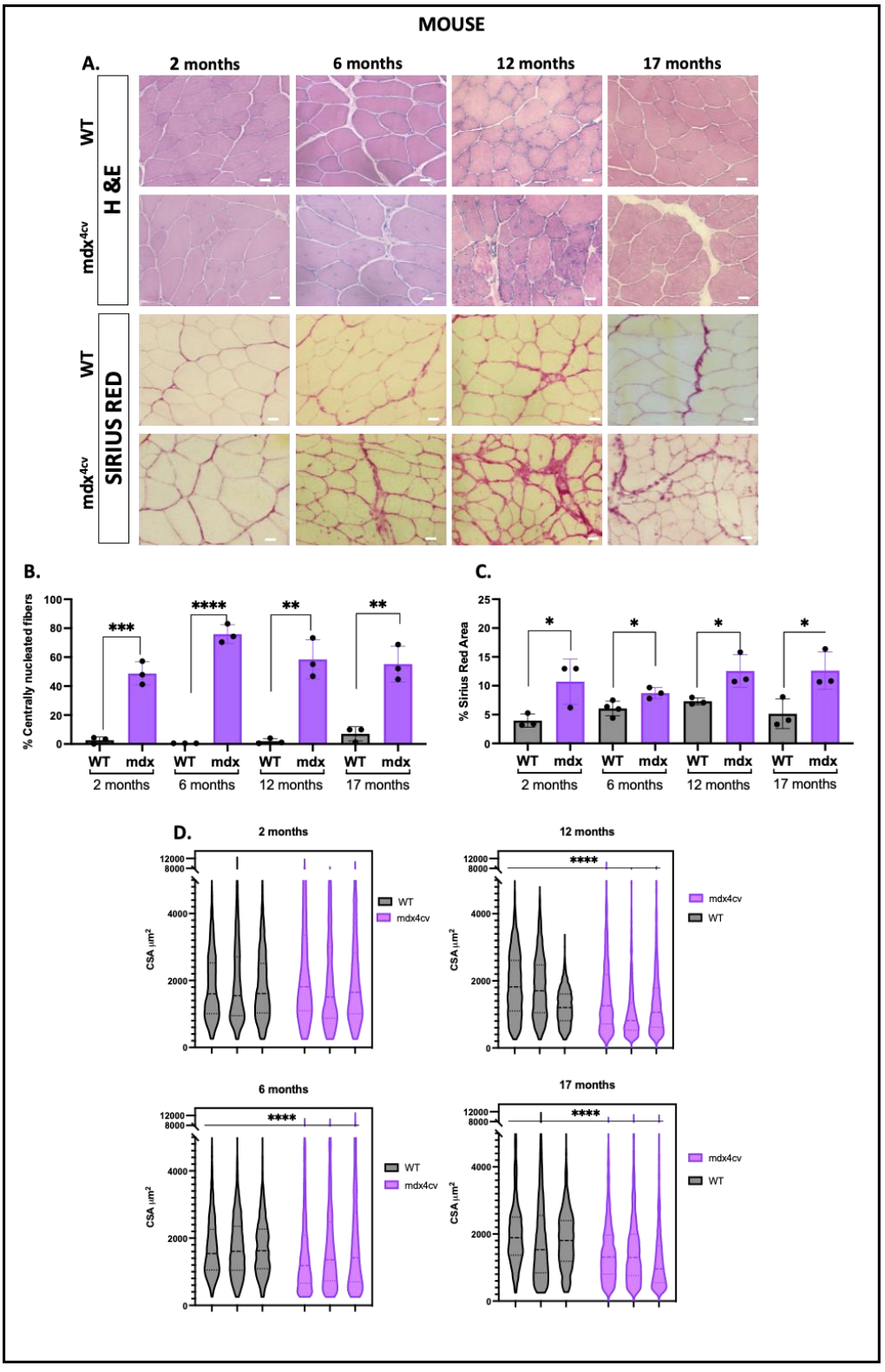

Figure 9 *Dystrophic phenotype of mdx^{4cv} Tibialis Anterior compared to age matched WT, the dystrophic pathology increases with age. (A) H&E and Sirius red-stained transverse section of Tibialis Anterior of mice. Scale bar is 20µm. (B) Percentage of centrally nucleated fibers on the total amount of fibers at different time points. (C) The fibrotic area increases with age. Percentage of Sirius red area on the total area of the section in WT and mdx^{4cv}mice at different time point. The data are presented as mean ± SEM; * p≤0,05 Student's t-test (B-C). (D)*

CSA Cross Sectional Area of fibers expressed in micrometers square. Violin plots showing the fibers caliber of the tibialis anterior of each animal. The data are presented as median and quartiles of the total amount of the fibers.

4.1.2 Fat tissue infiltration, inflammation, vessels and Fibro Adipogenic Progenitors (FAPs)

Variability is widely present in DMDs, however fat tissue infiltration increases progressively with aging p=0,02*, indeed in early stage patients (1-2 years old) the amount of fat tissue infiltration is near to zero 0,35 ±0,05 like in the control samples 0,11 ±0,05 and in patients with more than 7 years the values are 0,23 ±0,13 in controls and 4,19 ±1,52 in DMD. The mean of fat tissue area in percentage for the others time points is: 3-4 years old 0,19 ±0,08 in controls and 2,86 ±2,34 in DMD; 5-6 years old 0,43 ±0,25 in controls and 1,66 ±0,98 in DMD (Fig 10 F).

Becker patients does not show fat tissue infiltration 0,23 ±0,06 the mean is even lower that the controls one 0,31 ±0,12 (Fig 10 G).

In DMD rats is showed a significative increase of fat tissue infiltration in the muscle over time, starting from 3 months old to 12. At 3 months old the mean of the fatty area was 1,73 ±0,33 compared with the WT in which was 0,129 ±0,06 p=0,0099**; 6 months old DMD rats 2,36 ±0,24 and WT 0,08 ±0,011 p=0,0077***; 12 months old DMD rats 6,94 ±0,88 and WT 0,54 ±0,11 p=0,0019** (Fig 10 B).

Mdx mice showed a milder increase of adipose tissue with aging and it is present more variability compared to the rats. The mean of the fatty area in mice was 0,03 ±0,006 in WT mice 2 months old and 0,05 ±0,019 in 2mo mdx; 0,02 ±0,006 and 0,065 ±0,03 in WT and mdx 6 months mice respectively; at 12 months old 0,02 ±0,01 in WT and 0,092 ±0,05 in mdx; finally at 17 months old in WT 0,44 ±0,018 and in mdx 0,108 ±0,03(Fig 10 D).

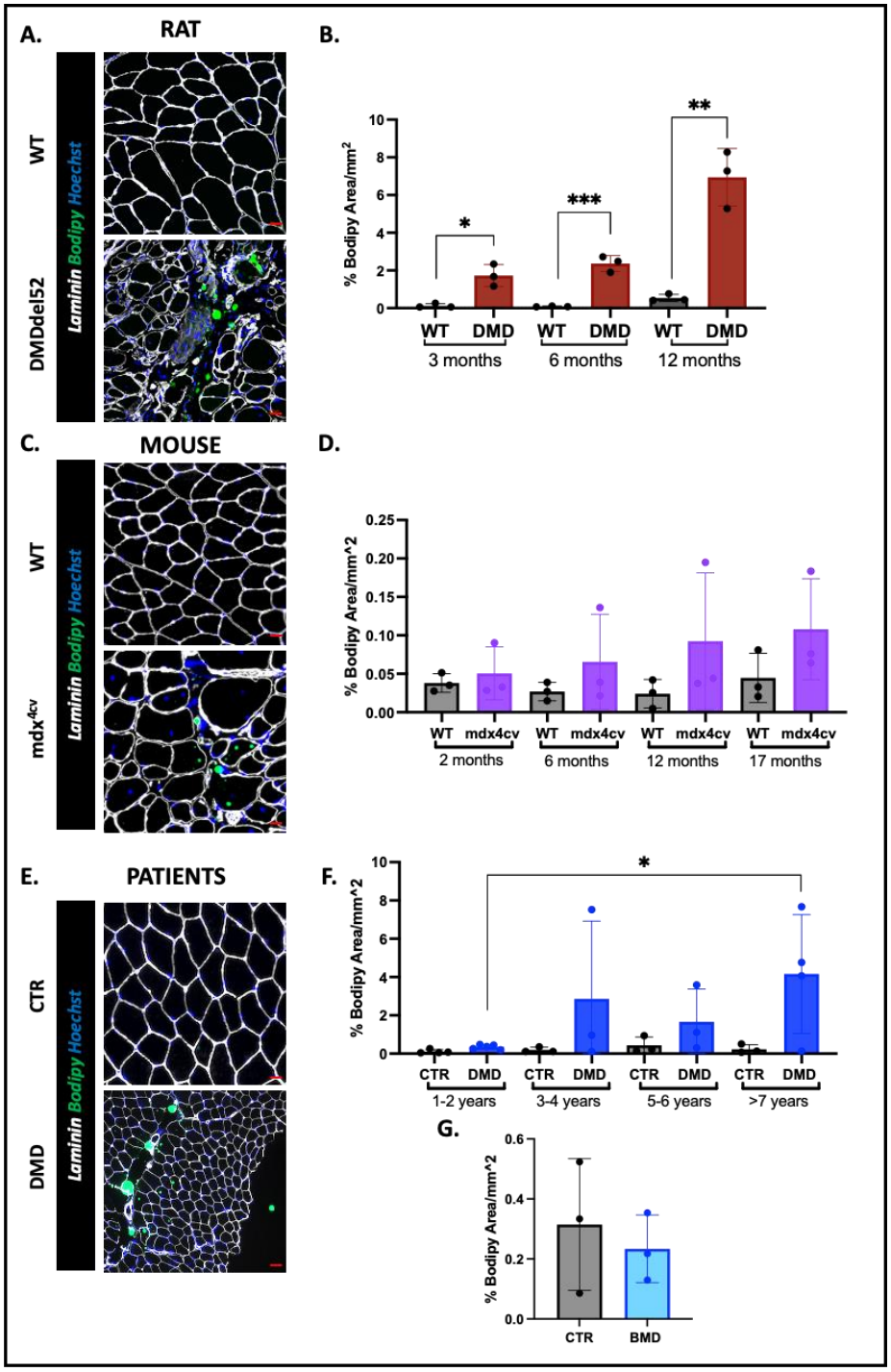

Figure 10 *Fat tissue infiltration increase over time in Duchenne muscular dystrophy models and patients. (A-C-E) Bodipy staining representation in Tibialis Anterior of rats and mice at 12 months old and relatives WT A-C and of quadriceps collected from patients and control of 4 years of age. Laminin is white, Bodipy area is the green stained area and in blue are stained the nuclei with Hoechst. Scale bar is 20µm. (B-D-F) Percentage of bodipy stained area on the total area of the section in DMD rats, mdx mice, WT, DMD patients and controls at different time points. (G) Percentage of bodipy stained area on the total area of the section in Becker patients and age matched controls. The data are presented as mean ± SEM; * p≤0,05 Student's t-test*

With CD45 we observed in DMDs an increase of inflammation infiltrates only after 7 years old, probably related to the variability between patients, reason why the Standard Error Mean

(SEM) is elevated. The media of values calculating the number of inflammatory cells is 12,68 ± 4,99 and 84,99 ±29,56 in CTR and DMDs patients of 1-2 years old, respectively p=0,05*; 18,16 ±4,51 and 85,77 ±37,44 in controls and DMDs patients of 3-4 years old respectively; 21,91 ±5,97 and 101,4 ±37,45 in Controls patients and DMDs patients of 5-6 years old respectively; 4,56 ±2,02 and 140,9 ±11,27 in Controls patients and DMDs patients with more than 7 years old respectively p<0,0001**** (Fig 11 F)

In BMDs the inflammation was higher comparing to the controls but was lower comparing with DMDs: 2,50 ±1,65 in controls and 18,15 ±10,70 in BMDs (Fig 11 G).

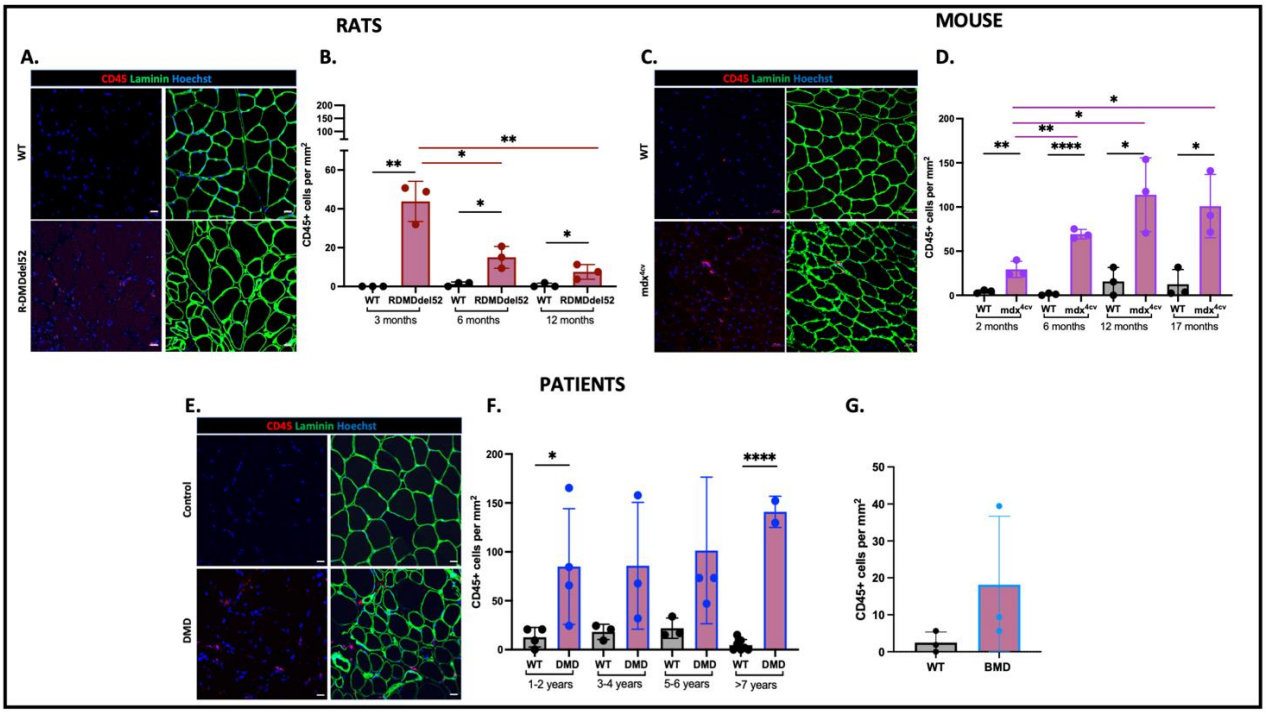

Figure 11 *Inflammatory cells in duchenne muscles. (A-C) Rapresentation of CD45/Laminin staining on Tibialis anterior of DMD rats mdx mice and relatives WT at 6 months old. CD45 cells are stained in red. In green is stained Laminin and in blue are visible the nuclei stained with Hoechst. Scale bar is 20μm. (B-D-F) Number of CD45 positive cells on the total area, expressed in mm2, of the section in DMD Rats, mdx mice WT, DMD patients and controls at different time points. The data are presented as mean ± SEM; * p≤0,05 Student's t-test (E) Rapresentation of CD45/Laminin staining on quadriceps of a patient and a control at 4 years old. In green is stained Laminin and in blue are visible the nuclei stained with Hoechst. Scale bar is 20μm.(G) Number of CD45 positive cells on the total area expressed in mm^2, of quadriceps and deltoid of becker patients and age matched controls. The data are presented as mean ± SEM*

In DMD rats we observed a decrease in the inflammatory infiltrates over time, meanwhile in mice is showed an increase in the number of inflammatory cells in the muscle during the progression of the disease. At 3 months old in rats is well known that there is a peak of

inflammation (Taglietti et al., submitted), indeed the media of values calculating the number of inflammatory cells at 3 mo was 43,82 ±5,97 in DMD rats and non represented in WT p=0,0018**. At 6 months the inflammation decreases to 15,06 ±3,2 cells per mm^2 in DMD p=0,013* and compared to 6 months WT 1,24 ±0,63 p=0,014*; at 12 months the number of inflammatory cells keep decreasing 7,50 ±2,16 in DMD p=0,0046** and compared to12 months WT 0,62 ±0,62 p=0,038* (Fig 11 B).

On the counterpart, in mdx mice was observed an increase of inflammation with aging. At 2 months old the mean of the inflammatory cells number in mdx muscle is 29,35 ±5,29, at 6 months is 69,26 ±3,1 p=0,0029** ; at 12 113,9 ±24,12 p=0,026* and at 17 months old the inflammation remains high 101 ±20,68 p=0,02*; comparing mdx with age matched WT important differences were observed as well: 2 months WT 4,30±1,03 p=0,0097**; 6 months WT 1,17 ±0,67 p<0,0001****; 12 months WT 15,65 ±9,15 p=0,019* and 17 months WT 12,52 ±9,59 p=0,017* (Fig 11 D).

Another point to understand was if there were any anomalies in the number of vessels in Duchenne muscular dystrophy, for this reason, staining with CD31 in mice and humans' samples was performed and isolectine has been used to detect capillaries on rats (Fig 12 A-C-E).

No changes and no alteration were observed in the number of vessels in both models and in human samples. The number of vessels seems to remain unchanged during the progression of the disease and as well in comparison with the controls.

In DMDs samples the number of vessels was at 1-2 years old 0,78 ±0,5 in DMD and 0,16 ±0,015 in controls, at 3-4 years old 0,71 ±0,13 in DMD and 0,35 ±0,10 in controls; at 5-6 years old 0,66 ±0,05 in DMD and 0,40 ±0,14 in controls; after 7 ears old 0,78 ±0,13 in DMD and 0,64 ±0,10 in controls (Fig 12 F).

In BMDs patients 0,70 ±0,11 and in controls 0,94 ±0,42 (Fig 12 G).

The number of vessels in TA of models was 1,46 ±0,03 and 1,19 ±0,09 in WT and DMD 3 months old rats respectively; 1,40 ±0,03 and 1,35 ±0,23 in WT and DMD 6 months old rats respectively; 1,88 ±0,03 and 1,44 ±0,09 in WT and DMD 12 months rats respectively (Fig 12 B). 2,12 ±0,20 and 2,14 ±0,15 in 2 months old WT and mdx mice respectively, 1,70 ±0,11 and 2,31 ±0,09 in 6 months old WT and mdx mice respectively; 1,18 ±0,15 and 2,21 ±0,06 in 12

months old WT and mdx mice respectively; 2,21 ±0,06 and 2,03 ±0,2 in 17 months old WT and mdx mice respectively (Fig 12 D).

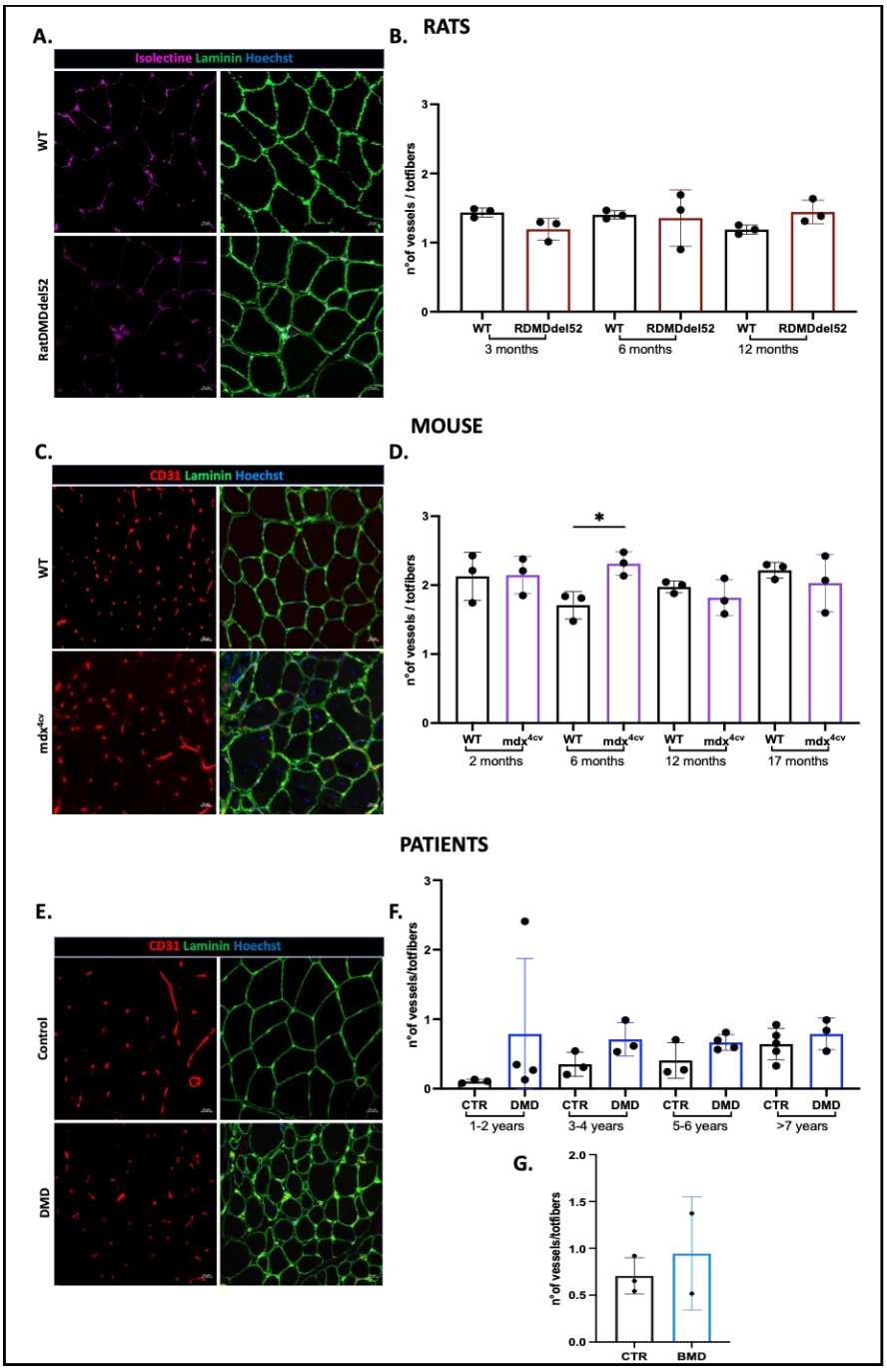

Figure 12 *Capillaries in Duchenne muscles. (A) Isolectine/Laminin co-staining in Tibialis Anterior of 6 months old DMD rat and WT. Scale bar is 20µm. (B) Quantification of capillaries in Tibialis Anterior of DMD and WT rats at different time points. (C) CD31/Laminin co-staining in Tibialis Anterior of 6 months old mdx and WT mouse. Scale bar is 20µm. (D) Quantification of capillaries in Tibialis Anterior of mdx and WT mice at different time points. (E) CD31/Laminin co-staining in quadriceps of 6 years old DMD patients and control. Scale bar is 20µm. (F) Quantification of capillaries in quadriceps and deltoids of DMD patient's samples and control samples*

*at different time points. (G) Quantification of capillaries in quadriceps and deltoids of Becker patient's samples and control samples. The data are presented as mean ± SEM * p≤0,05 Student's t-test.*

To check the number of how many Fibro Adipogenic Progenitors (FAPs) muscle PDGFRα has been used as a marker. In Fig 13 A and C is showed a progressive increase over time of the number of FAPs in the muscle of Duchenne models, instead in DMD patients the number of FAPs remain stable in all the analyzed stages of the disease, the variability between individuals is constant (Fig 13 E).

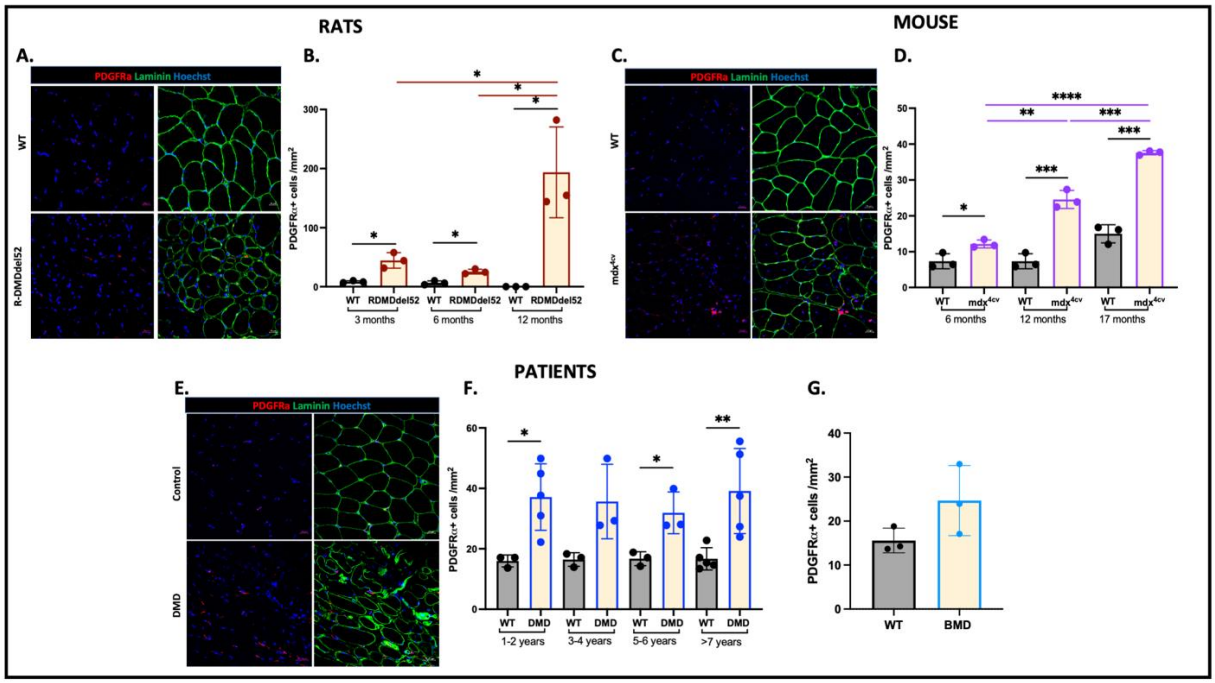

Figure 13 *Fibro Adipogenic Progenitos (FAPs) in Duchenne muscles. (A-C) Representation of PDGFRα/Laminin staining on Tibialis anterior of DMD rats mdx mice and relatives WT at 6 months old. FAPs are stained in red. In green is stained Laminin and in blue are visible the nuclei stained with Hoechst. Scale bar is 20μm. (B-D-F) Number of PDGFRα positive cells on the total area, expressed in mm2, of the section in DMD Rats, mdx mice WT, DMD patients and controls at different time points. The data are presented as mean ± SEM; * p≤0,05 Student's t-test (E) Representation of PDGFRα/Laminin staining on quadriceps of a patient and a control at 4 years old. FAPs are stained in red, in green is stained Laminin and in blue are visible the nuclei stained with Hoechst. Scale bar is 20μm.(G) Number of PDGFRα positive cells on the total area expressed in mm^2, of quadriceps and deltoid of Becker patients and age matched controls. The data are presented as mean ± SEM*

There was variability between DMDs, anyhow the number of FAPs in the muscle was higher compared to control muscle. At 1-2 years old the medium values were 15,96 ±1,14 in controls and 37,13 ±4,91 in DMD p=0,018*; at 3-4 years old 16,45 ±1,30 in controls and 35,66 ±7,12 in DMD; at 5-6 years old 16,72 ±1,33 in controls and 31,93 ±3,98 in DMD p=0,022*; in patients

with more than 7 years old 16,68 ±1,64 for the controls and 39,13 ±6,28 in DMD p=0,0086** (Fig 13 F).

In Becker patients (24,67 ±4,59) the number of FAPs was higher than the controls (15,58 ±1,63) (Fig 13 G).

The number of FAPs (red stained cells) was calculated manually and the medium values of the analyzed groups were: 3 months old rats 8,28 ±0,97 in WT and 44,66 ±7,58 in DMD p=0,0089**; 6 months old 6,49 ±1,95 in WT and 25,63 ±2,39 in DMD p=0,0035**; In 12 months old rats 0,00 ±0,00 in WT rats and 193,7 ±44,39 in DMD p=0,01*. The difference between 3- and 6-months old rat was significant with a p value of p=0,019* and between 3- and 12-months old p=0,029* (Fig 13 B).

In mouse model as mentioned before is observed an increase: between 6- and 17-months old p<0,0001***; between 6- and 12-months old p=0,0014** and between 12- and 17-months old p=0,0009 ***. Comparing the mdx with the controls the values obtained were: 7,35 ±1,21 in WT and 12,17 ±0,64 in mdx 6 months old mice p=0,02*; 7,35±1,21 in WT and 24,56 ±1,45 in mdx 12 months old mice p=0,0008***; 15,00 ±1,46 in WT and 37,59 ±0,33 mdx 17 months old mice p=0,0001***(Fig 13 D).

4.1.3 Dystrophin

Revertant fibers are fibers in which dystrophin expression is spontaneously restored despite the absence of Dystrophin.

In patients at 1-2 years old the percentage of revertant fibers was 0,00% ±0,00; at 3-4 years old 0,017% ±0,02; 5-6 years 0,18% ±0,29 and >7 years old the percentage was increate to 2,8% ±3,44 (Fig 14 F).

In rats, since 3 months of age was observed the 1,8% ±0,49 of revertant fibers. Their number increase with aging with 2,8% ±0,41 at 6 months, and 5,47% ±1,26 at 12 months old. (Fig 14 A, B).

In mice the revertant fibers were approximately absent in all the time points. At 2 months were not detected, at 6 months 0,1 ±0,022, at 12 months 0,04% ±0,00 and at 17 months 0,33% ±0,03 (Fig 14 C, D). The WT were taken as positive controls in which the expression of dystrophin was always 100% ±0,00 in both models and controls patients (Fig 14 A-D).

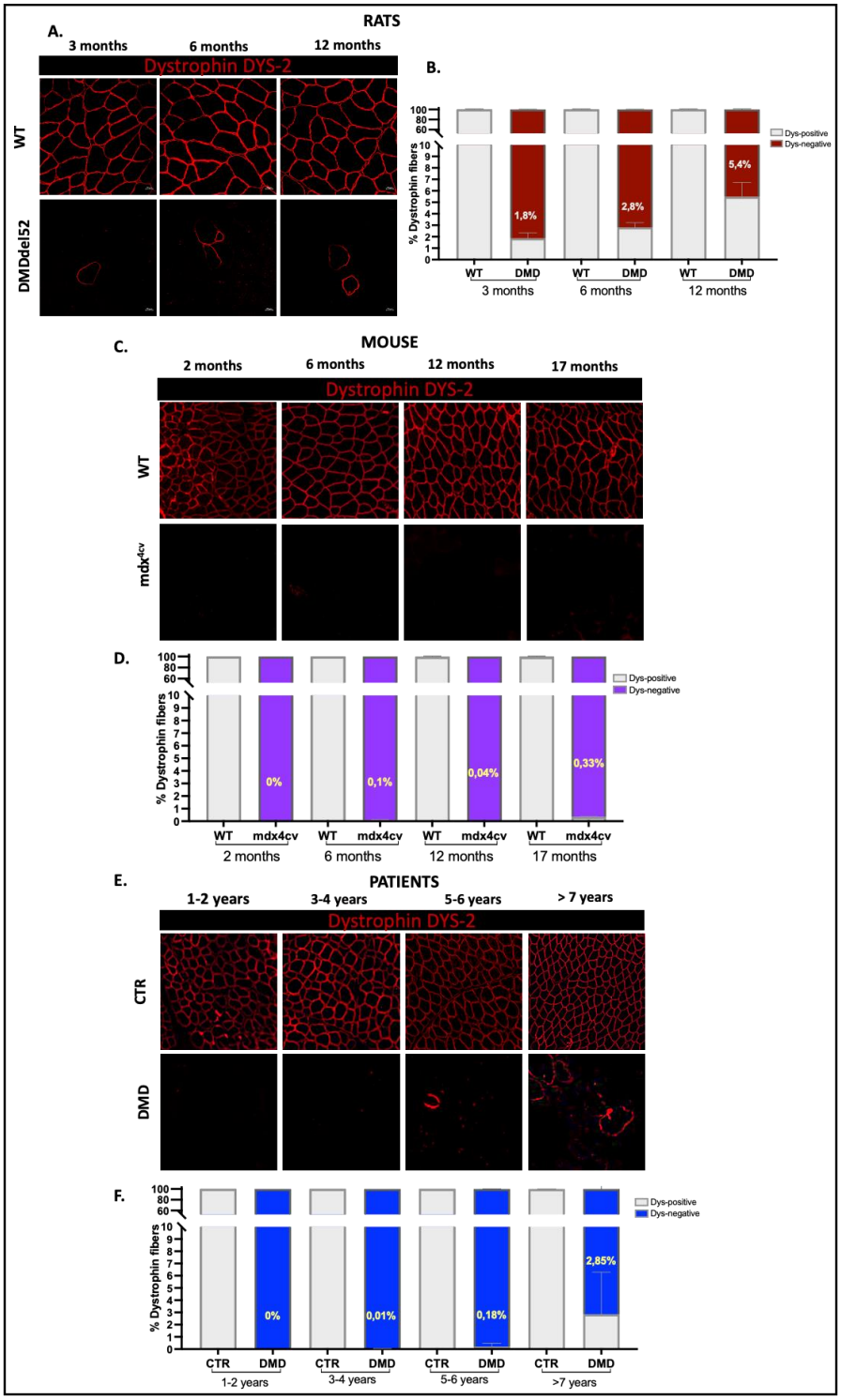

Figure 14 *Dystrophin and dystrophin revertant fibers increase during the progression of the disease. (A-C) Representation of the expression of dystrophin in Rats (A) and mice (C) in Tibialis Anterior muscle at different time points. DYS-2 detecting Rod-domain has been used. Scale bar 20µm. (B-D-F) Quantification of the positive fibers of dystrophin at different time points in Tibialis Anterior of animal models with age matched Wild Types, and in DMD patients with relative age matched histologically normal control muscles. Dystrophin positive fibers are expressed in percentage and normalized on the total number of fibers. The data are presented as percentage*

on the total and ±SD. (E) Representation of the expression of dystrophin in Quadriceps of DMD patients divided in groups according to age and age matched controls. DYS-2 detecting Rod-domain has been used.

4.2 Muscular Stem cells behavior

4.2.1 Regenerative capacity of Muscle fibers

We observed, a decrease in the number of regenerative fibers over time, during the progression of the disease in both models as well as in patients (Fig 15).

In WT and controls patient's muscles, no regenerative fibers were presents (Fig 15). In Becker patients muscles a little number of regenerative fibers is presents and in one patient are completely absent (Fig 15 G).

4.2.2 Activations and presence of Muscular satellite cells

In DMDs muscles SCs are slightly increased comparing to the controls and after 7 years old are significantly higher compared to the control p=0,002***. Furthermore, among DMD as well as among controls was observed an individual-to-individual variability. The mean values obtained counting satellite cells in human samples were 4,62 ±0,96 in controls and 17,27 ±10,40 in DMD 1-2 years old; 12,24 ±7,79 in controls and 17,88 ±2,88 in DMD 3-4 years old; 6,48 ±1,43 in controls and 19,23 ±5,89 in DMD 5-6 years old and finally after 7 years old 8,065 ±1,32 in controls and 24,08 ±1,24 in DMD (Fig 16 B). In BMDs and controls patients the number of satellite cells in the muscle was the same and always variability between individuals was present; 7,44 ±0,79 in controls and 10,21 ±3,8 in Becker (Fig 16 C).

In rats was observed an increase in the number of satellite cells in DMD muscle compared to WT muscle, however there is a slight decrease in the number of Pax7 positive cells during the progression of the disease.

In rats muscles the mean percentage of the number of satellite cells was 9,47 ±1,44 in WT and 19,66 ±3,68 in DMD months old; 6,95 ±0,91 in WT and 11,06±0,22 in DMD 6 months old rats p=0,04* and in 12 months old rats was 6,14±0,40 in WT and 10 ±0,22 in DMD p=0,005** (Fig 17 B).

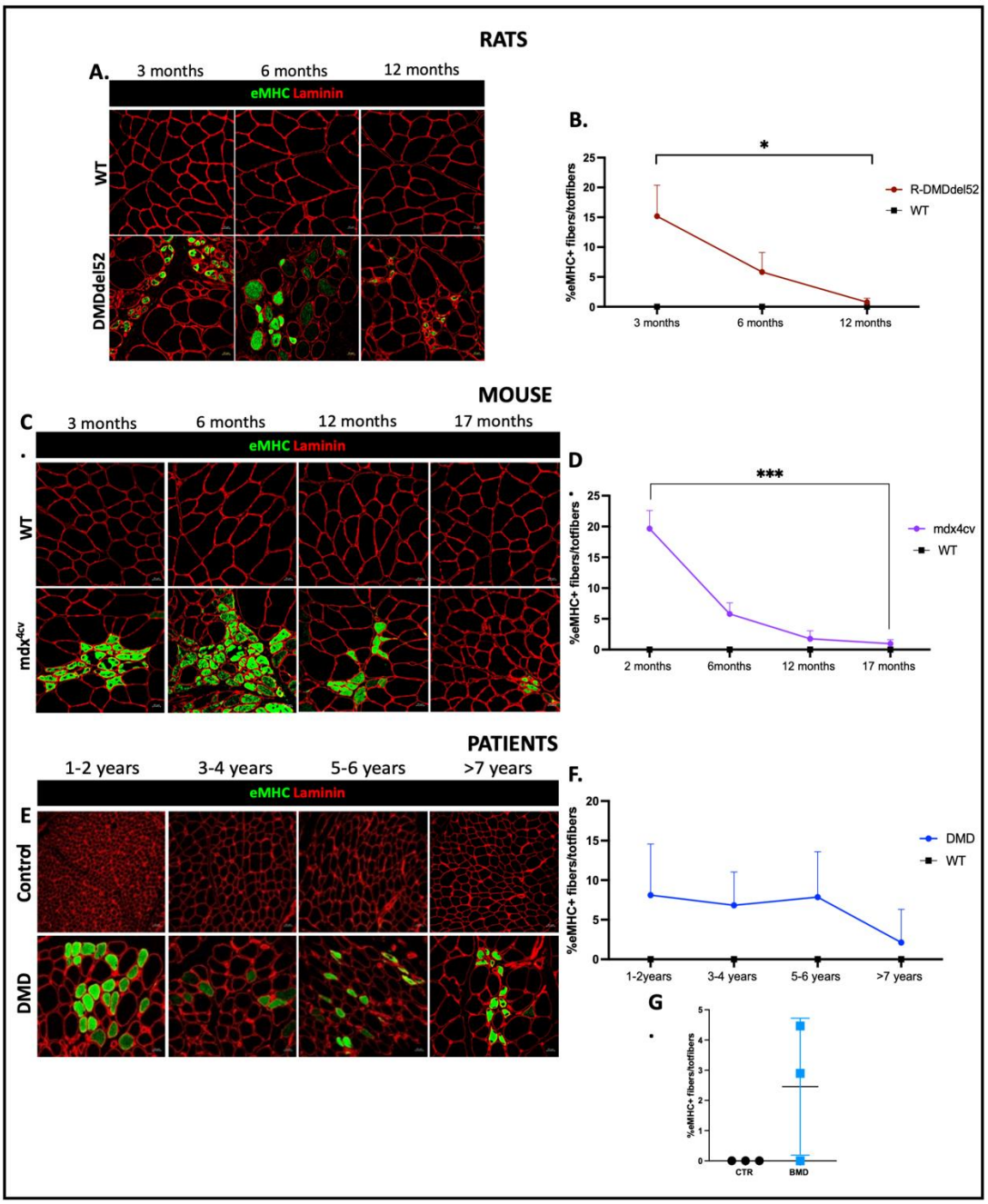

Figure 15 *Regenerative capacity of muscle fibers in Duchenne muscular dystrophy. (A-C) Representation of the co-staining eMHC/Laminin in transverse sections of Tibialis Anterior in DMD rats and mdx mice at different time points with age matched WT. Scale bar 20μm. (B-D-F) Quantification of eMHC positive cells, expressed in percentage, in Tibialis Anterioir of models at different time point and in human muscles in groups divided according to age. The data are presented as mean and ±SD. * p≤0,05 Student's t-test. (E) Representation of the co-staining eMHC/Laminin in transverse sections of quadriceps collected from DMD and control patient, divided in groups according to age. (G) Quantification of eMHC positive cells, expressed in percentage, in Becker patients and age matched controls. The data are presented as mean and ±SD. * p≤0,05 Student's t-test.*

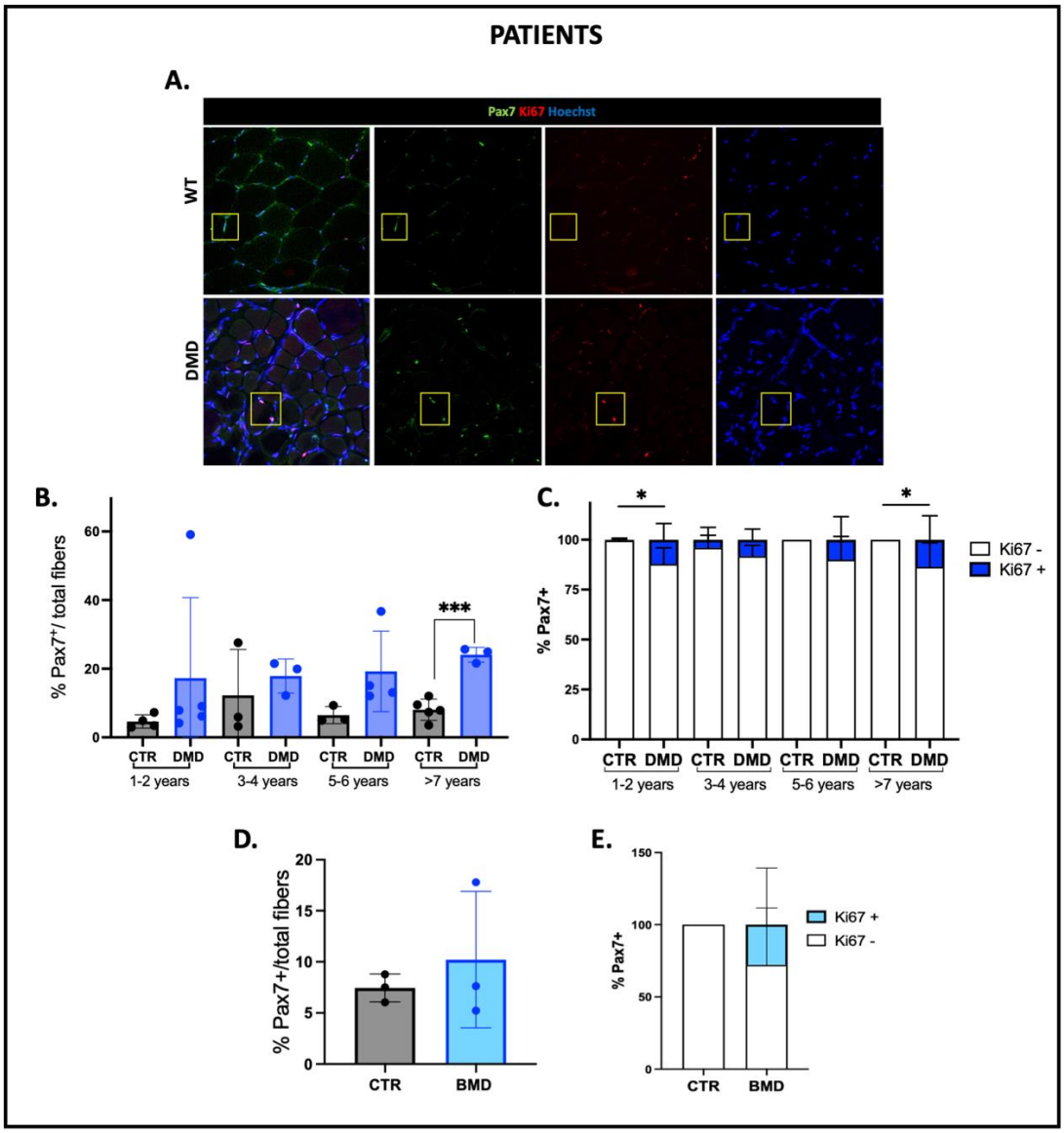

Figure 16 *Muscular satellite cells in Duchenne muscles and their activation. (A)Representation of a co-staining with PAX7-KI67 on Quadriceps of a 6-year-old patients and age matched control. Pax7 positive cells are green and Ki67 positive cells highlighted in red, in blue are stained the nuclei. Scale bar 20µm.(B) Quantification of the total number of Pax7 positive cells normalized on the total number of fibers in Quadriceps of DMD and control patients divided in groups according to age. The data are presented as mean ±SEM; * p≤0,05 Student's t-test (C) Quantification of actives satellite cells on the total number of satellite cells in the muscle of DMD patients and controls divided in groups according to age. The data are presented as percentage ±SD. * p≤0,05 Student's t-test. (D) Quantification of the total number of Pax7 positive cells normalized on the area of the section in Quadriceps of Becker and control patients. The data are presented as mean ±SEM. (E) Quantification of actives satellite cells on the total number of satellite cells in the muscle of Becker patients and controls. The data are presented as percentage ±SD.*

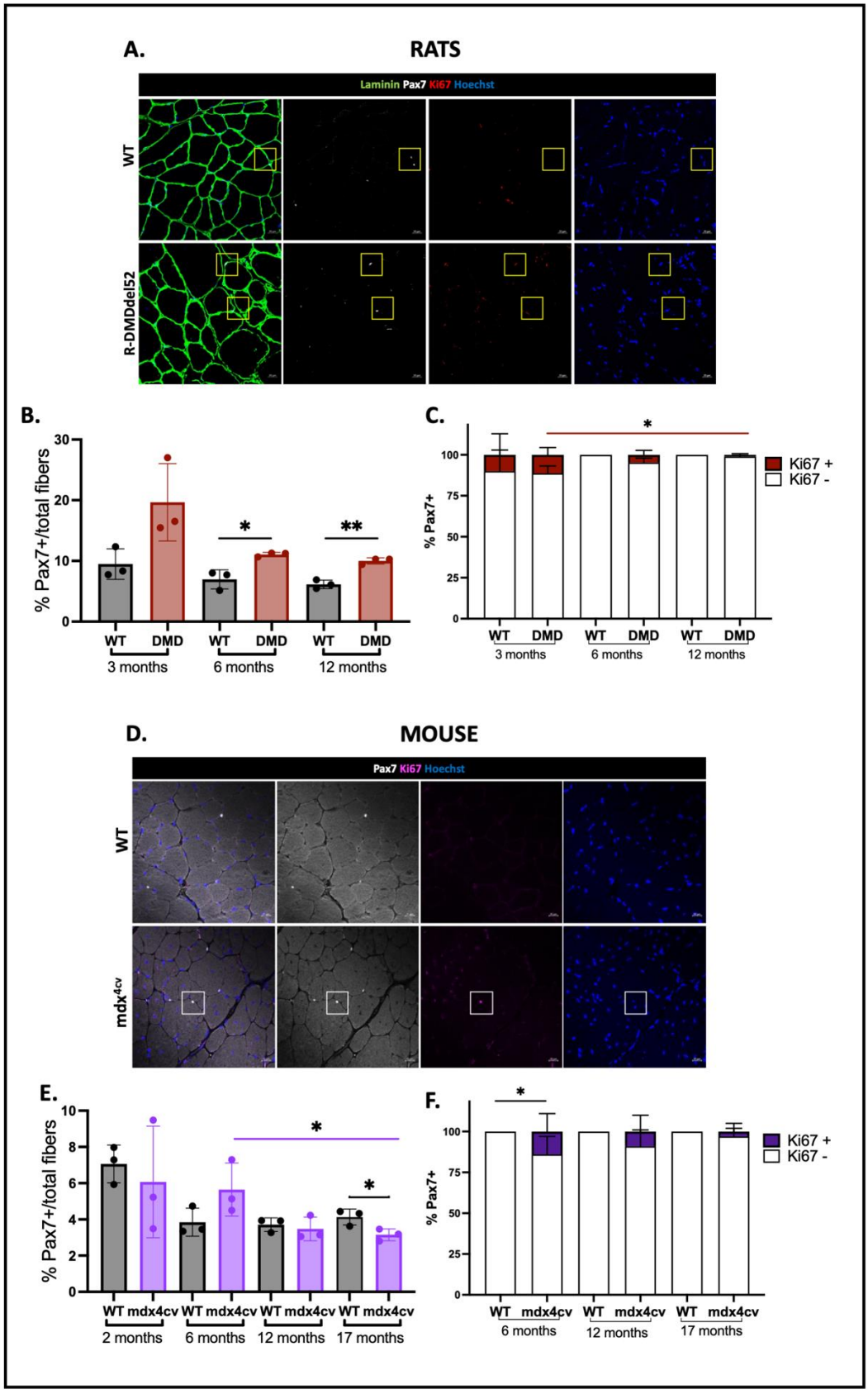

Figure 17 *Muscular satellite cells in Duchenne muscles and their activation. (A) Representation of a co-staining with PAX7-KI67-Laminin on a Tibialis Anterior in 6 months old DMD rat and WT. Laminin is highlighted in*

*green, Pax7 positive cells are white and Ki67 positive cells are red, in blue are stained the nuclei. Scale bar 20μm.(B) Quantification of the total number of Pax7 positive cells normalized on the total number of fibers in Tibialis Anterior of DMD rats and WT at different time points. The data are presented as mean ± SEM; * p≤0,05 Student's t-test (C) Quantification of actives satellite cells on the total number of satellite cells in the muscle of DMD rats and WT rats at different time points. The data are presented as percentage ±SD. (D) Representation of a co-staining with PAX7-KI67 on a Tibialis Anterior in 6 months old mdx mouse and WT. Pax7 positive cells are white and Ki67 positive cells highlighted in purple, in blue are stained the nuclei. Scale bar 20μm.(E) Quantification of the total number of Pax7 positive cells normalized on the total number of fibers in Tibialis Anterior of mdx mice and WT at different time points. The data are presented as mean ± SEM; * p≤0,05 Student's t-test (F) Quantification of actives satellite cells on the total number of satellite cells in the muscle of mdx mice and WT mice at different time points. The data are presented as percentage ±SD.*

In mdx mice muscles the number of satellite cells was not different comparing it with WT muscles, but a decrease was observed from 6 months old mice to 17 months old mice p=0,01*.

The mean values obtained counting the Pax7 positive cells in mice were 7,06 ±0,55 in WT and 6,06 ±1,79 in mdx 2 months old animals; 3,84 ±0,44 in WT and 5,64±0,84 in mdx 6 months old animals; 3,70±0,21 in WT and 3,47 ±0,37 in mdx 12 months old animals; 4,13 ±0,2 and 3,1 ±0,19 in 17 months old animals with a significative difference p=0,02* (Fig 17 E).

The activation of satellite cells was assessed with the co-staining Pax7-Ki67, in which only the double positive cells were counted as activated and normalized on the total number of satellite cells presents in the section. In animal models was observed a decrease in the number of active satellite cells during the progression of the disease. In rats the decrease is progressive till 12 months of age (Fig 17C), while in mice the active satellite cells start to decrease in a later time point, at 17 months of age (Fig 1 F). In human muscles the variability is constant, and a small number of satellite cells is always activated in all the stages of the disease. (Fig 16 C). Active satellites cells were also found in Becker muscles and again the variability between individuals was also noticed (Fig 16 E).

4.2.3 Satellite cells senescence

To see if the satellite cells were acquiring a senescent phenotype different co-staining with Pax7 and senescence markers have been performed. The chosen senescence markers where P16, Histon2AX (H2AX) and P21. Only the double positive cells were taken into account and considered senescent, then were normalized on the total number of Pax7 positive cells of the section and expressed in percentage.

The analysis which has been done in DMDs, BMDs and CTR muscles showed again an important variability among individuals. However, showed in Fig 21 A the expression of P16

in satellite cells increases with aging in DMD muscles. Furthermore, in the control the expression of P16 is about 1-2% which is lower than DMD.

The expression of H2AX did not follow a trend over time, but as is showed in Fig 18 B the expression of this marker in SCs of DMD muscles was always higher compared to the controls. These findings are completely different for P21 expression which in Human sample was highly variable because is expressed in controls as well as in DMD muscle without important differences (Fig 18 C). In Fig 21 D are showed the trends of the three markers over time confirming that only P16 increase during the progression of the disease, instead P21 and H2AX remain in the same range. In the muscles of Becker patients, the numbers of senescent satellites cells seem to be higher compared with the controls, in-fact the three markers are more expressed in BMD compared to the WT (Fig 18 E-F-G).

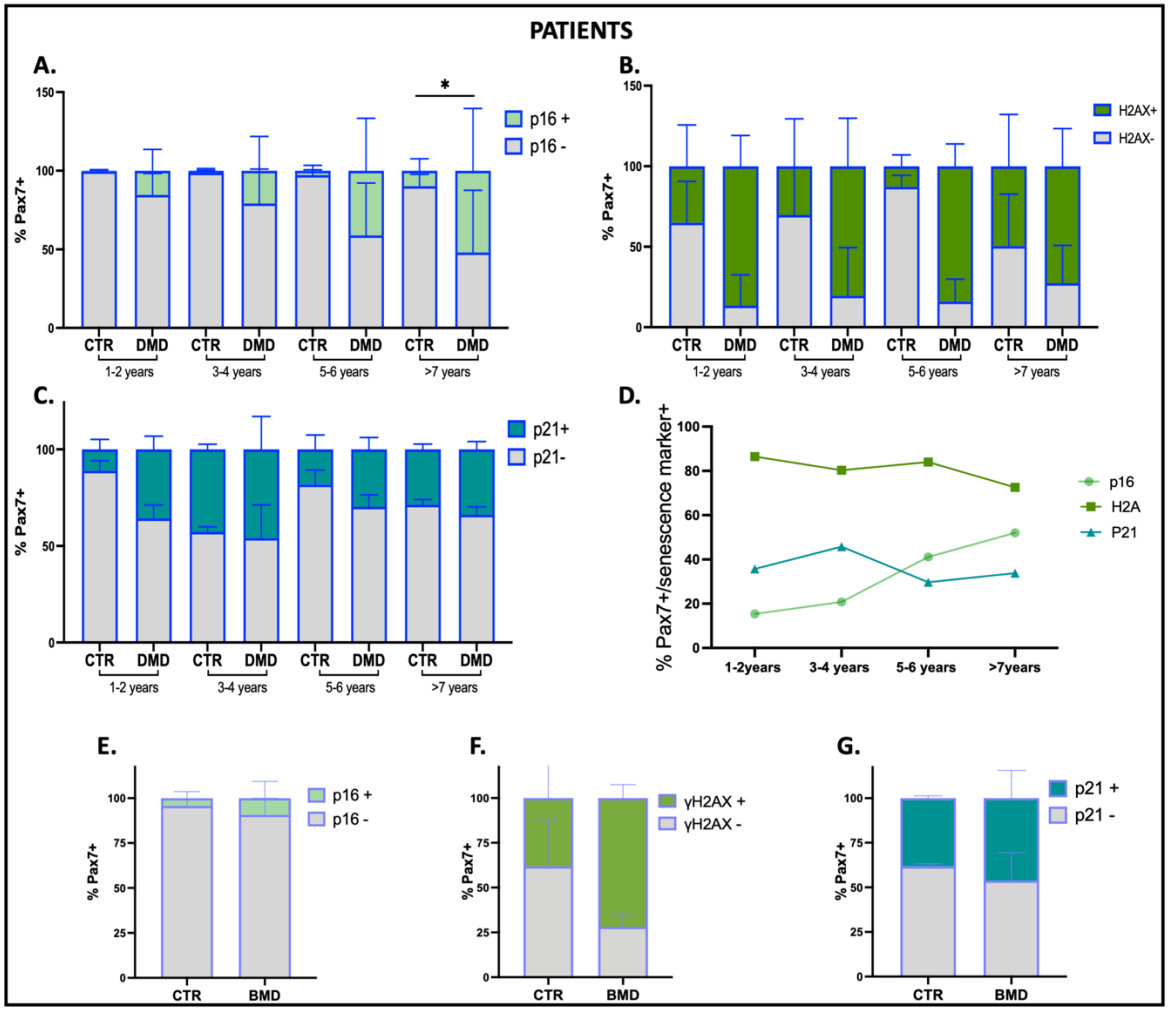

Figure 18 *Muscular satellite cells acquire a senescent phenotype during the progression of the disease. (A) Quantification of satellite cells expressing P16 on the total number of satellite cells in muscles of DMD patients and controls divided in groups according to age. (B)Quantification of satellite cells expressing H2AX on the total*

*number of satellite cells in the muscle of DMD patients and controls divided in groups according to age. (C) Quantification of satellite cells expressing P21 on the total number of satellite cells in the muscle of DMD patients and controls divided in groups according to age. The data are presented as percentage ±SD. * p≤0,05 Student's t-test. (D) Trend of senescent satellite cells number in the muscle of DMD patients and controls divided in groups according to age. The data are presented as mean. (E) Quantification of satellite cells expressing P16 on the total number of satellite cells in muscles of Becker patients and controls. (F) Quantification of satellite cells expressing H2AX on the total number of satellite cells in the muscle of Becker patients and controls. (G) Quantification of satellite cells expressing P21 on the total number of satellite cells in the muscle of Becker patients and controls. The data are presented as percentage ±SD.*

In DMD rat muscles, interestingly, was observed a significant progressive increase in the number of senescent satellite cells with aging. In Fig 19 is showed the increase of the three markers during the progression of the disease.

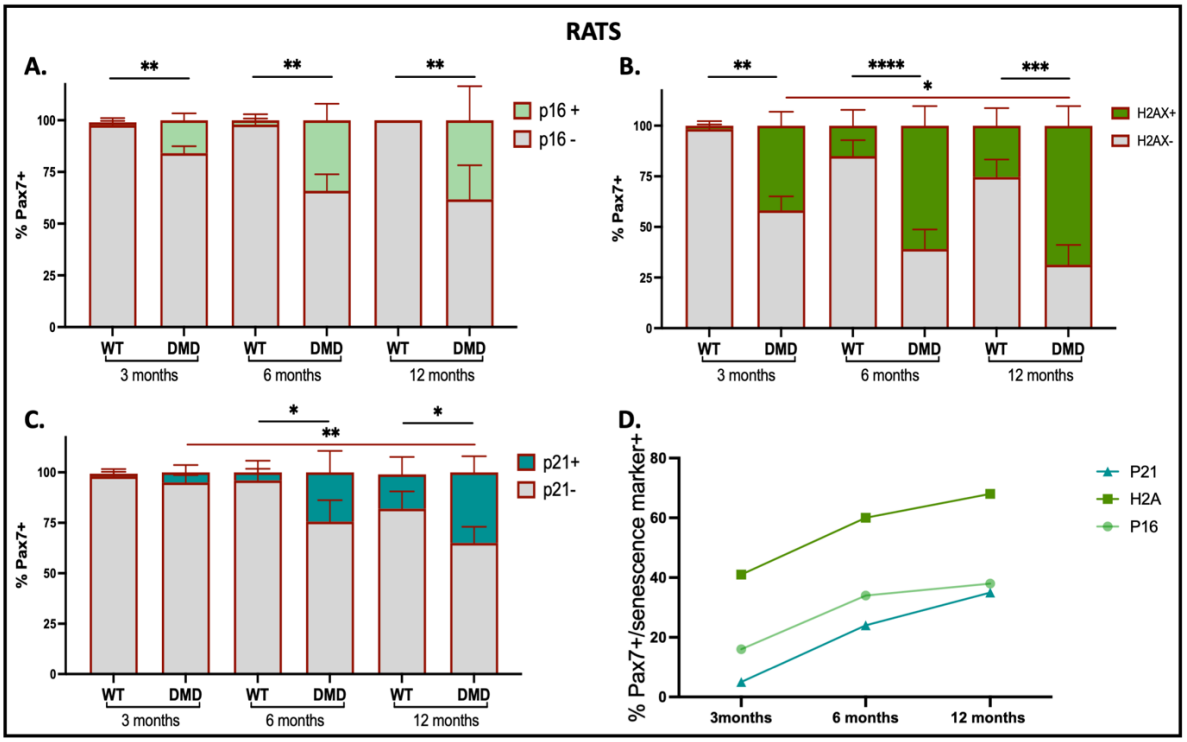

Figure 19 *Muscular satellite cells acquire a senescent phenotype during the progression of the disease. (A) Quantification of satellite cells expressing P16 on the total number of satellite cells in Tibialis Anterior of DMD rats and WT rats at different time points. (B)Quantification of satellite cells expressing H2AX on the total number of satellite cells in Tibialis Anterior of DMD rats and WT rats at different time points. (C) Quantification of satellite cells expressing P21 on the total number of satellite cells in Tibialis Anterior of DMD rats and WT rats at different time points. The data are presented as percentage ±SD. * p≤0,05 Student's t-test. (D) Trend of senescent satellite cells number in Tibialis Anterior of DMD and WT rats over time. The data are presented as mean.*

In mdx model the satellite cells acquire a senescent phenotype as well, but in an older time point. The SCs of the mouse starts to express senescent marker from 17 months old. H2AX and P21 increasing is higher than the P16 one at 17 months old which expression is very low, around

1% (Fig 20). However progressive increase in senescent satellite cells over time of the three markers was observed also in mdx model muscles while were absent in WT (Fig 20 D).

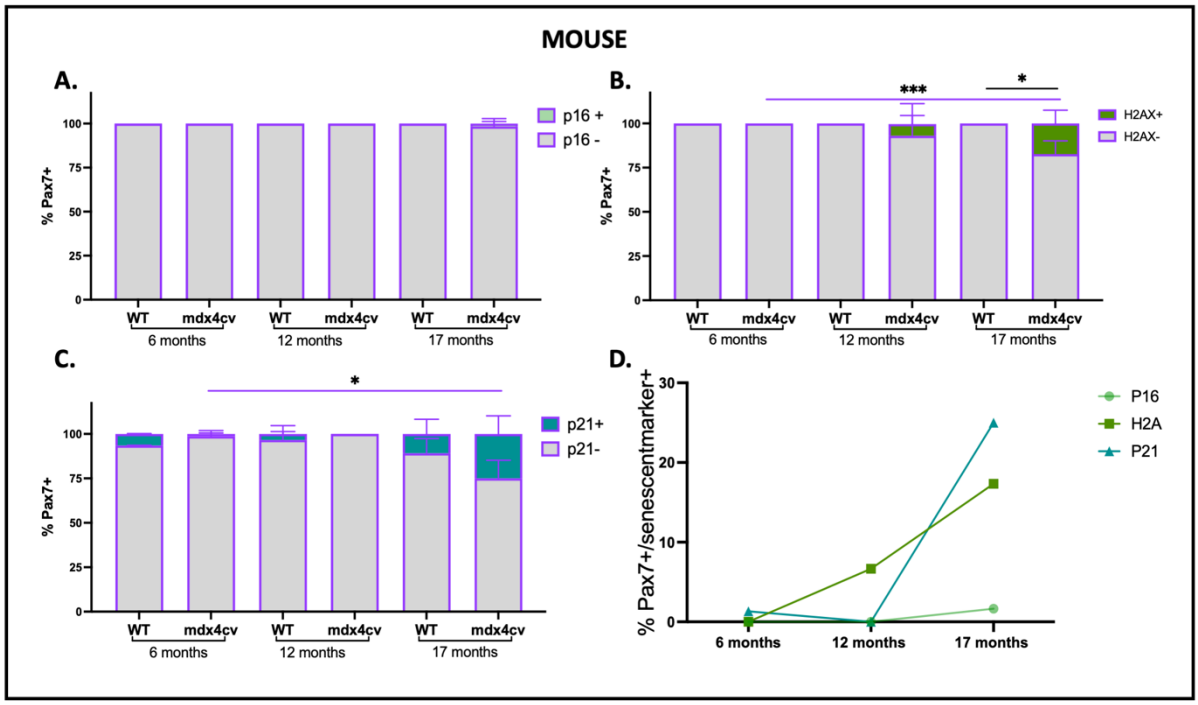

Figure 20 *Muscular satellite cells acquire a senescent phenotype during the progression of the disease. (A) Quantification of satellite cells expressing P16 on the total number of satellite cells in Tibialis Anterior of mdx and WT mice at different time points. (B)Quantification of satellite cells expressing H2AX on the total number of satellite cells in Tibialis Anterior of mdx and WT mice at different time points. (C) Quantification of satellite cells expressing P21 on the total number of satellite cells in Tibialis Anterior of mdx and WT mice at different time points. The data are presented as percentage ±SD. * p≤0,05 Student's t-test. (D) Trend of senescent satellite cells number in Tibialis Anterior of mdx and WT mice over time. The data are presented as mean.*

4.3Functional studies

4.3.1 Whole body Plethysmography

Plethysmography is an often used and reliable technique to assess the diaphragms' function (Huang et al., 2011; Nelson et al., 2011). In order to evaluate respiratory functions and to compare the diaphragm impairment, of the two models with age-matched WT different parameters has been measured (Fig. 21).

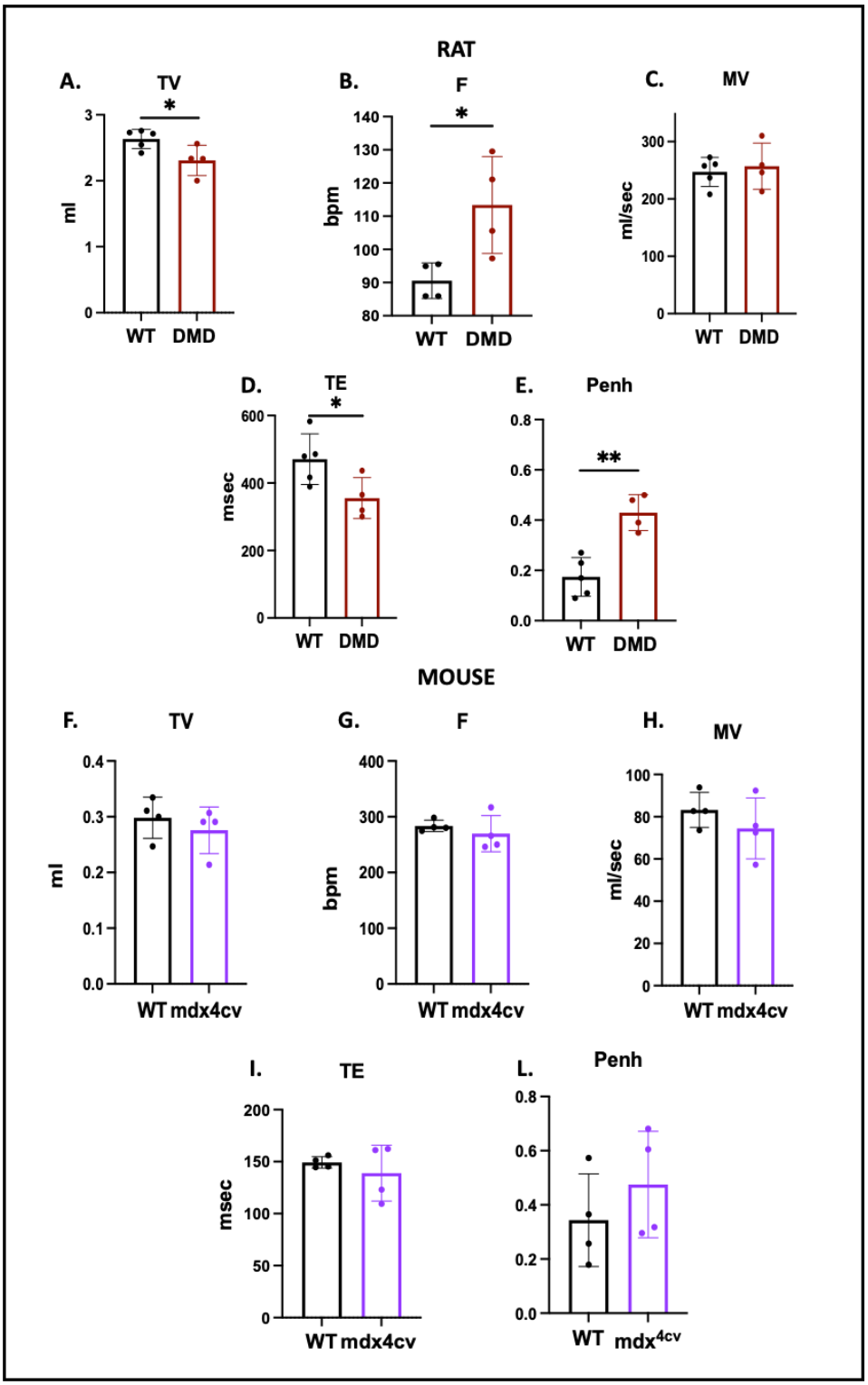

Figure 21 *Respiratory dysfunction in Rats DMDdel52 and mdx^{4cv} mice. The respiratory function of models and age-matched wild type was monitored by whole-body plethysmography, in which the animals were free to move around within an enclosed space. (A-F) Tidal Volume of Rats (6 months) (A) and mice (20 months) (F) normalized on body weight; (B-G) Frequency of breath measured breaths per minute (bpm); (C-H) Minute Volume measured in ml on seconds. (D-I) Time of expiration (E-L) Penh index, used to measure the bronchoconstriction of the models and the WT. The data are presented as mean ± SEM; * p≤0,05 Student's t-test.*

In rats the total (tidal volume TV) volume inspired was higher in WT compared to DMD with a p value p=0,03 *; in mice no significative difference was observed between the tidal volume of mdx^{4cv} and WT (Fig 21 A-F). The frequency of breaths measured breaths per minute was much higher in DMD rats compared to age matched WT p=0,02, no difference was found in the frequency between mdx4cv and their relative controls (Fig 21 B-G). Despite differences in TV and F in DMD rats and WT, no difference was observed in the MV (minute volume) as well as in mice (Fig 21 C-H).

Expiration time (TE) and Penh index are mostly used to measure the elasticity of the diaphragm which become thick and rigid due to fibrosis and scar tissue, and also to evaluate the strength and the lesser extend of intercostal muscles. The time of expiration in WT rats was longer than in DMD rats with a p value of p=0,04 *. In mice no differences were found between mdx4cv and WT's TE (Fig 21 D-I).

Regarding the Penh index, is the index used to assess respiratory function and broncho-constriction; the higher is the more are respiratory functions impaired. It is significantly elevated in DMD rats p=0,0014 compared to WT, but a slightly non-significative increase was observed in mdx4cv compared to WT.

4.3.2 Treadmill and Forelimb strength grip test

The results of the treadmill and the grip strength tests are showed in Fig. 22. Treadmill was used to assess dystrophic state, the protocol until exhaustion was used. In Figure 22 (A-B) are shown the cm on second routes by models and WT and dystrophic rats get exhausted way before mdx mice with a p value of p=0,0001****, moreover also the differences between DMD rats and age-matched WT are significative with a p value of p=0,0001****. Regarding mice instead there are no differences in the exhaustion and in the distance routes between mdx4cv and WT.

The strength of forelimb muscles was assessed with the grip test, in rats the DMD strength was lower compared to WT p=0,0077** and as expected the DMD rats seems to be weaker than mice; notwithstanding, a significative difference in the strength of mdx^{4cv} mice was observed comparing to WT p=0;03*.

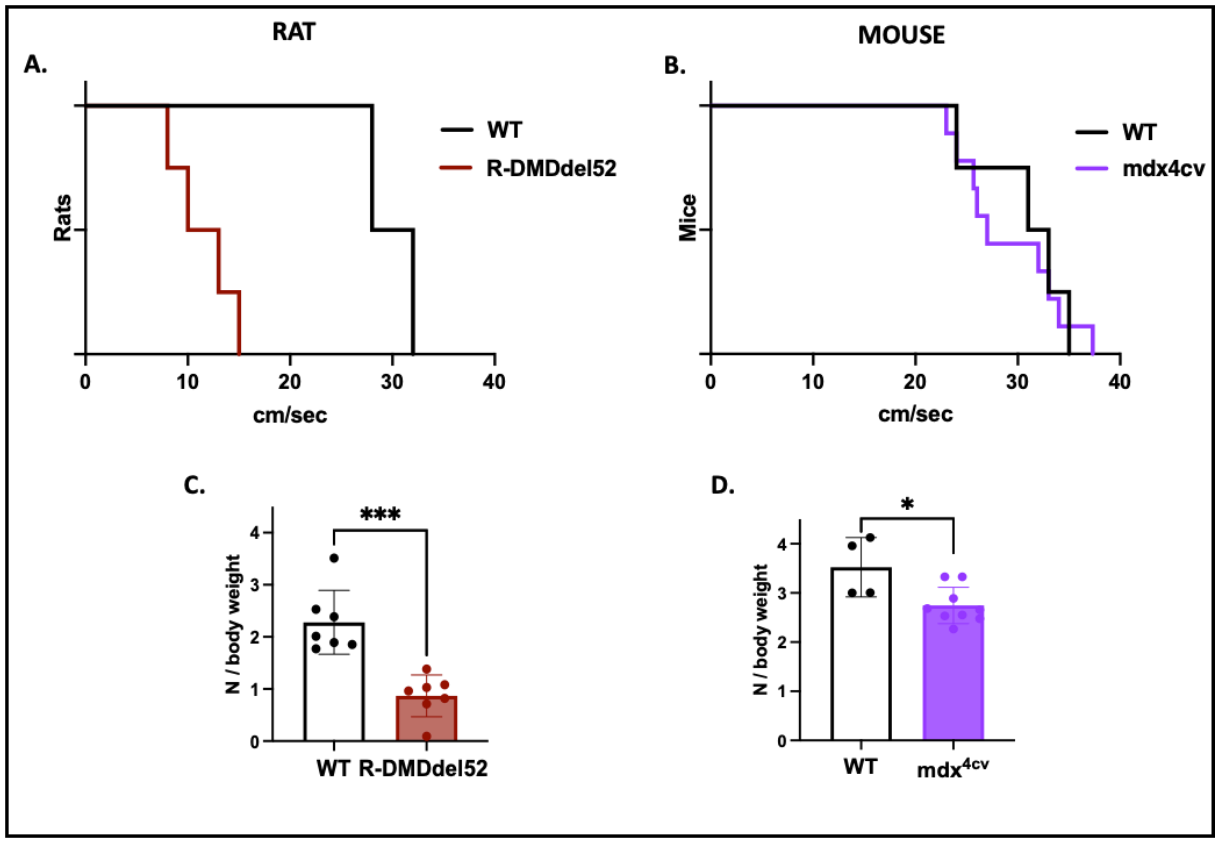

Figure 22 *Functional assessment and exercise capacity of mdx mice and DMD rats. (A.) Treadmill exhaustion protocol of rats. Distance routes is shown in cm/sec, each steps represent an animal; (B.) Treadmill exhaustion protocol of mice. Distance routes is shown in cm/sec, each steps represent an animal; (C-D) Grip test. The strength is expressed in Newton (N) and normalized on body weight. (C.) Rats (D.) Mice. The data are presented as mean ± SEM; * p≤0,05 Student's t-test.*

4.4 Correlation studies

Correlation studies has been also performed with Pearson r coefficient calculation. No correlation was found between regenerative fibers and FAPs, except for the mice in which a negative correlation was discovered r=0,90 p=0,0009*** meaning that to the increase of Faps correspond a decrease of regenerative fibers, however in rats and humans a negative correlation was discovered between regenerative fibers and fibrosis r=0,50 p=0,035* in Human and r=0,87 p=0,0020** in rats.

No correlation was found between regenerative fibers and Ki67 positive stem cells.

In patients no correlation was found between Ck levels and fibrosis. An interesting correlation was found in patients between the number of vessels and the number of active SCs r=0,90 p<0,007**

5. DISCUSSION

Duchenne muscular dystrophy (DMD) is an X-linked, genetic disease affecting 1:5000 males worldwide. DMD is a progressive, muscle-wasting disorder associated with wheelchair confinement around 15 years of age, and premature death around the age of 30 due to cardiorespiratory failure (Duan et al., 2021). Numerous of DMD animal models have been developed including porcine, canine and rhesus monkey models (Kornegay et al., 2017; Chen et al., 2015; Selsby et al., 2015). However, most early preclinical works were conducted on mdx mice that exhibit only a mild DMD pathological phenotype compared to human (Bulfirld et al., 1984; Chamberlain et al., 2007).

In our lab a new rat model of DMD has been developed (R-DMDdel52) with a deletion in the hot spot area of exons 45-55 where the majority of human mutations are occurring (Nakamura et al., 2017) (Taglietti et al., submitted). To evaluate the translational potential of our new generated R-DMDdel52 rats and the well-described *mdx*^{4cv} mouse model (McGreevy et al., 2015), we decided to perform a comparison study of these two animal models highlighting the constant and reproducible elements in common between human samples and model muscles. The protein restore of dystrophin alone is not enough to have improvements in the prognosis of the disease. Starting from human muscles we decided to identify parameters in models which better recapitulate the human disease that can be useful for pre-clinical trial and moreover useful to better understand the mechanisms behind DMD.

5.1 Analysis of histopathological markers showed variability among human DMD biopsies and confirmed the more severe phenotype of R-DMDdel52 rats

It is well known that Duchenne muscles undergo changes during the progression of the disease with degenerative-regenerative cycles (Blake et al., 2002), followed by accumulation of fibrosis, alterations in fiber size and morphology, diffuse atrophy, inflammation, necrosis, and fat tissue infiltration (Duan et al., 2021).

Affected boys appear clinically normal at birth; indeed, signs and symptoms usually become apparent around 4-5 years old, when the disease is diagnosed. However due the variability of phenotype, which may depend on the mutation, or on environment or treatment, the signs and

symptoms could appear in the early childhood around 1-2 years old (Guiraud et al., 2015; Mendell et al., 2012).

Disease progression in *mdx* is less severe than in patients. In adult *mdx*, fibrosis develops extensively only in the diaphragm muscle and never reaches the severity of human disease (Carnwath et al., 1987; Ardite et al., 2012). Keeping in mind the milder phenotype of the other mdx skeletal muscles compared to diaphragm, we decided to use for our comparative analysis the well characterized *tibialis anterior* muscle. Indeed, the available human biopsies are from limbs skeletal muscle, so to be able to perform a proper comparison between human and animal models we believed that TA muscles will be more appropriate.

The histopathological changes occurring during the progression of Duchenne muscular dystrophy, were analyzed in both dystrophic rats and mice at different time points and in DMDs and BMDs patients muscle samples divided in cohorts according to age.

A normal muscle is composed of fibres that are uniform in size, and polygonal in shape, while DMD muscle present variable degrees of atrophy, hypertrophy and an increased myofiber size variation (Blake et al., 2002). In *mdx* mice variation in size of the fibers appears in adulthood (10 months old) (Ben Larbi et al., 2021), and in DMD patients the signs are usually visible at 4-5 years old (Guiraud et al., 2015).

In humans the heterogeneity in the myofiber size and in shape is visible by H&E staining. The changes are evident at 4-year-old on, as described by Girauld et al. (Girauld et al., 2015). However, differences in the calibre of fibers were found also in younger patients, in which the control fibers result to be bigger (Duddy et al., 2015). In our cohort of DMD patients we also observed a greater number of fibers with a reduced calibre compared to controls, confirming the myofiber atrophy of DMD muscles (Duan et al., 2021). Importantly, compared to animal models, human muscle samples showed a higher variability. The variability between samples was also found in BMDs that develop a milder dystrophic phenotype than DMDs (Waldrop et al., 2019). The high heterogeneity in fiber size quantified in each BMD biopsy, combined with the low number of available samples, limited the analysis we can conduct on these samples. Indeed, the variability is too high to be able to drive any conclusion. Identifying the bases of such variability in both DMD and BMD samples is relevant for patient counselling, prognosis, stratification in trials, and identification of therapeutic targets. Numerous studies have been already conducted to elucidate the causes of this variability. For example, it has been seen that the type of mutation could influence the severity of the disease (Zatz et al., 2014; Winnard et

al., 1995; Wang et al., 2017; Muntoni et al., 1994; Aartsma-Rus et al., 2006). Indeed, patients carrying isolated deletion of exon 45 of *DMD* gene show a milder phenotype compared to what observed for other type of mutations (Pane et al., 2014; van den Bergen et al., 2014; Dwianingsih et al., 2014). In our cohort, patients present different mutations, and this could explain the high variability observed. The disease severity could also differ among patients with different socio-economic conditions and environmental factors (Hufton et al., 2017). Unfortunately, these data are often very difficult to obtain, limiting a better stratification of the patients.

Finally, mutations in different genes have been associated with variability of the phenotype in Duchenne muscular dystrophy, recently reviewed by Bello (Bello et al., 2019). For example, mutation in *SPP1, LTBP4, CD40* and *THBS1* genes, implicated in inflammatory pathways, play a role in influencing DMD severity (Bello et al., 2019). In the future, it would be useful to perform further genomic analysis with the aim to identify novel disease-related genes and correlate them with the muscle phenotype.

Regarding DMD rat and mouse animal models, we observed lower variability among each individual and that myofiber morphological alterations in calibre are significantly different in mdx mice compared to WT after 2 months of age, while in DMD rats these alterations appear earlier. Also, we observed that the number of centrally nucleated fibers does not correlate with the pathology progression in both rat and mouse DMD animal models, as well as in patients, only a slight decrease was observed in the samples of higher age animals and patients. Centrally nucleated fiber represents the fibers that underwent cycles of degeneration/regeneration (Narita et al., 1999). Although without a clear trend, the number of fibers with internalized nuclei is significantly higher in DMD samples (both from rats/mice and human) compared to WT/controls, suggesting that regenerative and degenerative cycles are occurring in DMD muscles independently of phenotype and age.

As already discussed, human sample variability reduces the statistical power of different histological analysis and quantifications for a small sample size. Indeed, due to this high variability, we were not able to appreciate an increase in fibrotic deposition with age in DMD human samples. On the other hands, the increase of fibrosis was clearly observed in DMD rats, while mdx muscles do not present a clear trend, as previously reported (Lefaucheur et al., 1995; Ben-Larbi et al., 2020). Interestingly, fat tissue infiltration increases in both animal models as well as in DMD patients over time, confirming previously data showing that the fat replacement

occurs late in the disease in a progressive way (Collins et al., 2003; Blake et al., 2002). To notice, *mdx4cv* muscles present only a very low percentage of fat tissue and at later stages (20 moths of age) as also showed by Ben-Larby in a cohort of mdx^{4cv} mice (Ben-Larbi et al., 2020). Both fibrosis and fat infiltration were also assessed in Becker patients in which no significance differences were observed compared to controls. Indeed, BMDs showed a mild muscle phenotype compared with DMD samples.

5.2 Dystrophin "revertant fibers" increase over time

Duchenne muscles are characterized by the absence of dystrophin protein expression, excepting some fibers that can present some level of dystrophin expression. These fibers are called "revertant fibers" (Shahnoor et al., 2018). In our analyses we observed than in the first stages of the disease in DMDs patients were not presents revertant fibers which start to be expressed after 7 years old, when the worsening of the disease is progressing.

In animals carrying a null mutation in *dystrophin* gene, the presence of revertant fibers is rarely occurring, and it increases with age (Lu et al., 2000). In our study, we reported a low percentage of dystrophin-positive fibers in *mdx,* while this percentage was higher in DMD rats and it also increases with age, reaching a percentage of *circa* 5%.

In literature, it is widely reported the notion that up to 50% of DMD patients presents revertant fibers in a percentage from 1 to 6% (Hoffman et al., 1987; Nicholson et al., 1989; Nicholson et al., 1990). Interestingly, there is a positive correlation between percentage of revertant fibers and the age or the progression of the disease (Fanin et al., 1992; Fanin et al .,1995).

We also observed an increase over time in presence of fibers expressing dystrophin which is consistent with the data previously cited.

Taking into account all these considerations, we can conclude that the expression pattern of dystrophin-revertant fibers is more similar between DMD patients and our rat than mdx mice.

What is fascinating, it is that the molecular mechanisms at the base of the expression of dystrophin in a DMD context are still unclear. Some hypotheses have been proposed as sporadic alternative splicing events able to skip the mutation in the DMD gene or newly generated mutations, occurring upon repetitive cycles of regeneration and able to correct the native mutation (Crawford et al., 2001; McGreevy et al., 2015). Our future aim is to increase the number of DMD patients, to be able to utilise other techniques to quantify dystrophin

expression. We could, indeed, verify if there is a correlation between Dystrophin levels and disease progression or severity.

5.3 Analyses of the behaviour of muscular satellite cells highlight their exhaustion and the acquisition of senescence traits in DMD muscles

In patients with Duchenne muscular dystrophy, it is reported an impaired muscle regeneration (Verhaart et al., 2019). The ability to regenerate muscle rely on muscle-specific stem cells (MuSCs), also called satellite cells, which after muscle tissue damage activate and proliferate to create a pool of myoblasts, able to differentiate in newly generated myofibers (Yin et al., 2013). To elucidate the extent of muscle regeneration in our DMD animal models and in DMD human biopsies we firstly quantified the number of regenerating myofibers over time. Our analysis showed a decrease in the number of new formed fibers with the progression of the disease in both animal models and also in DMD patients. These data are in agreement with previous studies conducted on another DMD rat model (Sugihara et al., 2020) and on mdx mice (vanPutten et al., 2019; Giraud et al., 2019).

Since satellite cells are responsible of muscle regeneration (Mauro et al., 1961; Dumont et al 2011; Boldrin et al., 2015), we decided to quantify the number of satellite cells in all our samples, to understand if the decline in muscle regeneration is due to a loss of the pool of these stem cells.

In DMD human muscles, is usually described an increase in the number of satellite cells (Maier et al., 1999; Ishimoto et al., 1983) followed by alteration in differentiation (Kottlors et al., 2010). Surprisingly in our patients we observed a slight decrease in the number of satellite cells and alterations in their activation. These data could explain the decline observed along time in muscle regeneration.

Conflicting data have been obtained regarding changes in the number of satellite cells in DMD samples compared to controls, making hard to drive precise conclusions (Ben-Larbi et al., 2019; Luz et al., 2002; Jasmin et al., 1984). In our study, we observed that the total number of satellite cells was not diminishing over time in R-DMDdel52 rats, and it was higher compared to WT. However, the activation of satellite cells is dropping starting from 3 months of age, correlating with the lower number of regenerating myofibers. Also, in mdx mice the total number of SCs was stable over time, with a decrease in their activation potential starting around 17 months old.

The higher activation capacity of mdx SCs compared to DMD rats could explain the mild phenotype of mdx mice. This hypothesis is strengthened by a previous study of Sacco et al. (Sacco et al., 2010) in which it has been demonstrated that the milder mdx phenotype is worsened if the satellite cells have shortened telomeres and thus a compromised regenerative capacity.

All together this data suggest that SC play a key role in DMD progression and that they may have crucial therapeutic implications for an effective DMD treatment.

Recently it has been showed that in an another DMD rat model, muscles satellite cells express senescent markers (Sugihara et al., 2020), hence we decided to explore whether this event occurred in mice and humans in addition to rats. The senescence markers we decided to investigate are p16, p21 and the phosphorylation of the histone variant H2AX. These are all well know senescence markers with p16 and p21 playing a role in cell cycle arrest, while the gamma H2AX marks DNA damage that triggers the entry into senescence (Sharma et al., 2012, Teramoto et al., 2021).

Mdx satellite cells started to express H2AX and P21 around 17 months of age and as slight expression of P16 is observed. On the counterpart these senescent markers, P21, P16 and H2AX were already observable in DMDdel52 rats SCs at 3 months of age and increased over time. Also, in DMD patients we observed an increased number of SCs expressing P16, and H2AX compared to control, while the expression of P21 was variable.

Senescence is involved in the progression of various diseases such as atherosclerosis (Childs et al., 2016), hepatic steatosis (Ogrodnick et al., 2017), diabetes and others (Schafer et al., 2017). The hypothesis is that senescent stem cells could be involved in the severity of Duchenne phenotype, impinging on muscle regeneration. Senolytic drugs has been tested on DMD rats, showing an improvement of muscle function and regeneration but the continuous activation of SC could lead to the development of rhabdomyosarcoma (Teramoto et al., 2021; Karimian et al., 2016; Sugihara et al., 2020). R-DMDdel52 better than mdx thanks to the early SC senescence phenotype could be useful to further elucidate the biological significance of stem cell senescence in DMD and to test new therapies that could modulate these aspects, favouring the maintenance of muscle regeneration over time.

5.3.1 Inflammation and FAPs could play a role in influencing satellite cell behaviour and phenotype of DMD muscles

Alteration in satellite cell number and activation might be determined by extrinsic factors constituting the muscle stem cell niche or microenvironment. Indeed, malfunction of geriatric satellite cells was linked to the niche factors and rescued after being exposed to a young milieu or serum (Carlson et al., 2005; Conboy et al., 2005; Brack 2007). In DMD, extracellular matrix (ECM) proteins that form the fibrosis might influence the regeneration capacity of SCs (Carlson et al., 1989; Zacks et al., 1982); indeed, we found a negative correlation between the number of eMHC positive fibers and fibrosis.

Skeletal muscle mesenchymal progenitors also known as Fibro-adipogenic progenitors (FAPs) are the cells mainly responsible of the secretion of ECM proteins constituting the fibrosis in skeletal muscle (Judson et al., 2017; Joe et al., 2010). FAPs have been also associated with the pathogenesis of Duchenne muscular dystrophy in *mdx*, because they contribute to the perivascular cardiac fibrosis, exerting they fibro-genic action via transforming growth factor-β1 (TGF-β1) (Uezumi et al., 2014; Ieronimakis et al., 2013). Herein we showed a high number of FAPs in DMD rats skeletal muscle with increase with age, although the increased number of FAPs compared to WT was not striking in mdx mice as it was for DMD rats and humans. This could explain the different severity of the fibrotic phenotype between the two models.

Recently it has been discovered that TGF-β is associated with senescence phenotype (Tominaga et al., 2019), and senescent cells not only cease the cell cycle but also secrete cytokines as TGF-β (Coppè et al., 2010). Given the large presence of FAPs in DMD rat muscles, we might also speculate that stem cell senescence may somehow depend on this signalling. Thus, giving a dual role to the action of TGF-β in stimulating fibrosis production and in inducing cell senescence.

High expression of TGF-β1 has been detected also in DMD patients (DePaepe et al., 2013) and correlate with the severity of the phenotype (Song et al., 2017). This corroborates the hypothesis that TGF-β1could be involved in the worsening of the phenotype and in the senescence of cells. Fitting with this concept, the application of losartan, drug counteracting TGF-β1 activity, to *mdx* mice has been shown to ameliorate differentiation and muscle regeneration with a

reduction of fibrosis (Cohn et al., 2007). We suggest that further studies are needed to better understand the correlation between TGF-β1 and DMD pathological and molecular mechanisms.

Moreover, inflammatory cells, mainly macrophages, are another source of TGF-β1 (DePaepe et al., 2013). A previous study on rats, demonstrated a high number of CD45+ cells in rat skeletal muscle, and improvements in the phenotype after anti-CD45 antibody treatment (Ouisse et al., 2019). Inflammatory infiltrates are highly presents in R-DMDdel52 at 3 months, followed by a decrease in their number with the disease progression. While in *mdx* mice we observed a constant increase in the number of inflammatory cells. We could explain the decrease in CD45+ cells observed in DMD rats after 3 months of age by the fact that the skeletal muscles begin to be replaced by fibrotic and fat tissue, leading to a decrease in the contraction activity of the muscle, and in the myonecrosis that recruits the inflammatory cells. On the other part, in mdx mice the muscles are less affected. Also, several studies have demonstrated that immunity cells could ameliorate lesions in the muscle. Training induces inflammation in muscles (Gordon et al., 2012), and in trained muscles the transcription of genes involved in the switch from pro- to an anti- inflammatory macrophage has been observed (Gordon et al., 2012). For example, NF-KB-binding activity, that promotes pro-inflammatory gene expression, has been found downregulated in muscles following adaptation to exercise (Xin et al., 2014). On the other side, up-regulation of the chemokine CCL2, which is the monocyte recruiter, may enhance processes involved in muscle repair (Hubal et al., 2008; Deyle et al., 2016). Further studies are necessary to elucidate the expression of these chemokines in mdx muscles and to understand if the presence of the inflammatory cells could play a role in softening the severity of the disease.

It is important also to emphasize that the sequence and timing of muscle inflammation phases are critical for muscle regeneration (Chazaud et al., 2016). All the subsequent phases of inflammation are parts of the recovery process occurring after injury. Indeed, prolonged presence of pro-inflammatory macrophages in dystrophic muscles (Ben Larbi et al., 2021), contribute to the establishment of chronic inflammation and fibrosis with a consequent regeneration impairment (Yahiaoui et al., 2008).

Also, chronic inflammation may play a role in inducing senescence. Indeed, senescence can be induced by several genotoxic stressors and damaging stimuli such as DNA damage, and oxidative stress (Pole et al., 2016; Hernandez et al., 2018). Persistent inflammation in Duchenne muscles leads to chronic damage resulting in accumulation of oxidative stress (Terril et al.,

2016). Progressive increase in oxidative stress levels have been found in Duchenne patient muscles (Petrillo et al., 2017).

Oxidative stress is characterised by the formation of free radicals that damage important biological molecules. These are therefore considered to be highly dangerous particles, as nitric oxide (NO) (Jones 2008). NO is a gaseous molecule secreted by endothelial cells when vasodilatation is needed in capillaries (Robbins et al., 1997). NO is also produced by the muscular enzyme, NO synthase (n-NOS), which normally binds proteins belonging to dystrophin complex. Lack of dystrophin lead to a delocalization of n-NOS floating in the cytoplasm with alterations in its functions (Brenman et al., 1995; Crosbie et al., 2002). During exercise when oxygen is needed, muscle ischemia may occur in Duchenne muscle (Sander et al., 2000), and NO may be involved in misregulation of the vascular supply (Crosbie et al., 2001). However, we did not observe any alterations in the number of vessels in Duchenne muscles, but we show an interesting correlation between the number of vessels and the number of activated satellite cells. This reinforces the knowledge of an existing cross-talk between vascular niche and SCs (Verma et al., 2018) and it is in line with previous studies that have shown that an higher vascular density is increasing SC number in mdx mice (Matsakas et., al 2013; Verma et al., 2010). Altogether this data suggests that in DMD muscles there are not major vascular alteration and that vessels can have a pro-myogenic influence on the muscles.

5.4 Functionals studies showed more severe phenotype of R-DMDdel52 rats compared to milder phenotype of *mdx*^{4cv} mice

We decided to perform muscle functional studies on the two models with the aim to compare the muscle strength and respiratory capacity.

To assess skeletal muscle performance in vivo, we measured both muscle strength and endurance of performing respectively the forelimb grip test and the treadmill until exhaustion.

The grip test highlighted loss of strength in both animal models in comparison with the respective 6 months WT controls. However, the decreased muscle strength observed in 6 and 20 mdx months old *mdx* mice was less strikingly than the one observed in R-DMDdel52 rats. Also, the decrease in the maximal force applied by R-DMDdel52 rats was bigger than those observed in another DMD rat model (Larcher et al., 2014).

Regarding the treadmill test, different protocols have been already used to analyse the consequences of exercise in mdx animals, and often the differences between 20 months old mdx and age-matched WT were not significant, confirming the mild phenotype of these models (Radley-Crabb et al., 2011; Zelikovich et al., 2019; Capogrosso et al., 2017).

In agreement with these previous publications, treadmill test conducted on 20-month-old mdx mice compared with aged-matched controls, did not reveal any differences between the two groups. On the other side much younger R-DMD-del52 rats (6 months) were unable to run as the same extent of WT rats showing a strong impairment in exercise capacity and advanced muscle weakness.

Duchenne muscular dystrophy is associated with respiratory impairments, which lead to the need of ventilators (Gozal et al., 1999). Decreasing of respiratory functions in DMD patients is progressive (Gayraud et al., 2010, LoMauro et al., 2010) and they are a consequence of abdominal, diaphragm and intercostal muscle weakness (LoMauro et al., 2018; Ishizaki et al., 2008). In adult (20 months old) *mdx* mice the respiratory capacity was compromised with increased respiratory rate and a decreased total inspired volume. Moreover, it has been demonstrated that double knockout (mdx/Sgcg $^{-/-}$ and mdx/utrn$^{+/-}$) mice showed a worse impairment of respiratory functions compared to *mdx* mice demonstrating the existence of compensatory effects in *mdx* mice that attenuate the severity of the disease (Roberts et al., 2014; Huang et al., 2011). Burns et al. assessed the respiratory capacity in *mdx* mice during hypercapnic hypoxia showing that *mdx* mice preserve the ventilatory capacity, which demonstrate again the mild respiratory impairment in those mice despite the weakness of the diaphragm which is the most severely affected muscle in mdx mice (Ishizaki et al., 2008; Burns et al., 2019). Whole body plethysmography performed on 20 months old mdx and 6 months old R-DMDdel52 rats show that DMD rats develop a wider respiratory impairment compared with *mdx* mice. Tidal volume (TV) and time of expiration, main indicators of muscle elasticity, were found to be significantly decreased in R-DMDdel52 rats comparing to WT, but not in *mdx* mice that showed only a slight decrease in the TV. This could suggest that the diaphragm of rats together with abdominal, and intercostal muscles is weaker and more affected than the one of mdx mice.

Another parameter used to assess respiratory impairments is the Penh (enhanced pause), that reflects respiratory functions and bronchoconstriction (Burns et al., 2019). We observed a high

increase of Penh in R-DMDdel52 rats compared with WT littermates, while its increase in mdx mice was less evident.

Another important point confirming the severity of disease in R-DMDdel52 rats is the significantly reduced lifespan. It is well known that mdx mice have a normal lifespan (McGeevy et al., 2015). While the DMD rats did not survive beyond 14 months of age, while the life expectancy of WT rats is around 24 months old. This strongly corroborates the evidence of the milder phenotype of the mdx mice.

With these functional results combined with life expectancy we can assert the milder phenotype of the mdx mice compared to the newly developed DMD rats which shows a much more severe phenotype, with reduced exercise capacity as well reduced respiratory functions. Since corticosteroid treatment is proven to delay respiratory impairment in DMD patients with extended life expectancy (Machado et al., 2012), through molecular mechanisms not fully understood, we suggest that R-DMDdel52 could be a good model to further elucidate these aspects.

6. CONCLUSIONS

Results obtained in this thesis showed the severe dystrophic phenotype of a new generated DMD rat model (R-DMDdel52) and confirmed the mild phenotype observed in *mdx* mice. Indeed, R-DMDdel52 rats showed an earlier and progressive deterioration of muscle morphology and function culminating in a more exacerbated phenotype compared to mdx mice. Indeed, mdx mice reach the severity observed in R-DMDdel52 rats only at advanced age (more than 17 months). Regarding the human biopsies we have collected and used in this study, the variability of phenotype developed by each DMD patient is sometimes too high to be able to drive clear conclusions. This variability may depend on a multitude of factors, such as genetic mutations, or epigenetic. Although the hard interpretation of the data obtained from human samples, our study reveals that R-DMDdel52 rat model recapitulates the major hallmarks of the human disease better than mdx4cv mice and could be used as a valuable and reliable model for DMD. Moreover, it can be considered as a preclinical model for the study of safety and efficiency for future novel DMD therapies. Also, R-DMDdel52 rats can be used for further studies to better elucidate the mechanisms behind the pathogenesis of Duchenne muscular dystrophy.

Another important conclusion highlighted by our study is the importance of muscle stem cells in the progression of Duchenne muscular dystrophy. We demonstrated that they become senescent, in the animal models as well as in humans, and this might explain the inability to repair the tissue damage occurred with the DMD. Thus, we suggest that stem cell senescence could be a crucial target for the development of future treatments.

At this point, we can speculate that niche extrinsic factors might be involved in the dysregulated behaviour occurring in satellite cells, rather than an intrinsic defects of satellite cells. Indeed, in mdx4cv mice with a milder muscle phenotype, the senescence of SCs is occurring much later during the progression of the disease. Thus, the role of inflammatory pathways as well as of fibrotic deposition in influencing the entry of SCs into a senescence state need to be deeper studied, as follow-up of our study.

7. BIBLIOGRAPHY

Aaron s. Zelikovich. Mattia Quattrocelli. Isabella M. salamone. Nancy L. Kuntz & Elizabeth M. McNally Moderate exercise improves function and increases adiponectin in the *mdx* mouse model of muscular dystrophy *Scientific RepoRts* | 2019 9:5770

Aartsma-Rus A. Antisense-mediated modulation of splicing: Therapeutic implications for Duchenne muscular dystrophy. *RNA Biology*. 2010 7(4):453–61

Aartsma-Rus A. Fokkema I. Verschuuren J. Ginjaar I. van Deutekom J. van Ommen G-J. Theoretic applicability of antisense-mediated exon skipping for Duchenne muscular dystrophy mutations. *Hum Mutat.* 2009 Mar;30(3):293–9

Aartsma-Rus A. Ginjaar IB. Bushby K. The importance of genetic diagnosis for Duchenne muscular dystrophy. *Med Genet J* 2016 53:145–151

Aartsma-Rus A. Krieg AM. FDA Approves Eteplirsen for Duchenne Muscular Dystrophy: The Next Chapter in the Eteplirsen Saga. *Nucleic Acid Therapeutics*. 2017 27(1):1–3

Aartsma-Rus A. Morgan J. Lonkar P. Neubert H. Owens J. Binks M. Montolio M. Phadke R. Datson M. Van Deutekom J. Morris GE. Ashutosh Rao V. Hoffman EP. Muntoni F Arechavala-Gomeza V. workshop participants Report of a TREAT-NMD/World Duchenne Organisation Meeting on Dystrophin Quantification Methodology. *J Neuromuscul Dis.* 2019 6(1):147-159.

Aartsma-Rus A. Straub V. Hemmings R. Haas M. Schlosser-Weber G. Stoyanova-Beninska V. Mercuri E. Muntoni F. Sepodes B. Vroom E. Balabanov P. Development of Exon Skipping Therapies for Duchenne Muscular Dystrophy:A Critical Review and a Perspective on the Outstanding Issues. *Nucleic Acid Ther.* 2017 27:251-259

Aartsma-Rus. A. Van Deutekom. J.T. Fokkema. IF. Van Ommen. GJB. Den Dunnen. JT. Entries in the Leiden Duchenne muscular dystrophy mutation database: An overview of mutation types and paradoxical cases that confirm the reading-frame rule. Muscle Nerve. 2006. 34. 135–144.

Ahn AH. Kunkel LM. The structural and functional diversity of dystrophin. *Nat Genet*. 1993 3(4):283–91

Amoasii L. Hildyard JCW. Li H. et al. Gene editing restores dystrophin expression in a canine model of duchenne muscular dystrophy. Science. 2018;51 1-6

Amthor H. Egelhof T. McKinnell I. Ladd ME. Janssen I. Weber J. Albumin targeting of damaged muscle fibres in the mdx mouse can be monitored by MRI. Neuromuscul Disord. 2004 14(12):791–6

Anthony K, Arechavala-Gomeza V, Ricotti V, Torelli S, Feng L, Janghra N, Tasca G, Guglieri M, Barresi R, Armaroli A, Ferlini A, Bushby K, Straub V, Ricci E, Sewry C, Morgan J, Muntoni F. Biochemical characterization of patients with in-frame or out-of-frame DMD deletions pertinent to exon 44 or 45 skipping. *JAMA Neurol*. 2014 71(1):32-40

Ardite. E. Perdiguero. B. Vidal. S. Gutarra. A. L. Serrano. and P. Mun˜ozCa´noves. “PAI-1-regulated miR-21 defines a novel age-associated fibrogenic pathway in muscular dystrophy.” *Journal of Cell Biology*. 2012. 196.1.163–175.

Baghdadi MB. Tajbakhsh S. Regulation and phylogeny of skeletal muscle regeneration. *Developmental Biology*. 2018;433(2):200-209

Banks GB and J. S. Chamberlain. “The value of mammalian models for duchenne muscular dystrophy in developing thera- peutic strategies.” *Current Topics in Developmental Biology*. 2008. 84 431–453.

Banks GD. Chamberlain JS. “The value of mammalian models for duchenne muscular dystrophy in developing therapeutic strategies.” *Current Topics in Developmental Biology*. 2008. 84. 431–453.

Barresi R. Disruption of heart sarcoglycan complex and severe cardiomyopathy caused by beta sarcoglycan mutations. *Journal of Medical Genetics*. 2000 1;37(2):102–7.

Bayliss OB. Adams CWM Bromine-Sudan Black: a general stain for lipids including free cholesterol *The histochemical journal* 1972 4.505-515

Ben Larbi S. Saclier M. Fessard A. Juban G and Chazaud B. Muscle of DMD MDX4CV Mice from 1 to 24 Months *Journal of Neuromuscular Diseases* (2021)

Bentzinger CF. Wang YX. Rudnicki MA. Building muscle: molecular regulation of myogenesis. *Cold Spring Harb Perspect Biol*. 2012 1;4(2)

Bernasconi P. Di Blasi C. Mora M. Morandi L. Galbiati S. Confalonieri P. Cornelio F. Mantegazza R. Transforming growth factor-beta1 and fibrosis in congenital muscular dystrophies. *Neuromuscul Disord* 1999 9:28–33

Bernasconi P. Torchiana E. Confalonieri P. Brugnoni R. Barresi R. Mora M. et al. Expression of transforming growth factor-beta 1 in dystrophic patient muscles correlates with fibrosis. Pathogenetic role of a fibrogenic cytokine. *J Clin Invest*. 1995 1;96(2):1137–44

Bettica P. Petrini S. D'Oria V. D'Amico A. Catteruccia M. Pane M. Sivo S. Magri F. Brajkovic S. Messina S. Vita GL. Gatti B. Moggio M. Puri PL. Rocchetti M. De Nicolao G. Vita G. Comi G. Bertini E. Mercuri E. Histological effects of givinostat in boys with Duchenne muscular dystrophy. *Neuromuscular Disorders.* 2016 26(10). 643–649

Biernacka A. Dobaczewski M. Frangogiannis NG. TGF-β signaling in fibrosis. *Growth Factors.* 2011 29(5):196–202.

Biressi S. Molinaro M. Cossu G. Cellular heterogeneity during vertebrate skeletal muscle development. *Developmental Biology* 2007 308: 281-293

Birnkrant DJ. Bushby K. Bann CM. Alman BA. Apkon SD. Blackwell A. et al. Diagnosis and management of Duchenne muscular dystrophy. part 2: respiratory. cardiac. bone health. and orthopaedic management. *The Lancet Neurology*. 2018 17(4):347–61

Birnkrant DJ. Bushby K. Bann CM. Apkon SD.Blackwell A. Brumbaugh D. Diagnosis and management of Duchenne muscular dystrophy. part 1: diagnosis. and neuromuscular. rehabilitation. endocrine. and gastrointestinal and nutritional management. *The Lancet Neurology* 2018 17(3):251–67

Bladen. C. L. Salgado D. Monges S The TREAT-NMD DMD global database: analysis of more than 7000 Duchenne muscular dystrophy mutations. *Hum. Mutat.* 2015 36. 395–402

Blake DJ. Weir A. Newey SE. Davies KE. Function and Genetics of Dystrophin and Dystrophin-Related Proteins in Muscle. *Physiological Reviews.* 2002 1;82(2):291–329.

Boldrin. L. Zammit. P. S. & Morgan. J. E. Satellite cells from dystrophic muscle retain regenerative capacity. *Stem Cell Res* 2015 14. 20–29.

Bradley WG. Fulthorpe JJ. Studies of sarcolemmal integrity in myopathic muscle. *Neurology*. 1978 28(7):670–7.

Bradley WG. Hudgson P. Larson F. Papapetropoulos TA. Jenkison M. Structural changes in the early stages of Duchenne muscular dystrophy. *J Neurol Neurosurg Psychiatry*. 1972 35(4): 451–455.

Brenman JE. Chao DS. Gee SH. McGee AW. Craven SE. Santillano DR. et al. Interaction of Nitric Oxide Synthase with the Postsynaptic Density Protein PSD-95 and α1-Syntrophin Mediated by PDZ Domains. Cell. 1996 84(5):757–67.

Brenman JE. Chao DS. Xia H. Aldape K. Bredt DS. Nitric oxide synthase complexed with dystrophin and absent from skeletal muscle sarcolemma in Duchenne muscular dystrophy. *Cell* 1995 82:734- 52.

Bulfield G. Siller WG. Wight PA. Moore KJ X chromosome-linked muscular dystrophy (mdx) in the mouse. *Proc Natl Acad Sci U S A* 1984 81: 1189-1192

Burns DP. Kevin H. Murphy. Eric F. Lucking and Ken D. O'Halloran Inspiratory pressure-generating capacity is preserved during ventilatory and non-ventilatory behaviours in young dystrophic *mdx* mice despite profound diaphragm muscle weakness *J Physiol* 2019 831–848

Burns DP. Kevin H. Murphy. Eric F. Lucking and Ken D. O'Halloran Inspiratory pressure-generating capacity is preserved during ventilatory and non-ventilatory behaviours in young dystrophic *mdx* mice despite profound diaphragm muscle weakness *J Physiol* 2019 597.3 831–848

Burton EA. Tinsley JM. Holzfeind PJ. Rodrigues NR. Davies KE. A second promoter provides an alternative target for therapeutic up-regulation of utrophin in Duchenne muscular dystrophy. *Proc Natl Acad Sci U S A* 1999 23;96(24):14025-30.

Bushby K. Finkel R. Birnkrant DJ. Case LE. Clemens PR. Cripe L. et al. Diagnosis and management of Duchenne muscular dystrophy. part 1: diagnosis. and pharmacological and psychosocial management. *The Lancet Neurology*. 2010 9(1):77–93

Bushby K. Sheerin UM. The muscular dystrophies. *Neurogenetics: A Guide for Clinicians*. 2012 359:148-165.

Byers TJ. Lidov HGW. Kunkel LM. An alternative dystrophin transcript specific to peripheral nerve. *Nat Genet*. 1993 4(1):77–81

Capogrosso RF. Mantuano P. Cozzoli A. Sanarica F. Massari AM. Conte E. Fonzino A. Giustino A. Rolland JF. Quaranta A. De Bellis M. Camerino GM. Grange RW. and De Luca A. Contractile efficiency of dystrophic mdx mouse muscle: in vivo and ex vivo assessment of adaptation to exercise of functional end points *J Appl Physiol* 2017.122: 828–843.

Carlson BM. Faulkner JA Muscle transplantation between young and old rats: age of host determines recovery. *Am J Physiol* 1989 256:C1262–C1266

Carnwath JW. Shotton DM. "Muscular dystrophy in the mdx mouse: histopathology of the soleus and extensor digitorum longus muscles." *Journal of the Neurological Sciences*. 1987 80. 1. 39–54.

Carnwath JW. Shotton DM. "Muscular dystrophy in the mdx mouse: histopathology of the soleus and extensor digitorum longus muscles." *Journal of the Neurological Sciences*. 1987.80:1. 39–54.

Carter. John C. Sheehan. Daniel W. Prochoroff A. Birnkrant DJ. *Muscular Dystrophies. Clinics in Chest Medicine* 2018. *39(2). 377–389.*

Chamberlain JS. Metzger J. Reyes M. Townsend D. Faulkner JA. Dystrophin-deficient mdx mice display a reduced life span and are susceptible to spontaneous rhabdomyosarcoma. FASEB J 2007 21: 2195-2204

Chargé SBP. Rudnicki MA. Cellular and Molecular Regulation of Muscle Regeneration. *Physiological Reviews*. 2004 84(1):209-238.

Charleston JS. Schnell FJ. Dworzak J. Donoghue C. Lewis S. Chen L. Eteplirsen treatment for Duchenne muscular dystrophy: Exon skipping and dystrophin production. *Neurology.* 2018 12;90(24): e2146–54.

Chazaud B. Inflammation during skeletal muscle regeneration and tissue remodeling: application to exercise-induced muscle damage management. *Immunol Cell Biol* 2016. 94: 140–145.

Chemello F. Bassel-Duby R. Olson EN. Correction of muscular dystrophies by CRISPR gene editing. *Journal of Clinical Investigation*. 2020 1;130(6):2766–76

Chen Y-W. Nagaraju K. Bakay M. McIntyre O. Rawat R. Shi R. Hoffman EP. Early onset of inflammation and later involvement of TGF in Duchenne muscular dystrophy. *Neurology*. 2005 27;65(6):826–34.

Childs BG. Baker D. Wijshake T. Conover CA. Campisi J. vanDeursen JM. Senescent intimal foam cells are deleterious at all stages of atherosclerosis *Science* 2016 354.472–477

Ciafaloni E. Fox DJ. Pandya S. Delayed Diagnosis in Duchenne Muscular Dystrophy: Data from the Muscular Dystrophy Surveillance. Tracking. and Research Network (MD STARnet). *Journal of Pediatrics* 2009;155(3):380-385

Cirak S. Arechavala-Gomeza V. Guglieri M. Feng L. Torelli S. Anthony K. Abbs S. Garralda ME. Bourke J. Wells DJ. Dickinson G. Wood MJA. Wilton SD. Straub V. Kole R. Shrewsbury SB. Sewry C. Morgan JE. Bushby K. Muntoni F. Exon skipping and dystrophin restoration in patients with Duchenne muscular dystrophy after systemic phosphorodiamidate morpholino oligomer treatment: an open label phase 2 dose- escalation study. *The Lancet*. 2011 378(9791):595–605.

Cohn RD. van Erp C. Habashi JP. Soleimani AA. Klein EC. Lisi MT. Gamradt M. Rhys CM. Holm TM. Loeys BL. Ramirez F. Judge DP. Ward CW. Dietz HC Angiotensin II type 1 receptor blockade attenuates TGF-beta-induced failure of muscle regeneration in multiple myopathic states. *Nat Med* 200713:204–210

Collins. C. A. and Morgan. J. E. Duchenne's muscular dystrophy: Animal models used to investigate pathogenesis and develop therapeutic strategies. *Int J Exp Pathol* 2003 84. 165–72.

Collins. C. Olsen. I. Zammit. P. Heslop. L. Petrie. A. Partridge. T. Morgan. J. Stem cell function. self-renewal. and behavioral heterogeneity of cells from the adult muscle satellite cell niche. *Cell* 2005.122. 289–301.

Colussi C. Gurtner A. Rosati J. Illi B. Ragone G. Piaggio G. Moggio M. Lamperti C. D'Angelo G. Clementi E. Minetti G. Mozzetta C. Antonini A. Capogrossi MC. Puri PL. Gaetano C. Nitric oxide defciency determines global chromatin changes in Duchenne muscular dystrophy. *FASEB J Of Publ Fed Am Soc Exp Biol* 2009 23:2131–2141

Consalvi S. Mozzetta C. Bettica P. Germani M. Fiorentini F. Del Bene F. Rochhetti M. Leoni F. Monzani V. Mascagni P. Puri PL. Saccone V. Preclinical studies in the mdx mouse model of duchenne muscular dystrophy with the histone deacetylase inhibitor givinostat. *Mol Med*; 2013 19:79–87.

Coppé JP. Desprez PY. Krtolica A. Campisi J. The senescence-associated secretory phenotype: the dark side of tumor suppression. *Annu. Rev. Pathol* 2010 5. 99–118

Cossu. G. Biressi. S. Satellite cells myoblasts and other occasional myogenic progenitors: possible origin. phenotypic features and role in muscle regeneration. Semin. *Cell Dev. Biol.* 2005 16. 623–631.

Crawford GE. Lu QL. Partridge TA. Chamberlain JS. Suppression of revertant fibers in mdx mice by expression of a functional dystrophin. *Hum Mol Genet* 2001 10:2745–50.

Crosbie RH. Barresi R. Campbell KP. Loss of sarcolemma n-NOS in sarcoglycan-deficient muscle. *FASEB* 2002; 16:1786-91.

Crosbie RH. NO vascular control in Duchenne muscular dystrophy. *Nat Med* 2001 7:27-9

D'Amore PA. Brown RH. Ku PT. Hoffman EP. Watanabe H. Arahata K. et al. Elevated basic fibroblast growth factor in the serum of patients with Duchenne muscular dystrophy. *Ann Neurol*. 1994 35(3):362–5.

D'Souza VN. Man N t. Morris GE. Karges W. Pillers D-AM. Ray PN. A novel dystrophin isoform is required for normal retinal electrophysiology. *Human Molecular Genetics*. 1995 4(5):837–42

Dalkilic I. & Kunkel LM. Muscular dystrophies: genes to pathogenesis *Curr Op In Genet and Develop* 2003 13:231-238

De Paepe B. De Bleecker JL. Cytokines and chemokines as regulators of skeletal muscle inflammation: presenting the case of Duchenne muscular dystrophy. *Mediators Inflamm.* 2013 2013:540370

De Palma C. Morisi F. Cheli S. Pambianco S. Cappello V. Vezzoli M. Rovere-Querini P. Moggio M. Ripolone M. Francolini M. Sandri F. Clementi E. Autophagy as a new therapeutic target in Duchenne muscular dystrophy. *Cell Death Dis* 2012 3: e418

Decary S. Ben Hamida C. Mouly V. Barbet JP. Hentati F. Butler-Browne GS. Shorter telomeres in dystrophic muscle consistent with extensive regeneration in young children. *Neuromuscular Disorders*. 2000 10(2):113–20

Deconinck N. Dan B. Pathophysiology of Duchenne Muscular Dystrophy: Current Hypotheses 2007 *by Elsevier Inc*

Desguerre I. Mayer M. Leturq F. Barbet JP. Gherardi RK. Christov C. Endomysial fibrosis in Duchenne muscular dystrophy: a marker of poor outcome associated with macrophage alternative activation *J neuropathol exp Neurolog* 2009 68(7) 762-733

Deyhle MR. Gier AM. Evans KC. Eggett DL. Nelson WB. Parcell AC. Hyldahl RD. Skeletal muscle inflammation following repeated bouts of lengthening contractions in humans. *Front Physiol* 2016 6: 424

Dos Santos M. Backer S. Saintpierre B. Single-nucleus RNA-seq and FISH identify coordinated transcriptional activity in mammalian myofibers. *Nature Communications*. 2020 11(1)

Duan D. Goemans N. Takeda S. Mercuri E. Aartsma-Rus A. Duchenne muscular dystrophy. *Nature reviews* 2021 7:13

Dubowitz V. Sewry CA. Oldfords A. Muscle Biopsy fifth edition Elsevier 202110:214-236

Duchenne GBA Rechercher sur la paralysie musculaire pseudohypertrophique ou paralyse myosclerosique. *Generals Archives of medicine* 1968 11(5) :179 305.421.552

Duddy W. Duguez S. Johnston H. Cohen TV. Phadke A. Gordish-Dressman H. Nagaraju K. Gnocchi V. Low S. Partridge Muscular dystrophy in the mdx mouse is a severe myopathy compounded by hypotrophy. hypertrophy and hyperplasia. T.*Skelet Muscle.* 2015 1;5:16.

Dumont NA. Wang YX. Maltzahn JV. Pasut A. Bentzinger CF. Brun CE. Rudnicki MA. Dystrophin expression in muscle stem cells regulates their polarity and asymmetric division. *Nat. Med.* 2016 211455–1463

Dumont. NA. Bentzinger CF. Sincennes MC. Rudnicki MA. Satellite cells and skeletal muscle regeneration. *Compr. Physiol* 2011 5. 1027–1059

Dwianingsih EK. Malueka RG. Nishida A. Itoh K. Lee T. Yagi M. Iijima. K. Takeshima Y. Matsuo M. A novel splicing silencer generated by DMD exon 45 deletion junction could explain upstream exon 44 skipping that modifies dystrophinopathy. *J. Hum. Genet.* 2014. *59*. 423–429

E. Ardite. E. Perdiguero. B. Vidal. S. Gutarra. A. L. Serrano. and P. Mun˜oz-Ca´noves. "PAI-1-regulated miR-21 defines a novel age-associated fibrogenic pathway in muscular dystrophy." *Journal of Cell Biology* 2012. 196. 1.163–175.

Ervasti J. Campbell K. A role for the dystrophin-glycoprotein complex as a transmembrane linker between laminin and actin. *Journal of Cell Biology*. 1993 15;122(4):809–23.

Exter D. Connel DA. Skeletal Muscle: Functional Anatomy and Pathophysiology *Semin Musculoskelet Radiol* 2010 14:97-105

Falzarano MS. Scotton C. Passarelli C. Ferlini A. Duchenne muscular dystrophy: from diagnosis to therapy. *Molecules* 2015 20:18168-18184

Fanin M. Danieli GA. Cadaldini M. Miorin M. Vitiello L. Angelini C. Dystrophin- positive fibers in Duchenne dystrophy: origin and correlation to clinical course. *Muscle Nerve* 1995; 18:1115–20

Fanin M. Danieli GA. Vitiello L. Senter L. Angelini C. Prevalence of dystrophin- positive fibers in 85 Duchenne muscular dystrophy patients. *Neuromuscul Disord* 1992; 2:41–5

Feener CA. Koenig M. Kunkel LM. Alternative splicing of human dystrophin mRNA generates isoforms at the carboxy terminus. *Nature.* 1989 338(6215):509–11

Ferlini A. Neri M. Gualandi F. The medical genetics of dystrophinopathies: Molecular genetic diagnosis and its impact on clinical practice. *Neuromuscular Disorders.* 2013 23(1):4–14

Fletcher S. Meloni PL. Johnsen RD. Wong BL. Muntoni F. Wilton SD. Antisense suppression of donor splice site mutations in the dystrophin gene transcript. *molecular Genetics & Genomic Medicine* 2013

Frontera WR. Ochala J. Skeletal Muscle: A Brief Review of Structure and Function. *Behavior Genetics*. 2015 45(2):183-195.

Galpin AJ. Raue U. Jemiolo B. Trappe TA. Harber MP. Minchev K. Trappe S. Human skeletal muscle fiber type specific protein content. *Analytical Biochemistry*. 2012 425(2):175-182.

Gao Q. McNally E. The Dystrophin Complex: Structure. Function. and Implications for Therapy Compr Physiol. 2015 5(3):1223-1239

Gayraud J. Ramonatxo M. Rivier F. Humberclaude V. Petrof B. Matecki S. Ventilatory parameters and maximal respiratory pressure changes with age in Duchenne muscular dystrophy patients. *Pediatr Pulmonol* 2010 45(6):552-9.

Giovarelli M. Zecchini S. Catarinella G. Moscheni C. Sartori P. Barbieri C. De Palma C. Givinostat as metabolic enhancer reverting mitochondrial biogenesis deficit in Duchenne Muscular Dystrophy. *Pharmacological Research* 2021 170. 105751

Glancy B. Balaban RS. Protein composition and function of red and white skeletal muscle mitochondria. *Am J Physiol Cell Physiol.* 2011 300(6): C1280–C1290.

Gordon PM. Liu D. Sartor MA. IglayReger HB. Pistilli EE. Gut- mann L. Nader GA. Hoffman EP. Resistance exercise training influ- ences skeletal muscle immune activation: a microarray analysis. *J Appl Physiol* 2012 112: 443–453.

Gozal D. Thiriet P. Respiratory muscle training in neuromuscular disease: long-term effects on strength and load perception. *Med Sci Sports Exerc* 1999 31:1522–1527.

Grozdanovic Z. Baumgarten HG. Nitric oxide synthase in skeletal muscle fibers: a signaling component of the dystrophin– glycoprotein complex. *Histol Histopathol* 1999 14:243–256

Guiraud S. Davies KE regenerative biomarkers for duchenne muscular dystrophy *Neural Regen Res* 2019 8:1317-1320

Guiraud S. Edwards B. Squire SE. Moir L. Berg A. Babbs A. Ramadan N. Wood MJ. Davies KE. Embryonic myosin is a regeneration marker to monitor utrophin-based therapies for DMD *Human Molecular Genetics.* 2019. 28. 2 307–319

Guiraud. S. Aartsma-Rus. A. Vieira. N. M. Davies. K. E. van Ommen. G. J. and Kunkel. L. M. The pathogenesis and therapy of muscular dystrophies. *Annu Rev Genomics Hum Genet* 2015 16. 281–308

Harper SQ. Hauser MA. DelloRusso C. Duan D. Crawford RW. Phelps SF. Harper HA. Robinson AS. Engelhardt JF. Brooks SV. Chamberlain JS. Modular flexibility of dystrophin: Implications for gene therapy of Duchenne muscular dystrophy. *Nat Med.* 2002 8(3):253–61

Hathout Y. Seol H. Han MHJ. Zhang A. Brown KJ. Hoffman EP. Clinical utility of serum biomarkers in Duchenne muscular dystrophy. *Clin Proteomics*. 2016 13:9.

Heier CR. Yu Q. Fiorillo AA. Tully CB. Tucker A. Mazala DA. Uaesoontrachoon K. Srinivassane S. Damsker JM. Hoffman E. Nagaraju K. Spurney CF. Vamorolone targets dual nuclear receptors to treat inflammation and dystrophic cardiomyopathy. *Life Sci Alliance.* 2019 11;2(1)

Hawke TJ. Garry DJ. Myogenic satellite cells: physiology to molecular biology. *J Appl Physiol* 2001 91(2):534–51

Hendriksen JG. Vles JS. Neuropsychiatric disorders in males with duchenne muscular dystrophy: frequency rate of attention-deficit hyperactivity disorder (ADHD). autism spectrum disorder. and obsessive – compulsive disorder. *J. Child Neurol*. 2008; 23: 477–81

Henriques-Pons A. Yu Q. Rayavarapu S. Cohen TV. Ampong B. Cha HJ. Jahnke V. Van der Meulen J. Wang D. Jiang W. Kandimalla ER. Agrawal S. Spurney CF. Nagaraju K. Role of toll-like receptors in the pathogenesis of dystrophin-deficient skeletal and heart muscle. *Human Molecular Genetics*. 2014 15;23(10):2604–17.

Heo Y-A. Golodirsen: First Approval. *Drugs.* 2020 ;80(3):329–33.

Heredia JE. Mukundan L. Chen FM. Mueller AA. Deo RC. Locksley RM. Rando TA. Chawla A. Type 2 innate signals stimulate fibro/adipogenic progenitors to facilitate muscle regeneration. *Cell*. 2013 11;153(2):376–88.

Hernández-Hernández JM. García-González EG. Brun CE. Rudnicki MA. The myogenic regulatory factors. determinants of muscle development. cell identity and regeneration. Semin *Cell Dev Biol.* 2017 72:10–8

Hernandez-Segura A. Nehme J. Demaria M. Hallmarks of cellular senescence. *TrendsCellBiol.* 2018 28.436–453

Hoffman EP. Arahata K. Minetti C. Bonilla E. Rowland LP. Dystrophinopathy in isolated cases of myopathy in females. *Neurology*. 1992 42(5):967–75.

Hoffman EP. Brown Jr RH. Kunkel LM. Dystrophin: the protein product of the Duchenne muscular dystrophy locus. *Cell* 1987; 51:919–28.

Hoffman EP. Schwartz BD. Mengle-Gaw LJ. Smith EC. Castro D. Mah JK. McDonald CM. Kuntz NL. Finkel RS. Guglieri M. Bushby K. Tulinius M. Nevo Y. Ryan MM. Webster R. Smith AL. Morgenroth LP. Arrieta A. Shimony M. Siener C. Jaros M. Shale P. McCall JM. Nagaraju K. van den Anker J. Conklin LS. Cnaan A. Gordish-Dressman H. Damsker JM. Clemens PR. Cooperative International Neuromuscular Research Group. Vamorolone trial in Duchenne muscular dystrophy shows dose-related improvement of muscle function. *Neurology*. 2019 24;93(13): e1312-e1323

Huang P. Cheng. G. Lu H. Aronica M. Ransohoff RM. Zhou ML. IMPAIRED RESPIRATORY FUNCTION IN *MDX* AND *MDX/UTRN*+/ − MICE *Muscle Nerve.* 2011 43(2): 263–267. .

Huang.PG. Cheng.H. Lu.M. Aronica.RM. Ransohoff L. Zhou L. "Impaired respiratory function in *mdx* and *mdx/utrn*$^{+/-}$ mice." *Muscle & Nerve*. 2011. 43. 2. 263–267.

Hubal MJ. Chen TC. Thompson PD. Clarkson PM. Inflammatory gene changes associated with the repeated-bout effect. *Am J Physiol Regul Integr Comp Physiol* 2008 294: R1628–R1637.

Hufton M. Roper H. Variations in Duchenne muscular dystrophy course in a multi-ethnic UK population: Potential influence of socio-economic factors. *Dev. Med. Child Neurol.* 2017. *59*. 837–842.

Hugnot JP. Gilgenkrantz H. Vincent N. Chafey P. Morris GE. Monaco AP. Berwald-Netter Y. Koulakoff A. Kaplan JC. Kahln A. Distal transcript of the dystrophin gene initiated from an alternative first exon and encoding a 75- kDa protein widely distributed in non-muscle tissues. *Proceedings of the National Academy of Sciences.* 1992 89(16):7506–10

Hutcheson DA. Zhao J. Merrell A. Haldar M. Kardon G. Embryonic and fetal limb myogenic cells are derived from developmentally distinct progenitors and have different requirements for β-catenin. *Genes and Development.* 2009 23(8):997-1013

Ibraghimov-Beskrovnaya O. Ervasti JM. Leveille CJ. Slaughter CA. Sernett SW. Campbell KP. Primary structure of dystrophin-associated glycoproteins linking dystrophin to the extracellular matrix. *Nature.* 1992 355(6362):696–702

Ibrahim GA. Zweber BA. Awad EA. Muscle and serum enzymes and isoenzymes in muscular dystrophies. *Arch Phys Med Rehabil.* 1981 62(6):265–9

Ieronimakis N. Hays AL. Janebodin K. Mahoney WM. Duffield JS. Majesky MW. Reyes M. Coronary adventitial cells are linked to perivascular cardiac fibrosis via TGFβ1 signaling in the *mdx* mouse model of Duchenne muscular dystrophy. *J Mol Cell Cardiol* 2013; 63: 122 – 134.

Ishitobi M. Haginoya K. Zhao Y. Ohnuma A. Minato J. Yanagisawa T. Tanabu M. Kikuchi M. Iinuma K. Elevated plasma levels of transforming growth factor beta1 in patients with muscular dystrophy. *Neuroreport.* 2000 18;11(18):4033–5.

Ishizaki M. Suga T. Kimura E. Shiota T. Kawano R. Uchida Y. Uchino K. Yamashita S. Maeda Y. Uchino M. Mdx respiratory impairment following fibrosis of the diaphragm *Neuromuscular Disorders* 2008 18 342–348

Ishizaki M. Suga Y. Kimura E. Shiota T. Kawano R. Uchida Y. Uchino K. Yamashita S. Maeda Y. Uchino M. Mdx respiratory impairment following fibrosis of the diaphragm. *Neuromuscular Disorders* 2008 18:342–348

Jasmin G. Tautu C. Vanasse M. Brochu P. Simoneau R. Impaired muscle differentiation in explant cultures of Duchenne muscular dystrophy. *Lab Invest* 1984 50:197–207

Joe AWB. Yi L. Natarajan A. Le Grand F. So L. Wang J. Rudnicki MA. Rossi FMV. Muscle injury activates resident fibro/adipogenic progenitors that facilitate myogenesis. *Nat Cell Biol*. 2010 12(2):153–63.

Jones. D. P. Radical-free biology of oxidative stress. *AJP: Cell Physiology* 2008 295(4). C849–C868.

Juan-Mateu J. Gonzalez-Quereda L. Rodriguez MJ. Baena M. Verdura E. Nascimento A. Ortez C. Baiget M. Gallano P. DMD Mutations in 576 Dystrophinopathy Families: A Step Forward in Genotype-Phenotype Correlations. *PLoS One.* 2015 18;10

Judson RN. Low M. Eisner C. Rossi FM. Isolation Culture and Differentiation of Fibro/Adipogenic Progenitors (FAPs) from Skeletal Muscle *Mol Biol* 2017 1668:93-103.

Karimian A. Ahmadi Y. Yousefi B. Multiple functions of p21 in cell cycle. apoptosis and transcriptional regulation after DNA damage. *DNA Repair (Amst*). 2016 42:63-71

Kasai T. Abeyama K. Hashiguchi T et alDecreased total nitric oxide production in patients with duchenne muscular dystrophy. *J Biomed Sci* 2004 11:534–537.

Kaye D. Pimental D. Prasad S. Mäki T. Berger HJ. McNeil PL. Smith TW. Kelly RA. Role of transiently altered sarcolemmal membrane permeability and basic fibroblast growth factor release in the hypertrophic response of adult rat ventricular myocytes to increased mechanical activity in vitro. *J Clin Invest*. 1996 15;97(2):281–91

Keefe AC. Kardon GA. New role for dystrophin in muscle stem cells. *Nat. Med*. 2015 21. 1391–1393

Keegan NP. Pseudoexons of the DMD Gene. *Journal of Neuromuscular Diseases* 2020 7:77–95

Kharraz Y. Guerra J. Pessina P. Serrano AL. Muñoz-Cánoves P. Understanding the Process of Fibrosis in Duchenne Muscular Dystrophy. *BioMed Research International*. 2014 2014:1–11.

Koenig M. Monaco AP. Kunkel LM. The complete sequence of dystrophin predicts a rod-shaped cytoskeletal protein. *Cell*. 1988 53(2):219–28.

Kollu S. Abou-Khalil R. Shen C. Brack AS. The Spindle Assembly Checkpoint Safeguards Genomic Integrity of Skeletal Muscle Satellite Cells. *Stem Cell Rep.* 2015 9;4(6)1061-74

Kornegay JN The golden retriever model of Duchenne muscular dystrophy. *Skelet Muscle* 2017 7.9

Larcher T. Lafoux A. Tesson L. Remy S. Thepenier V. Francois V. Le Guiner C. Goubin H. Dutilleul M. Guigand L. Toumaniantz G. De Cian A. Boix C. Renaud JB. Cherel Y. Giovannangeli C. Concordet JP. Anegon I. Huchet C. Characterization of Dystrophin Deficient Rats: A New Model for Duchenne Muscular Dystrophy. *PLoS ONE* 2014 9(10): e110371

Le Grand F. Rudnicki MA. Skeletal muscle satellite cells and adult myogenesis. *Current Opinion in Cell Biology*. 2007 19(6):628–33

Leask A. Abraham DJ. TGF-beta signaling and the fibrotic response. *FASEB J.* 2004 18(7):816–27

Lee KH. Baek MY. Moon KY Song WK. Chung CH. Ha DB. Kang MS. Nitric oxide as a messenger molecule for myoblast fusion. *J Biol Chem* 1994 269:14371–14374

Lefaucheur JP. Pastoret C. Sebille A. Phenotype of dys- 590 trophinopathy in old mdx mice. *Anat Rec*. 1995 242: 591 70-6.

Leinonen H. Juntunen J. Somer H. Rapola J. Capillary circulation and morphology in Duchenne muscular dystrophy *Eur Neurol* 1979 18:249-255

Li S. Kimura E. Ng R. Fall BM. Meuse L. Reyes M. Faulkner JA. Chamberlain JS. A highly functional mini- dystrophin / GFP fusion gene for cell and gene therapy studies of Duchenne muscular dystrophy. *Human Molecular Genetics*. 2006 15;15(10):1a610–22.

Lidov HGW. Selig S. Kunkel LM. Dp140: a novel 140 kDa CNS transcript from the dystrophin locus. *Hum Mol Genet.* 1995 4(3):329–35

Lo Mauro A. D'Angelo MG. Romei M. et al. Abdominal volume contribution to tidal volume as an early indicator of respiratory impairment in Duchenne muscular dystrophy. *Eur Respir J* 2010; 35: 1118–1125.

Łoboda A. Dulak J. Muscle and cardiac therapeutic strategies for Duchenne muscular dystrophy: past. present. and future. *Pharmacol Rep.* 2020 72(5):1227–63

LoMauro A. Romei M. Gandossini S. Pascuzzo R. Vantini S. D'Angelo MG. Aliverti A. Evolution of respiratory function in Duchenne muscular dystrophy from childhood to adulthood. *Eur Respir J* 2018 51: 1701418

Lu QL. Morris GE. Wilton SD. Ly T. Artem'yeva OV. Strong P. Partridge TA. Massive idiosyncratic exon skipping corrects the nonsense mutation in dystrophic mouse muscle and produces functional revertant fibers by clonal expansion. *J Cell Biol* 2000 148:985–96.

Luce LN. Carcione M. Mazzanti C. Ferrer M. Szijan I. Giliberto F. Small mutation screening in the DMD gene by whole exome sequencing of an argentine Duchenne/Becker muscular dystrophies cohort. *Neuromuscul Disord*. 2018 28(12):986-995

Luz MA. Marques MJ. Santo NH Impaired regeneration of dystrophin-deficient muscle fibers is caused by exhaustion of myogenic cells. *Braz J Med Biol Res* 2002 35:691–695

Machado DL. Silva EC. Resende MB. Carvalho CRF. Zanoteli E. Reed UC. Lung function monitoring in patients with Duchenne muscular dystrophy on steroid therapy. *BMC Res Notes* 2012; 5: 435.

Maier F. Bornemann A. Comparison of the muscle fiber diameter and satellite cell frequency in human muscle biopsies. *Muscle Nerve* 1999 22:578–583

Malfatti E. Romero NB. Diseases of skeletal muscle. *Handbook of Clinical Neurology* 2017 145 (30) 429-451

Manning J. O'Malley D. What has the mdx mouse model of duchenne muscular dystrophy contributed to our understanding of this disease? *Journal of Muscle Research and Cell Motility*. 2015;36(2):155-167

Martini FH. Timmons FJ. Tallitsch RB. Human Anatomy *Edises* 2012

Matsumura K. Campbell KP. Dystrophin-glycoprotein complex: Its role in the molecular pathogenesis of muscular dystrophies. *Muscle Nerve.* 1994 17(1):2–15

Matsakas A. Yadav V. Lorca S. Narkar V. Muscle ERRγ mitigates Duchenne muscular dystrophy via metabolic and angiogenic reprogramming. *FASEB* J. 2013 27(10):4004-16

Matthews E. Brassington R. Kuntzer T. Jichi F. Manzur AY. Corticosteroids for the treatment of Duchenne muscular dystrophy. *Cochrane Database of Systematic Reviews*. 2016;2016(5)

Mauro A. Satellite cell of skeletal muscle fibers. *J Biophys Biochem Cytol*. 1961 9:493–5.

McGreevy. J. W. Hakim. C. H. McIntosh. M. A. and Duan. D. Animal models of Duchenne muscular dystrophy: From basic mechanisms to gene therapy. *Dis Model Mech*. 2015 8 195–213.

Mehlem A. Hagberg CE. Muhl L. Eriksson U. Falkeval A. Imaging of neutral lipids by oil red O for analyzing the metabolic status in health and disease *Nat Protoc* 2013 8(6) 1149-1154

Mendell JR. Campbell K. Rodino-Klapac L. Sahenk Z. Shilling C. Lewis S. et al. Dystrophin Immunity in Duchenne's Muscular Dystrophy. *N Engl J Med*. 2010 7;363(15):1429–37

Mendell JR. Lloyd-Puryear M. Report of MDA muscle disease symposium on newborn screening for Duchenne muscular dystrophy. *Muscle Nerve*. 2013 48(1):21–6.

Mendell JR. Sahenk Z. Lehman K. Nease C. Lowes LP. Miller NF. Iammarino MA. Alfano LN. Nicholl A. Al-Zaidy S. Lewis S. Church K. Shell R. Cripe LH. Potter RA. Griffin DA. Pozsgai E. Dugar A. Hogan M. Rodino-Klapac LR. Assessment of Systemic Delivery of rAAVrh74.MHCK7 micro-dystrophin in Children with Duchenne Muscular Dystrophy: A Nonrandomized Controlled Trial. *JAMA Neurol.* 2020 1;77(9):1122

Mendell JR. ShillingC. LeslieND. Flanigan KM. al-Dahhak R. Gastier-Foster J. Kneile K. Dunn DM. Duval B. Aoyagi A. Hamil C. Mahmoud M. Roush K. Bird L. Rankin C. Lilly H. Street N. Chamdrasekar R. Weiss RB. Evidence-based path to newborn screening for Duchenne muscular dystrophy. *Ann Neurol* 2012 71. 304–13.

Meng J. Bencze M. Asfahani R. Muntoni F. Morgan JE. The effect of the muscle environment on the regenerative capacity of human skeletal muscle stem cells. *Skelet Muscle* 2015 5. 11

Messina G. Cossu G. The origin of embryonic and fetal myoblasts: a role of Pax3 and Pax7. *Genes and Development*. 2009 23(8):902-905

Miike T. Sugino S. Ohtani Y. Taku K. Yoshioka K. Vascular endothelial cell injury and platelet embolism in Duchenne muscular dystrophy at the preclinical stage. *J Neurol Sci* 1987 82:67–80.

Mirski KT. Crawford TO. Motor and Cognitive Delay in Duchenne Muscular Dystrophy: Implication for Early Diagnosis. *The Journal of Pediatrics*. 2014 165(5):1008–10.

Mokri B. Engel AG. Duchenne dystrophy: electron microscopic findings pointing to a basic or early abnormality in the plasma membrane of the muscle fiber. *Neurology*. 1975 25(12):1111–20

Monaco AP. Bertelson CJ. Liechti-Gallati S. Moser H. Kunkel LM. An explanation for the phenotypic differences between patients bearing partial deletions of the DMD locus. *Genomics.* 1988 2(1):90–5

Mukund K. Subramanian S. Skeletal muscle: A review of molecular structure and function. in health and disease 2019 *WIREs Syst Biol Med*. 12:1462

Muntoni F. Gobbi P. Sewry C. Sherratt T. Taylor J. Sandhu SK. Abbs S. Roberts R. Hodgson SV. Bobrow M. Deletions in the 5' region of dystrophin and resulting phenotypes. *J. Med. Genet.* 1994. *31*. 843–847.

Muntoni F. Torelli S. Ferlini A. Dystrophin and mutations: one gene. several proteins. multiple phenotypes. *Lancet Neurol*. 2003 2(12):731–40.

Nagy S. Hafner P. Schmidt S. Rubino-Nacht D. Schädelin S. Bieri O. Fischer D. Tamoxifen in Duchenne muscular dystrophy (TAMDMD): study protocol for a multicenter, randomized, placebo-controlled, double-blind phase 3 trial. *Trials.* 2019 21;20(1):637.

Nakamura A. Shiba N. Miyazaki D. Nishizawa H. Inaba Y. Fueki N. Maruyama R. Echigoya Y. Yokota T. Comparison of the phenotypes of patients harboring in-frame deletions starting at exon 45 in the Duchenne muscular dystrophy gene indicates potential for the development of exon skipping therapy. *J. Hum. Genet* 2017 62. 459–463

Nakamura K. Generation of muscular dystrophy model rats with a CRISPR/Cas system. *Sci. Rep* 2014. 4.5635

Narita S. Yorifuji H. Centrally nucleated fibers (CNFs) compensate the fragility of myofibers in mdx mouse. Neuroreport 1999 19;10(15):3233-5.

Nelson. CA. R. B. Hunter. L. A. Quigley et al. "Inhibiting TGF-βactivity improve srespiratory function in mdx mice."*The American Journal of Pathology*. 2011 178. 6. 2611–2621.

Nicholson LV. Davison K. Johnson MA. Slater CR. Young C. Bhattacharya S. Gardner-Medwin D. Dystrophin in skeletal muscle. II. Immunoreactivity in patients with Xp21 muscular dystrophy. *J Neurol Sci* 1989 94:137–46.

Nicholson LV. Johnson MA. Gardner-Medwin D. Bhattacharya S. Harris JB. Heterogeneity of dystrophin expression in patients with Duchenne and Becker muscular dystrophy. *Acta Neuropathol* 1990 80:239–50.

Nigro V. Moreira E de S. Piluso G. Vainzof M. Belsito A. Politano L. Puca AA. Passos-Bueno MR. Zatz M. Autosomal recessive limbgirdle muscular dystrophy. LGMD2F. is caused by a mutation in the δ– sarcoglycan gene. *Nat Genet.* 1996 14(2):195–8.

Noguchi S. McNally EM. Othmane KB. Hagiwara Y. Mizuno Y. Yoshida M. Yamamoto H. Bonnemann CG. Gussoni E. Denton PH. Kyriakides T. Middleton L. Hentati F. Ben Hamida M. Nonaka I. Vance JM. Kunkel LM. Ozawa E. Mutations in the Dystrophin-Associated Protein [IMAGE]-Sarcoglycan in Chromosome 13 Muscular Dystrophy. *Science.* 1995 3;270(5237):819–22

Ogrodnik M. Miwa S. Tchkonia T. Tiniakos D. Wilson CL. Lahat A. Day CP. Burt A. Palmer A. Anstee QM. Grellscheid SN. Hoeijmakers JHJ. Barnhoorn S. Mann DA. Bird TG. Vermeij WP. Kirkland JL. Passos JF. von Zglinicki T. Jurk D. Cellular senescence drives age-dependent hepatic steatosis. *Nat Commun.* 2017 13;8:15691.

Ouisse LH. Immunophenotype of a rat model of Duchenne's disease and demonstration of improved muscle strength after anti-CD45RC antibody treatment. *Front. Immunol.* 2019 10. 2131.

Pane. M. Mazzone ES. Sormani MP. Messina S. Vita GL. Fanelli L. Berardinelli A. Torrente Y. D'Amico A. Lanzillotta V. Viggiano E. D'Ambrosio P. Cavallaro F. Mercuri E. 6 minute

walk test in Duchenne MD patients with different mutations : 12 month changes. *PLoS ONE* 2014. *9.* e83400.

Petrillo S. Pelosi L. Piemonte F. Travaglini L. Forcina L. Catteruccia M. Petrini S. Verardo M. D'Amico A. Musaro A. Bertini E. Oxidative stress in Duchenne muscular dystrophy: focus on the NRF2 redox pathway. *Hum. Mol. Genet* 2017. 26. 2781–2790

Peverelli L. Testolin S. Villa L. D'Amico A. Petrini S. Favero C. Magri F. Morandi L. Mora M. Mongini T. Bertini E. Sciacco M.. Comi GP. Moggio M. Histologic muscular history in steroid-treated and untreated patients with Duchenne dystrophy. *Neurology* 2015 85:1886–1893.

Plantié E. Migocka-Patrzałek M. Daczewska M. Jagla K Model organisms in the fight against muscular dystrophy: lessons from drosophila and Zebrafish. *Molecules* 2015.

Podkalicka P. Mucha O. Dulak J. Loboda A. Targeting angiogenesis in Duchenne muscular dystrophy *Cellular and molecular life sciences* 2019 76:1507-1528

Podkalicka P. MuchaO. KaziródK. Bronisz-Budzynska I. Ostrowska-Paton S. Tomczyk M. Andrysiak K. Stepniewski J. Dulak J. Łoboda A. Age-Dependent Dysregulation of Muscle Vasculature and Blood Flow Recovery after Hindlimb Ischemia in the *mdx* Model of Duchenne Muscular Dystrophy. *Biomedicines* 2021 .*9.*481.

Pole A. Dimri M. Dimri GP. Oxidative stress cellular senescence and ageing. *AIMSMol.Sci. 2016*

Potikanond S. Nimlamool W. Noordermeer J. Fradkin LG. Muscular Dystrophy Model. Adv *Exp Med Biol.* 2018 1076:147-172.

Prins KW. Humston JL. Mehta A. Tate V. Ralston E. Ervasti JM. Dystrophin is a microtubule-associated protein. *J Cell Biol*. 2009 186:363–369

Prior TW. Bartolo C. Papp AC. Snyder PJ. Sedra MS. Burghes AHM. Kissel JT. Luquette MH. Tsao CY. Mendell JR. Dystrophin expression in a Duchenne muscular dystrophy Patient with a frame shift deletion. *Neurology.* 1997 1;48(2):486–8.

Qiu B. Simon MC. BODIPY 493/503 staining of neutral lipid droplets for microscopy and quantification by flow cytometry *Bio Protoc* 2016 6(17)

Radàk Z. Skeletal muscle. Function. and Muscle fyber types. *The pathology of physical training* 2018 2:15-31

Radley-Crabb H. Terrill J. Shavlakadze T. Tonkin J. Arthur P. Grounds M. A single 30 min treadmill exercise session is suitable for 'proof-of concept studies' in adult mdx mice: A comparison of the early consequences of two different treadmill protocols *Neuromuscular Disorders* 2012 22:170–182

Radley-Crabb H. Terrill J. Shavlakadze T. Tonkin J. Arthur P. Grounds M. A single 30 min treadmill exercise session is suitable for 'proof-of concept studies' in adult mdx mice: A comparison of the early consequences of two different treadmill protocols. *Neuromuscular Disorders* 2012 170–182

Ramos JN. Hollinger K. Bengtsson NE. Allen JM. Hauschka SD. Chamberlain JS. Development of Novel Micro-dystrophins with Enhanced Functionality. *Molecular Therapy.* 2019 27(3):623–35

Reimann J. Irintchev A. Wernig A. Regenerative capacity and the number of satellite cells in soleus muscles of normal and mdx mice. *Neuromuscul Disord.* 2000; 10:276–282.

Reitter B and Goebel HH Dystrophinopathies *Seminars in pediatric neurology* 1996 3 :99-109

Relaix F. Montarras D. Zaffran S. Gayraud-Morel B. Rocancourt D. Tajbakhsh S. Mansouri A. Cumano A. Buckingam M. Pax3 and Pax7 have distinct and overlapping functions in adult muscle progenitor cells. *J Cell Biol.* 2006;172(1):91–102.

Relaix F. Skeletal muscle progenitor cells: From embryo to adult. *Cellular and Molecular Life Sciences.* 2006 63(11):1221-122

Rentschler S. Linn H. Deininger K. Bedford MT. Espanel X. Sudol M. The WW Domain of Dystrophin Requires EF-Hands Region to Interact with β-Dystroglycan. *Biological Chemistry* 1999 380(4).

Ribeiro AF. Souza LS. Almeida CF. IshibaR. Fernandes SA. Guerrier DA. Santos ALF. Onofre-Oliveira PCG. Vainzof M. Muscle satellite cells and impaired late stage regeneration in different murine models for muscular dystrophies. *Nature. scient reports* 2018 9:11842

Robbins RA. Grisham M B Nitric oxide. *Int J Biochem Cell Biol.* 1997 Jun;29(6):857-60

Roberts N. Holley-Cuthrell J. Gonzalez-Vega M. Mull AJ. Heydemann A. Biochemical and Functional Comparisons of mdx and Sgcg$^{-/-}$ Muscular Dystrophy Mouse Models Volume *Bio Med research Internat* 2015. 11

Rodriguez Cruz PM. Cossins J. Beeson D. Vincent A. The Neuromuscula Junction in Health and Disease: Molecular mechanisms governing Synaptic Formation and Homeostasis. *Front. Mol. Neurosci.* 2020 13:610964

Rosalki SB. Serum enzymes in disease of skeletal muscle. *Clin Lab Med.* 1989 9(4):767–81

Rosenberg S. Puig M. Nagaraju K. Hoffman E P. Villalta SA. RaoV. Lalage Wakefield M. Woodcock J. Immune-mediated pathology in Duchenne muscular dystrophy *Sci Transl Med.* 2015 7(299): 299

Roshmi R R. Yokota T. Viltolarsen for the treatment of Duchenne muscular dystrophy. *Drugs Today.* 2019;55(10):627.

Sadoulet-Puccio HM. Rajala M. Kunkel LM. Dystrobrevin and dystrophin: An interaction through coiled-coil motifs. *Proceedings of the National Academy of Sciences.* 1997 11;94(23):12413–8

Saito T. Yamamoto Y. Matsumura T. Serum levels of vascular endothelial growth factor elevated in patients with muscular dystrophy. *Brain Dev* 2009 31:612–617

Sander M. Chavoshan B. Harris SA. Functional muscle ischemia in neuronal nitric oxide synthase-deficient skeletal muscle of children with Duchenne muscular dystrophy. *Proc Natl Acad Sci USA* 2000;97:13818-23.

Sander M. Chavoshan B. Harris SA. Iannacone ST. Stull JT. Thomas GD. Victor RG. Functional muscle ischemia in neuronal nitric oxide synthase-deficient skeletal muscle of children with Duchenne muscular dystrophy. *Proc Natl Acad Sci USA* 2000;97:13818-23.

Schafer MJ. White TA. Iijima K. Haack AJ. Ligresti G. Atkinson EJ. Oberg AL. Birch J. Salmonowicz H. Zhu Y. Mazula DL. Brooks RW. Fuhrmann-Stroissnigg H. Pirtskhalava T. Prakash YS. Tchkonia T. Robbins PD. Aubry MC: Passos JF. Kirkland JL. Tschumperlin DJ. Kita H. LeBrasseur NK. Cellular senescence mediates fibrotic pulmonary disease. *Nat.Commun* 2017 .8.1–11

Schiaffino S. Fibre types in skeletal muscle: A personal account. *Acta Physiologica*. 2010 199(4):451-463

Schiaffino S. Reggiani C. Fiber types in Mammalian skeletal muscles. *Physiological Reviews.* 2011 91(4):1447-1531

Schiaffino S. Rossi AC. Smerdu V. Leinwand LA. Reggiani C. Developmental myosins: expression patterns and functional significance. *Skeletal Muscle.* 2015 5(1):22.

Schultz E. Gibson MC. Champion T. Satellite cells are mitotically quiescent in mature mouse muscle: An EM and radioautographic study. *Journal of Experimental Zoology*. 1978 206(3):451-456.

Seale P. Sabourin LA. Girgis-Gabardo A. Mansouri A. Gruss P. Rudnicki MA. Pax7 Is Required for the Specification of Myogenic Satellite Cells. *Cell.* 2000 102(6):777–86.

Selsby JT. Ross JW. Nonneman D. Hollinger K. Porcine models of muscular dystrophy. ILAR *Journal* 2015 56:1 116-126

Shahnoor N. Siebers EM. Brown KJ. and Lawlor MW. Pathological Issues In Dystrophinopathy in the Age of Genetic Therapies *Annu. Rev. Pathol. Mech. Dis.* 2019. 14:105–26

Shahnoor N. Siebers EM. Brown KJ. Lawlor MV. Pathological Issues In Dystrophinopathy in the Age of Genetic Therapies *Annual Review of Pathology: Mechanisms of Disease* 2015 12:25

Shandrin IY. Khodabukus A. Bursac N. Striated Muscle Function. Regeneration. and Repair *Cell Mol Life Sci.* 2016 73(22): 4175–4202

Sharma A. Singh K. Almasan A. Histone H2AX phosphorylation: a marker for DNA damage. *Methods Mol Biol*. 2012 920:613-26.

Smith AD. Koreska J. Moseley CF. Progression of scoliosis in Duchenne muscular dystrophy. *J. Bone Joint Surg. Am.* 1989; 71: 1066–74.

Smith EC. Conklin LS. Hoffman EP. Clemens PR. Mah JK. Finkel RS. Guglieri M. Tulinius M. Nevo Y. Ryan MM. Webster R. Castro D. Kuntz NL. Kerchner L. Morgenroth LP.

Arrueta A. Shimony M. Jaros M. Shale P. Gordish-Dressman H. Hagerty L. Dang U. Damsker JM. Schwartz BD. Mengle-Gaw L. McDonald CM. Efficacy and safety of vamorolone in Duchenne muscular dystrophy: An 18-month interim analysis of a non-randomized open-label extension study. *PLoS Med* 2020 17(9): e1003222

Song Y. Yao S. Liu Y. Long L. Yang H. Li Q. Liang J. Li X. Lu Y. Zhu H. Zhang N. Expression levels of TGF-β1 and CTGF are associated with the severity of Duchenne muscular dystrophy. *Exp Ther Med.* 2017 13. 1209–1214.

Sotgia F. Lee JK. Das K. Bedford M. Petrucci TC. Macioce P. Sargiacomo M. Bricarelli FD. Minetti C. Sudol M. Lisanti MP. Caveolin-3 Directly Interacts with the C-terminal Tail of β-Dystroglycan: IDENTIFICATION OF A CENTRAL WW-LIKE DOMAIN WITHIN CAVEOLIN FAMILY MEMBERS. *J Biol Chem*. 2000 1;275(48):38048–58

Spencer MJ. Montecino-Rodriguez E. Dorshkind K. Tidball JG. Helper (CD4+) and Cytotoxic (CD8+) T Cells Promote the Pathology of Dystrophin-Deficient Muscle. *Clinical Immunology*. 2001 98(2):235–43

Spencer MJ. Walsh CM. Dorshkind KA. Rodriguez EM. Tidball JG. Myonuclear apoptosis in dystrophic mdx muscle occurs by perforin-mediated cytotoxicity. *J Clin Invest*. 1997 1;99(11):2745–51.

Starosta A. Konieczny P. Therapeuthic aspects of cell signaling and communication in Duchenne muscular dystrophy. *Cellular and molecular life science.* 2021

Stone MR. O'Neill A. Catino D. Bloch RJ. Specific interaction of the actin-binding domain of dystrophin with intermediate filaments containing keratin 19. *Mol Biol Cell.* 2005; 16:4280–4293

Sugihara H. Teramoto N. Nakamura K. Shiga T. Shirakawa T. Matsuo M. Ogasawara M. Nishino I. Matsuwaki T. Nishihara M. Yamanouchi K. Cellular senescence-mediated exacerbation of Duchenne muscular dystrophy *Scientific RepoRtS* 2020 10:16385

Tajbakhsh S. Rocancourt D. Cossu G. Buckingham M. Redefining the genetic hierarchies controlling skeletal myogenesis: Pax- 3 and Myf-5 act upstream of MyoD. *Cell*. 1997;89(1):127-138.

Talts JF. Andac Z. Göhring W. Brancaccio A. Timpl R. Binding of the G domains of laminin α1 and α2 chains and perlecan to heparin. sulfatides. α-dystroglycan and several extracellular matrix proteins. *EMBO J.* 1999 15;18(4):863–70.

Taylor J. Muntoni F. Dubowitz V. Sewry A. The abnormal expression of utrophin in Duchenne and becker muscular dystrophy is age related. *Neuropathology and applied Neurobiology* 1977 23:399-405

Teramoto N. Ikeda M. Sugihara H. Shiga T. Matsuwaki T. Nishihara M. Uchida K. Yamanouchi K. Loss of p16/Ink4a drives high frequency of rhabdomyosarcoma in a rat model of Duchenne muscular dystrophy. *J Vet Med Sci*. 2021 15;83(9):1416-1424.

Terrill. J. R. Duong MN. Turner R. Le Guiner C. Boyatzis A. Kettle AJ. Grounds M/ Arthur PG/. Levels of inflammation and oxidative stress. and a role for taurine in dystropathology

of the Golden Retriever Muscular Dystrophy dog model for Duchenne Muscular Dystrophy. *Redox Biol* 2016. 9. 276–286

Tian PC. Wang Y. Shi DD. Chen Z. Luo Q. Wang HL. Application of next-generation sequencing in the molecular diagnosis of Duchenne muscular dystrophy. *Zhongguo Dang Dai 2019* 21(3): 244-248

Tominaga K. & Suzuki HI. TGF-β signaling in cellular senescence and aging-related pathology .*Int.J.Mol.Sci* 2019. 20.5002

Tozawa T. Itoh K. Yaoi T. Tando S. Umekage M. Dai H. Hosoi H. Fushiki S. The Shortest Isoform of Dystrophin (Dp40) Interacts with a Group of Presynaptic Proteins to Form a Presumptive Novel Complex in the Mouse Brain. *Mol Neurobiol.* 2012 45(2):287–97

Turgeman T. Hagai Y. Huebner K. Jassal DS. Anderson JE. Genin O. et al. Prevention of muscle fibrosis and improvement in muscle performance in the mdx mouse by halofuginone. *Neuromuscular Disorders*. 2008;18(11):857–68

Uezumi A. Fukada S. Yamamoto N. Ikemoto-Uezumi M. Nakatani M. Morita M. Yamaguchi A. Yamada H. Nishino I. Hamada Y. Tsuchida K. Identification and charac- terization of PDGFRα + mesenchymal progenitors in human skeletal muscle. *Cell Death Dis* 2014; 5: e1186.

Uezumi A. Fukada S. Yamamoto N. Takeda S. Tsuchida K. Mesenchymal progenitors distinct from satellite cells contribute to ectopic fat cell formation in skeletal muscle. *Nat Cell Biol.* 2010 12(2):143–52.

van den Bergen JC. Ginjaar HB. Niks EH. Aartsma-Rus A. Verschuuren JJGM. Prolonged ambulation in Duchenne patients with a mutation amenable to exon 44 skipping. *J. Neuromuscul. Dis.* 2014 *1*. 91–94.

Van Putten M. Putker K. Overzier M. Adamzec A. Pasteuning-Vuhman S. Plomp JJ. Aarstma Rus A. Natural disease history of the D2-*mdx* mouse model for Duchenne muscular dystrophy *FASEB J* 2019 33(7): 8110–8124

van Putten M. van der Pijl EM. Hulsker M. Verhaart IEC. Nadarajah VD. Van der Weerd L. Aartsma-Rus A. Low dystrophin levels in heart can delay heart failure in mdx mice. *Journal of Molecular and Cellular Cardiology.* 69:17–23

Verhaart IEC Aartsma-Rus A. Therapeutic developments for Duchenne muscular dystrophy. *Nat.Rev.Neurol.* 2019 15.373–386

Verma M. Asakura Y. Hirai H. Watanabe S. Tastad C. Fong GH. Ema M. Call JA. Lowe DA. Asakura A. Flt-1 haploinsufficiency ameliorates muscular dystrophy phenotype by developmentally increased vasculature in mdx mice. *Hum Mol Genet.* 2010 1;19(21):4145-59

Verma M. Asakura Y. Murakonda BSR. Pengo T. Latroche C. Chazaud B. McLoon LK. Asakura A. Muscle Satellite Cell Cross-Talk with a Vascular Niche Maintains Quiescence via VEGF and Notch Signaling. *Cell Stem Cell.* 2018 Oct 4;23(4):530-543

Villalta SA. Nguyen HX. Deng B. Gotoh T. Tidball JG. Shifts in macrophage phenotypes and macrophage competition for arginine metabolism affect the severity of muscle pathology in muscular dystrophy. *Hum Mol Genet.* 2009 1;18(3):482–96

Villalta SA. Rosenberg AS. Bluestone JA. The immune system in Duchenne muscular dystrophy: Friend or foe. *Rare Diseases*. 2015 3(1):e1010966

von Maltzahn J. Jones AE. Parks RJ. Rudnicki MA. Pax7 is critical for the normal function of satellite cells in adult skeletal muscle. *Proc Natl Acad Sci U S A.* 2013 8;110(41):16474–9.

Wagers AJ. Conboy IM. Cellular and molecular signatures of muscle regeneration: current concepts and controversies in adult myogenesis. *Cell* 2005 122:659–667

Waldrop MA. Flanigan KM. Update in Duchenne and Becker muscular dystrophy. curr Opin Neurol 2019 32(5):722-727

Wang DN. Wang ZQ. Yan L. He J. Lin MT. Chen WJ. Wang. N. Clinical and mutational characteristics of Duchenne muscular dystrophy patients based on a comprehensive database in South China. *Neuromuscul. Disord.* 2017. *27*. 715–722

Wang Y. Yang Y. Liu J. Chen X-C. Liu X. Wang C-Z. He XY. Whole dystrophin gene analysis by next-generation sequencing: a comprehensive genetic diagnosis of Duchenne and Becker muscular dystrophy. *Mol Genet Genomics*. 2014 289(5):1013–21

Webb C. Smooth muscle contraction and relaxation. *Adv physiol educ* 2003 27/201-206

Webster C. Silberstein L. Hays AP. Blau HM Fast muscle fibers are preferentially affected in Duchenne muscular dystrophy. *Cell* 1988 52: 503-513

Wein N. Vulin A. Falzarano MS. Al-Khalili Szigyarto C. Maiti B. Findlay A. Heller KN. Uhlén M. Bakthavachalu B. Messina S. Vita G. Passarelli C. Gualandi F. Wilton SD. Rodino-Klapac L. Yang L. Dunn DM. Schoenberg D. Weiss RB. Howard MT. Ferlini A. KM. Flanigan A novel DMD IRES results in a functional N-truncated dystrophin. providing a potential route to therapy for patients with 5' mutations *Nat Med.* 2014 20(9): 992–1000

Welch EM. Barton ER. Zhuo J. Tomizawa Y. Friesen WJ. Trifillis P. PTC124 targets genetic disorders caused by nonsense mutations. *Nature.* 2007 447(7140):87–91

Wilson K. Faelan C. Patterson-Kane JC. Rudmann DG. Moore SA. Frank D. Charleston J. Tinsley J Young GD. Milici AJ. Duchenne and Becker Muscular Dystrophies: A Review of Animal Models. Clinical End Points. and Biomarker Quantification. *Toxicologic Pathology*. 2017;45(7):961-976

Winnard. AV. Mendell. JR. Prior. TW. Florence. J. Burghes. AH. Frameshift deletions of exons 3-7 and revertant fibers in Duchenne muscular dystrophy: Mechanisms of dystrophin production. *Am. J. Hum. Genet.* 1995. *56*. 158–166.

Xin L. Hyldahl RD. Chipkin SR. Clarkson PM. A contralateral repeated bout effect attenuates induction of NF-KB DNA binding fol- lowing eccentric exercise. *J Appl Physiol 1985* 116: 1473–1480

Yahiaoui L. Gvozdic D. Danialou G. Mack M. Petrof BJ. CC family chemokines directly regulate myoblast responses to skeletal muscle injury. *J Physiol* 2008 586: 3991–4004.

Yin H. Price F. Rudnicki MA. Satellite Cells and the Muscle Stem Cell Niche. *Physiological Reviews.* 2013 93(1):23–67

Yiu E. Kornberg AJ Duchenne muscular dystrophy. *Jorn of Pediatric and child health*. 2015

Yuasa K. Nakamura A. Hijikata T. Takeda S Dystrophin deficiency in canine X-linked muscular dystrophy in Japan (CXMDJ) alters myosin heavy chain expression profiles in the diaphragm more markedly than in the tibialis cranialis muscle. *BMC Musculoskelet Disord* 2008 9: 1

Zacks SI. Sheff MF Age-related impeded regeneration of mouse minced anterior tibial muscle. *Muscle Nerve* 1982 5:152–161

Zamani GR. Mohammadi MF. Tavasoli AR. Ashrafi MR. Hosseinpour S. Ghabeli H. Pourbakhtyaran E. Haghighi R. Hosseiny SMM. Mohammadi P. Heidari M. Genetic Analysis of Forty MLPA-Negative Duchenne Muscular Dystrophy Patients by Whole-Exome Sequencing. *J Mol Neurosci*. 2022

Zatz M. Pavanello RCM. Lazar M. Yamamoto GL. Lourenço NCV. Cerqueir A. Nogueira L. Vainzof M. Milder course in Duchenne patients with nonsense mutations and no muscle dystrophin. *Neuromuscular Disorders.* 2014 24(11). 986–989.

Zelikovich AS . Quattrocelli M. Salamone IM. Kuntz NL. McNally EM. Moderate exercise improves function and increases adiponectin in the *mdx* mouse model of muscular dystrophy. *Scientific RepoRts* | 2019 9:5770

AKNOWLEDGMENTS

First of all, I would like to thank Professor Frederic Relaix for allowing me to work on this project by hosting me in his lab and thanks to Professor Edoardo Malfatti for believing in me and letting me work under his great guidance. Thank you both for giving me this valuable opportunity.

I would like to give a special thanks to the most precious help I received during this work, thank you Valentina Taglietti. Thank you for transmitting to me everything scientific that you could transmit to me and thank you for being a friend more than a colleague.

Thanks to my tutor Professor Alessandro Malandrini, who despite these difficult times with an ongoing epidemic allowed me to have this experience abroad and for having always believed in me.

Thanks to all the doctors, biologists and technicians at the Gaslini Institute of Genova, without you this work would not have been possible. Thanks, in particular to Dr. Chiara Fiorillo and Serena Baratto.

Thanks to Prof Jerome Authier and Dr Cyril Gitiaux for your precious help.

Thanks to sweet Kauthar she has been like my big sister in this lab, helping me literally for everything always with a lot of patience.

I would like to thank all the people from the lab for the help, the advice, the company, the support, thanks to all.